The Contribution of Lymphatic and Blood Endothelial Cell PD-L1 to Leukocyte Accumulation in Skin

Ryan S. Lane

A DISSERTATION

Presented to the Cancer Biology Program

& The Oregon Health & Science University

School of Medicine

In partial fulfillment of the requirements of the degree of

Doctor of Philosophy

July 2019

School of Medicine

Oregon Health & Science University

Certificate of Approval

This is to certify that the Ph.D. Dissertation of

Ryan Lane

"*The Contribution of Lymphatic and Blood Endothelial Cell PD-L1 to Leukocyte Accumulation in Skin*"

Has been approved

_____

Mentor: Amanda Lund, Ph.D.

_____

Member/Chair: Pepper Schedin, Ph.D.

_____

Member: Ann Hill, Ph.D.

_____

Member: Owen McCarty, Ph.D.

_____

Member: Pamela Cassidy, Ph.D.

_____

Member: Jeffrey Iliff, Ph.D.

Abstract

Mechanisms of immune suppression in peripheral tissues counteract protective immunity to prevent immunopathology and are coopted by tumors for immune evasion. Blood and lymphatic vessels contribute to the immune landscape within a tissue by providing selective entry and exit routes, respectively. The work here investigates potential mechanisms by which peripheral lymphatic and blood vessel expression of the T cell inhibitory molecule PD-L1, regulate antitumor immunity. Here I test the hypothesis that PD-L1 expression by blood and lymphatic vasculature limits T cell accumulation in skin and tumors. Initial studies demonstrated that both lymphatic and blood endothelial cells (LECs and BECs, respectively) express PD-L1 in the tumor microenvironment and loss of non-hematopoietic PD-L1 results in increased T cell accumulation in tumors. I show that LECs express PD-L1 following cutaneous viral infection in response to IFNγ produced by infiltrating $CD8^+$ T cells and prevent immunopathology by limiting T cell accumulation. Additionally, this feedback mechanism limiting T cell accumulation by lymphatic vessels is coopted by melanoma tumors. The inability for LECs to respond to IFNγ increases T cell-dependent tumor control and extends survival in mice. Therefore I identify tumor associated lymphatic vessels as a component of adaptive immune resistance in tumors that likely contributes to patient response to immune checkpoint blockade. Though BECs express PD-L1 at sites of ongoing inflammation, I show that BECs also express PD-L1 constitutively at steady state in the skin of mice. Here I test the hypothesis that PD-L1 expression by BECs inhibits leukocyte transmigration across poorly or uninflamed endothelial barriers. I demonstrate that this BEC PD-L1 expression is actively maintained by STAT1 signals and marks a subset of capillary endothelial cells. Interestingly, I demonstrate that blockade of PD-L1, but not PD-1, following viral infection increases monocyte accumulation in uninfected skin, indicating that BEC PD-L1 may inhibit monocyte accumulation independent of PD-1. Moving forward I will test the hypothesis that PD-L1 signals internally within cutaneous BECs and stabilizes endothelial cell-cell junctions.

Acknowledgements

I first want to thank my mentor Amanda Lund. Amanda, you have taught me how to be a scientist that truly thinks outside the box. I am so happy that I joined your lab when you first started and got to be a part of establishing what will become your legacy in the lymphatic field. Thank you for your mentorship and taking time to teach me how to be a better scientist and writer.

Thank you to all of the current and former members of the Lund lab. I would like to give a special thanks to Jamie Booth, I would not have been able to do any of this without your help in the beginning. Julia, Maria, Madeline (Maddog), Taylor, Haley, and Aubrey, you guys have been such fun to work with and I will miss you all. Shout out to Big Breazy, thanks for gettin big with me at the wellness center and for making procrastination way too easy.

I want to thank my friends for always providing an escape from the monotony that grad school can be sometimes. Thank you to A Jesus Youth and all the awesome middle school and high school guys that I have gotten to mentor and hang out with over the years. Tanner, Radley, and Tyler, you guys have reminded me about the joy of letting go and having fun.

Thank you Mom and Dad for raising me into the man I am today and for putting up with my busy life during grad school. Thanks Kyle, you have become an amazing fire fighter and I'm so proud of you. I'm so thankful that you are my brother and best friend.

Most importantly, I want to thank my amazing wife Mary. We have been through so much this last 5 years and I cannot possibly thank you enough for putting everything on hold so that I could do this. I could not have made it without you. Your love is the best thing to come home to every night. You are going to be an amazing mother to our little girl and I am excited to see what the next step in our journey holds. I love you forever!

Lastly, thank you God for being right by me and loving me through this whole journey.

“I like to have fun all the time, even when I’m working.”

– Tom Brady

List of Figures

List of Tables

List of abbreviations

ADAM10	A disintegrin and metalloproteinase 10
AKT	Protein kinase B
APC	Antigen presenting cell
B8R	MHCI restricted immunodominant epitope in vaccinia virus
BATF	Basic Leucine Zipper ATF-Like Transcription Factor
BEC	Blood endothelial cell
bFGF	Basic fibroblast growth factor
CCL	Chemokine (C-C motif) ligand
CCR,	C-C motif chemokine receptor
CD103	Integrin alpha E
CD11b	Integrin alpha M
CD11c	Integrin alpha X
CD28	TCR costimulatory molecule
CD31	Platelet endothelial cell adhesion molecule
CD4	TCR coreceptor
CD45	Lymphocyte common antigen
CD8	TCR coreceptor
CD80/86	T lymphocyte activation antigen 80/86
CDK	Cyclin dependent kinase
CKIT	A receptor tyrosine kinase
CLEVER-1	Common lymphatic endothelial and vascular endothelial receptor-1
CTL	Cytotoxic T lymphocyte
CTLA4	Cytotoxic T Lymphocyte Antigen 4
CX_3CL	C-X3-C motif chemokine ligand
CXCL	Chemokine (C-X-C motif) ligand
CXCR	C-X-C motif chemokine receptor
DC	Dendritic cell
DTH	Delayed-type hypersensitivity
EAE	Experimental Autoimmune Encephalomyelitisl
EC	Endothelial cell
ECM	Extracellular matrix
FDA	Food and drug administration
FRC	Fibroblastic reticular cell
gp38	Podoplanin
ICAM	Intercellular Adhesion Molecule 1
IDO	Indoleamine 2,3-dioxygenase
IFNγ	Interferon gamma
IFNγR	Interferon gamma receptor
IGF-1R	Insulin-like growth factor 1 receptor
IL	Interleukin
irAEs	Immune related adverse events
JAK	Janus activating kinase
LAG3	Lymphocyte activating 3

LCMV	Lymphocytic choriomeningitis
LEC	Lymphatic endothelial cell
LFA-1	Lymphocyte function-associated antigen 1
LM	Listeria monocytogenes
LN	Lymph node
LS	Lymphatic score
LV	Lymphatic vessel
LVD	Lymphatic vessel density
Ly6C	Lymphocyte antigen 6 complex C
Ly6G	Lymphocyte antigen 6 complex G
LYVE1	Lymphatic Vessel Endothelial Hyaluronan Receptor 1
MAPK	Mitogen-activated protein kinase
MC1R	Melanocortin receptor
MHCI	Major histocompatability complex class I
MHCII	Major histocompatability complex class II
MTOR	Mechanistic target of rapamycin
NF1	Neurofibromin 1
OT-I	Transgenic T cell specific for OVA
OVA	Ovalbumin
P-W	PD-L1$^{-/-}$ into WT chimera
PD-1	Programmed cell death receptor 1
PD-L1	Programmed cell death receptor ligand 1
PDAC	Pancreatic ductal adenocarcinoma
PDGFR-β	Platelet-derived growth factor receptor beta
PI3K	Phosphoinositide 3-kinase
Prox-1	Prospero homeobox 1
PTA	Peripheral tissue antigen
S1P	Sphingosine-1-phosphate
SHP-2	Src homology region 2 domain-containing phosphatase-2
STAT	Signal transducer and activator of transcription
TCGA	The Cancer Genome Atlas
TCR	T cell receptor
TGF-β	Transforming growth factor beta
TIL	Tumor infiltrating Lymphocyte
TIM-3	T-cell immunoglobulin and mucin-domain containing-3
TME	Tumor microenvironment
TNFα	Tumor necrosis factor alpha
UV	Ultraviolet
VacV	Vaccinia virus
VCAM	Vascular cell adhesion protein 1
VE-cadherin	Vacular endothelial cadherin
VEGF	Vascular endothelial growth factor
VLA-4	Very late antigen 4
W-P	WT into PD-L1$^{-/-}$ chimera
W-W	WT into WT chimera

Contents

Chapter 1:

Introduction

Melanoma

Epidemiology

Skin cancer is on the rise[1] and it is estimated that 1 in 5 individuals over the age of 70 will have had skin cancer in their lifetime[2]. While melanoma makes up only 1% of all skin cancer, it accounts for a majority of skin cancer related deaths. In the United States, melanoma represents 5.5% of all cancer[3] and the lifetime risk of melanoma is 1/56 for women and 1/37 for men[4], with an estimated 96,480 new cases and 7,230 deaths in the United States in 2019[3]. The rise of melanoma is likely due to the increase in ultraviolet (UV) radiation exposure from breakdown of the ozone[5] combined with popularity of outdoor recreational activities and the perceived glamorous look of tanned skin. Early detection and removal of localized melanoma, termed melanoma *in situ*, leads to cure rates of 98.7%[3]. However, the presence of distant metastasis at time of diagnosis bears only a 24.8% survival rate[3]. Unfortunately, melanoma is affecting younger people with the median age of diagnosis at 57[4] while most other cancers are diagnosed after age 65[4]. There is a clear need for earlier detection and better treatments for patients diagnosed with metastatic disease.

Melanocytes and Melanoma

Melanin produced by melanocytes in the epidermis provides the skin with its ability to protect DNA from UV radiation induced damage. UV radiation induces modifications to DNA (e.g. cyclobutane-pyrimidine dimers or 6-4 photoproducts) that, during replication, causes mutations (e.g. C to T transistions)[6]. There are about 1,500 melanocytes per square mm of human skin[7] interspersed throughout the basal membrane of the epidermis. They

are outnumbered 1:10 by basal keratinocytes[8] and extend dendrites to between 30-40 different neighboring keratinocytes[9]. Their main function is to synthesize melanin, package it into melanosomes and pass it through these dendrites to keratinocytes[10] where it absorbs and scatters UV light[11] thereby protecting nuclei from UV damage. The amount and type of melanin in the skin dictates the darkness of skin complexion, UV sensitivity, and cancer risk[12–14]. While the baseline level of melanin in the skin protects against UV from the sun, it also increases during sun exposure. UV-induced production of α-melanocyte stimulating hormone, by keratinocytes, signals to melanocytes through the melanocortin receptor (MC1R) to increase melanin synthesis[15] and breakdown of this pathway can cause loss of protection. In fact, germline mutation in MC1R, confers increased risk for melanoma formation[16]. Ultimately, failure to protect against UV radiation will lead to DNA damage in cells in the skin, and if that damage results in mutation in an oncogenic pathway in a melanocyte, it can cause melanoma.

The most common oncogenic driver pathway mutated in melanoma is the mitogen-activated protein kinase (MAPK) pathway[17,18]. 38-60% of MAPK pathway mutations occur in the BRAF gene[19–21], and most commonly results in a substitution of valine for a glutamic acid at residue 600 ($BRAF^{V600E}$) and accounts for 79% of all BRAF mutations[20]. The $BRAF^{V600E}$ mutation results in 500-fold higher activation of the catalytic domain of BRAF and subsequently hyperactivate MAPK signaling[21,22]. The other common pathway often disrupted in melanoma is the PI3K/AKT/mTOR pathway[17], although this usually occurs as the disease progresses[20,23]. MAPK activation may lead to uncontrolled proliferation of melanocytes, however 82% of benign nevi, or moles, also harbor the same $BRAF^{V600E}$ mutation[24], therefore it is not the only factor required for complete melanoma formation. In fact, forced $BRAF^{V660E}$ expression in normal melanocytes eventually leads to growth arrest and a senescence-like phenotype via expression of cyclin-dependent kinase (CDK) inhibitors such as p16, leading to G_1 phase arrest[25,26]. In this regard, it is not surprising that CDKN2A mutations, the gene encoding p16 are found exclusively in invasive melanoma and rarely in precursor lesions[27]. These observations indicate that benign nevi, can acquire additional mutations and turn into malignant disease, however this is

rarely the case as most melanomas arise *de novo* or as dysplastic precursor lesions[7,23,27]. Thus, while MAPK pathway mutations may initiate melanoma formation, it is likely additional UV-induced mutations are acquired to tip the scale to metastatic disease.

TARGETED THERAPY

Targeted therapy to treat metastatic melanoma has been successful in the clinic, but tumors often develop resistance and many patients relapse, warranting something better. Targeted therapy utilizes small molecules or antibodies that specifically bind to and block the function of mutated, but not normal versions of proteins, and therefore are very specific and often possess little off target effects. Vemurafenib, a selective inhibitor of $BRAF^{V600E}$, which up to 60% of patients possess[19–21], was the first FDA approved targeted therapy for patients with unresectable metastatic melanoma possessing this mutation[28,29]. It causes tumor regression in up to 90% of patients and improves progression free survival by 5-6 months compared to then standard-of-care dacarbazine chemotherapy[29]. Unfortunately, this clinical benefit is short-lived and tumors quickly develop mechanisms to circumvent BRAF inhibition[28]. Vemurafenib resistance can occur through MAPK pathway intrinsic mechanisms, such as elevated cyclin D amplification[30], alternative splicing of BRAF[31], or activating mutations in NRAS or MEK[32]. Resistance can also occur in MAPK pathway extrinsic mechanisms such as increased PI3K/AKT/mTOR pathway activation through its amplification by either increased IGF-1R[31] or PDGFR-β expression[28] or by loss of PTEN expression[31]. Importantly, as these resistance mechanisms become identified, their inhibition simultaneously with BRAF inhibition may be an answer to acquired resistance. In fact, inhibitors targeting MEK[33], CKIT[32] and mTOR[32] are already in clinical trials in combination with vemurafenib[32]. The MEK inhibitor, cobimetinib, in combination with vemurafenib was approved by the FDA for the treatment of unresectable melanoma and improved progression-free survival by 3.7 months compared to vemurafenib alone[33], demonstrating that combination therapy can be beneficial. Unfortunately, only about half of patients harbor the $BRAF^{V600E}$ mutation and therefore vemurafenib as a mono or combination therapy is not an option for those that harbor NRAS or NF1 driver mutations[17,20]. There is a need for effective, long-lasting treatments both for patients who become resis-

tant to BRAF/MEK inhibition and those that do not possess $BRAF^{V600E}$.

IMMUNOTHERAPY

Immunotherapy, unleashing the patients own immune system to fight the tumor, is the future of treating metastatic melanoma. Though tumors were previously thought to be poorly immunogenic and not capable of activating an immune response, we now know that somatic mutations (created by DNA instability and environmental challenge) generate neoantigens that are sufficiently distinct from self, such that T cells are capable of expanding and directing tumor-specific killing[34,35]. Despite this, tumors still evolve in ways that evade immune elimination, often by using naturally occurring immune inhibitory mechanisms. Such mechanisms are the targets of immunotherapy in melanoma. The first immunotherapy drug to treat metastatic melanoma, ipilimumab, targets the T cell inhibitory receptor CTLA4 and when compared to standard chemotherapy, extends median survival to 10.1 months[36,37], with a ten year survival rate of 20%[38]. As the first FDA-approved immunotherapy for metastatic melanoma, ipilimumab blazed the trail for approval of other immunotherapies, such as those targeting another T cell inhibitory receptor PD-1 or its ligand, PD-L1. The PD-1 inhibitor, pembrolizumab, has a 33% response rate and median survival of 23 months in patients with metastatic melanoma[39], and nivolumab, another PD-1 inhibitor, has a 52% overall survival rate at 36 months[40]. Head to head clinical trials have demonstrated that both pembrolizumab and nivolumab out perform ipilimumab in treating metastatic melanoma and have less high-grade toxicity[40,41], and pembrolizumab even has efficacy in ipilimumab refractory melanoma patients[42]. Combination of ipilimumab and pembrolizumab has an even greater effect, increasing survival to nearly 60%[40], however this comes at a cost – dramatically increased toxicity[40]. Termed immune related adverse events (irAEs), these side affects are markedly distinct from chemotherapy-related toxicities and manifest as autoimmunity and inflammatory pathologies of many different organs[43]. While most are mild (e.g. skin rash or pruritis), more severe irAEs such as colitis and pneumanitis can be life threatening and require discontinuation of treatment[43]. As these therapies become frontline and adjuvant treatments for melanoma, and used more often to treat other cancer types, there is a need

to know which patients will respond favorably, thereby protecting nonresponders from unnecessary irAEs. However, despite this widespread use of immune checkpoint blockade immunotherapy in the clinic, we, as a field, lack a complete understanding of the underlying biological mechanisms that these therapies inhibit. Subsequently, we also lack understanding needed to differentiate the mechanisms that contribute favorable clinical response from those that contribute to irAEs. Thus, in order to improve immunotherapy, extend it to other cancer types, and predict patient responses, we first need to understand the biology of antitumor immuntiy.

Regulation of T cell Responses

Immunity vs. Immunopathology

T cell-mediated immunity is very potent and provides protection from pathogenic challenge. However, if directed towards self or not turned off following pathogen clearance, the resulting autoimmunity or immunopathology, respectively, can be fatal. Therefore a careful balance between T cell stimulatory and inhibitory processes maintains the hosts ability to protect from pathogenic challenge, but not at the expense of self tissue destruction. The elimination of potentially harmful, self-reactive T cell clones is achieved through (1) central tolerance, which occurs in the thymus during lymphocyte development and negatively selects and deletes T cells whose T cell receptor (TCR) has either very high or no affinity for self antigens[44]; and (2) peripheral tolerance, which occurs after thymic development in secondary lymphoid organs and ensures self-reactive T cells that escaped central tolerance do not generate autoimmunity[45]. During an ongoing immune response, protective immunity is dependent upon sequential, rapid activation and mobilization of leukocytes that undergo multiple intercellular interactions to mediate immune control while simultaneously preventing self-tissue destruction. Therefore, rather than being stochastic, the activation, recruitment, and local function of lymphocytes is guided by stimulatory and inhibitory signals, termed immune checkpoints (e.g. the T cell inhibitory receptor PD-1), provided by interacting hematopoietic and non-hematopoietic cells throughout its lifetime which limit the size and functionality of the T cell response.

Another way the host balances protective immunity and self tissue destruction is through the spatial restriction of T cells within the host. Lymphatic and blood endothelial cells (LECs and BECs, respectively) form selective barriers that spatially compartmentalize leukocytes during the immune response and determine where they can be within the host. Importantly, both lymphatic and blood endothelium are in constant communication with their local environments and modulate immune responses according to the cues they receive. The mechanisms used by lymphatic and blood endothelium to instruct T cell responses are discussed in detail later (See Lymphatic Endothelium as a Selective Barrier of Immunity & Vascular Endothelium as a Selective Barrier of Immunity). Importantly, this global architecture within the host set up by endothelial barriers works in concert with T cell-intrinsic mechanisms of regulation throughout the immune response to achieve optimal immune function while limiting collateral damage. In cancer the balance shifts towards self-tissue protection and the tumors do not get eliminated.

THE CANCER IMMUNITY CYCLE

The generation of an effective T cell response to a pathogen occurs in a stepwise manner and, in the context of a tumor, it is referred to as the cancer immunity cycle (Figure 1.1)[34]. One of the hallmarks of cancer is avoiding this immunity[46], and as such, tumors coopt mechanisms of immune suppression throughout this cycle that normally function to counteract protective immunity and avoid immune elimination. The accumulation of neoantigens in tumors is likely a prerequisite to antitumor immunity across tumor types, and consistently, those tumors that exhibit highest somatic mutational burden (e.g. melanoma) exhibit good overall response to immune checkpoint blockade[47]. Even in the presence of potent neoantigens, however, some tumors still fail to respond to therapy and somatic mutational burden is not sufficient to predict T cell infiltration within and across tumor types[48]. Thus, multiple overlapping mechanisms of immune suppression occurring throughout the cancer immunity cycle (Figure 1.1) create a more complex immune landscape such that, processes of T cell activation, recruitment, retention, survival, and exit from tumors may underscore intratumoral T cell presence and thus influence response to therapy.

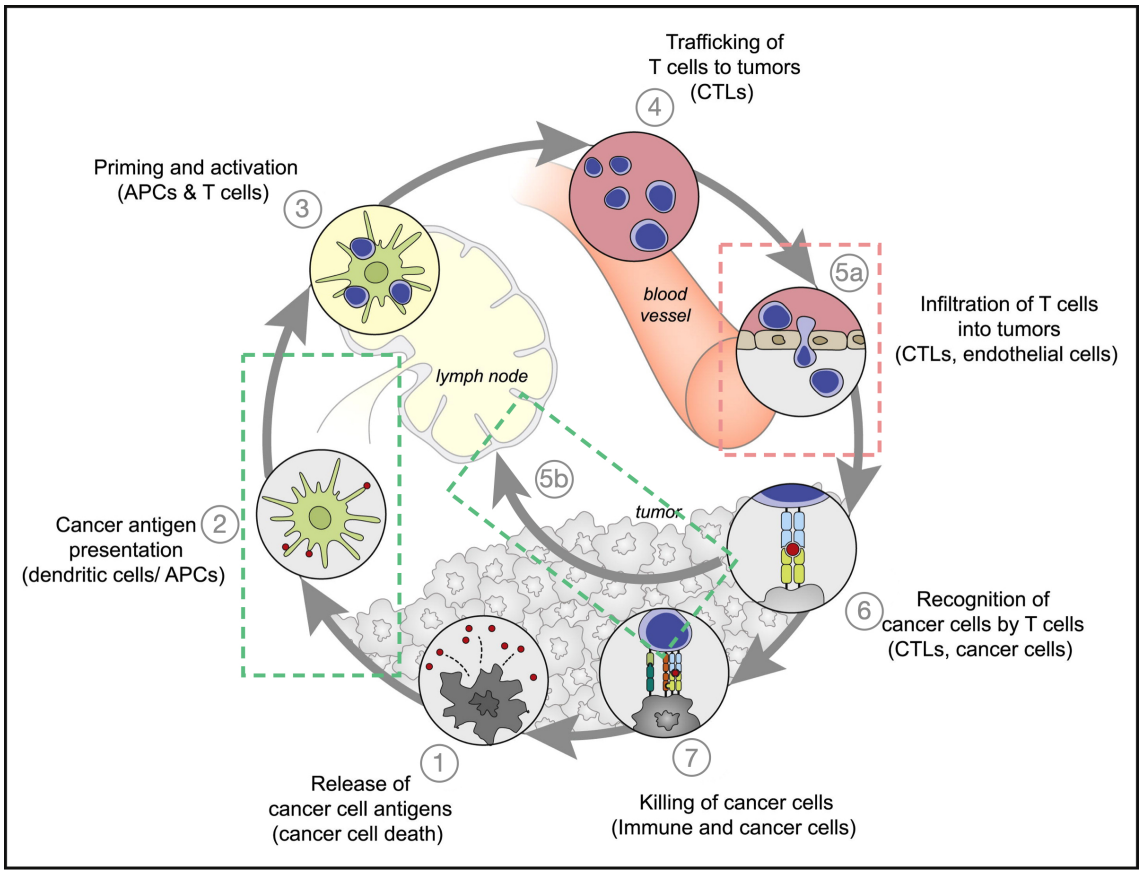

Figure 1.1: The Cancer Immunity Cycle: The generation of immunity to cancer is a cyclic process that can be self propagating, leading to an accumulation of immune-stimulatory factors that in principle should amplify and broaden T cell responses. The cycle is also characterized by inhibitory factors that lead to immune regulatory feedback mechanisms, which can halt the development or limit the immunity. This cycle can be divided into seven major steps, starting with the release of antigens from the cancer cell and ending with the killing of cancer cells. Each step is described below, with the primary cell types involved and the anatomic location of the activity listed. Green boxes highlight those steps regulated by peripheral lymphatic vessels and the red box highlights the step regulated by peripheral blood vessels. Abbreviations are as follows: APCs, antigen presenting cells; CTLs, cytotoxic T lymphocytes. Adapted from Chen & Mellman *Immunity* 2013

Lymphatic vessels are required for T cell priming during the onset of the cancer immunity cycle. Following antigen release from the tumor (step 1), lymph-borne antigen is transported to lymph nodes (LNs) through afferent lymphatic vessels (step 2, green box) that connect to the subcapsular sinus allowing delivery of large particulate antigens (>70kDa) to interfollicular dendritic cells (DC) and subcapsular macrophages[49,50]. Small antigens (<70kDa) enter fibroblast reticular cell-lined (FRC) conduits and are sampled by LN resident DCs[51]. Both the packing of collagen fibers within FRC-conduits and direct filtration by LECs lining the lymphatic sinus floor determine LN size exclusion properties and thus dictate antigen delivery[51,52]. While lymph flow is constitutive at steady state, lymphatic fluid transport is rapidly reduced following cutaneous infection, indicating that peripheral tissue context dictates lymphatic vessel function and antigen delivery[53]. In

addition to soluble antigen delivery in lymph fluid, $CD103^+$ cross-presenting DCs can capture antigens and traffic them to draining LNs, and is a major mechanism of antitumor T cell activation in melanoma[54]. Importantly, cutaneous infection and melanomas fail to activate adaptive immunity in mice lacking dermal lymphatic vessels[53,55]. As such, lymphatic vessels are fundamentally required for both soluble antigen delivery[51,56] and DC migration[53,57,58] (Figure 1.1, green box) to secondary lymphoid organs to prime T cells.

The next step, T cell priming, (step 3, Figure 1.1) occurs in the LN, where the signals a T cell receives from an APC during activation shape the size and functionality of the immune response. $CD8^+$ T cell priming, also called activation, requires 2 signals from licensed DCs[59]: ligation of their TCR by their cognate antigen presented on MHCI (signal 1) and ligation of the costimulatory receptor CD28 by CD80 and CD86 on DCs (signal 2)[60]. Upon activation and clonal expansion, however, effector $CD8^+$ T cells also upregulate many inhibitory receptors that interfere with TCR signaling and put boundaries on the size and behavior of the effector T cell population[61]. One such inhibitory receptor, CTLA-4, is expressed on the surface promptly after T cell activation and is crucial for dampening immunity and preventing fatal multi-organ destruction in mice[62]. CTLA-4 has a higher affinity for the ligands (CD80/86) that bind CD28 than CD28 itself does and therefore sequesters the costimulatory signal transmitted through CD28[63]. CTLA-4 is just one of many inhibitory receptors (e.g. PD-1, TIM-3, LAG3)[64] expressed by $CD8^+$ T cells during an ongoing immune response that altogether counterbalance activation and effector function, resulting in a properly tuned T cell response – pathogen clearance and minimal self tissue destruction. In antitumor immunity, however, the inhibitory pathways prevail and T cells fail to eliminate the tumor. Importantly though, blocking these checkpoints restores antitumor immunity[65] and is efficacious in the clinic[36,37,40], demonstrating that if we can identify the pathways used and block them, immunity can be restored.

In addition to T cell intrinsic checkpoint molecules, the blood and lymphatic endothelium provide selective barriers that determine the physical location where T cells can operate (steps 5a & 5b Figure 1.1). Following activation, effector T cells enter circulation in search of their target, and although they express the machinery required for tissue

entrance[66], it is the vascular endothelium that marks sites of inflammation and grants tissue access[67]. The mechanisms by which blood endothelial cells (BECs) maintain this selectivity is discussed in detail later (see Vascular endothelium as a selective barrier of immunity). The second endothelial cell barrier providing spatiotemporal regulation is the lymphatic vasculature. Lymphatic vessels in peripheral tissues, and tumors, provide an exit route for T cells[68] and their impact on lymphocyte accumulation and behavior during inflammation is also discussed in detail later (See Lymphatic endothelium as a selective barrier of immunity). Similar to the other steps in the cancer immunity cycle, the lymphatic and blood vasculature can also become dysregulated, tip the scale to self-tissue protection and prevent proper tumor elimination.

Once effector T cells get in, stay there, and home to their target, there is one last regulated step to adaptive immunity – killing their target. While this may seem straightforward, in tumors it is a major hurdle of the T cell response as tumors acquire many mechanisms to avoid this step. When antigen specific $CD8^+$ T cells recognize their cognate antigen presented on MHCI and start killing, they also produce the effector cytokine IFNγ, which has a double-edged effect on the local environment. First, it signifies an ongoing immune response, which in turn recruits more leukocytes to the site, increasing protection from the pathogen. Second, IFNγ also initiates mechanisms of immune resolution[69] within the affected tissue to prevent unnecessary bystander damage and immunopathology[70], essentially acting as a $CD8^+$ T cell off switch once the pathogen is cleared and T cells are no longer needed. When this occurs in tumors it is called adaptive immune resistance and T cells are inhibited prematurely *before* the tumor is completely eliminated[71]. While the inhibitory mechanisms of adaptive immune resistance are multifaceted[71,72], one particular component is tumor cell expression of T cell inhibitory molecule PD-L1[69], which prevents $CD8^+$ T cell killing of tumor cells[73]. Tumor cell PD-L1 is the source thought to be blocked with PD-1/PD-L1 checkpoint immunotherapy, however PD-L1 expression by tumor cells does not completely predict response to PD-1 checkpoint therapy[74]. For example, some patients whose tumor cells do not express PD-L1 still respond to therapy[74]. This suggests that there may be other, non-tumor-cell,

sources of PD-L1 that suppress antitumor CD8$^+$ T cells and that these sources of PD-L1 may be located outside of the tumor microenvironment.

THE PD-1/PD-L1 INHIBITORY AXIS

PD-1 is a T cell inhibitory checkpoint molecule that delivers a negative signal to the T cell at many points throughout the cancer immunity cycle and models of chronic infection demonstrate that the PD-1 inhibitory axis is crucial for limiting immunity and preventing fatal immunopathology[75,76]. PD-1 was first described by Tasuku Honjo in 1996[77] and is an inhibitory receptor on CD8$^+$ T cells that interferes with TCR signal propagation. PD-1 is expressed on the surface of CD8$^+$ T cells upon activation[77] and declines over time as antigen encounter is resolved[78]. PD-1 engagement by its ligand, PD-L1, inhibits lymphocyte activation[79] by recruiting the phosphatase SHP-2 to the immunological synapse where it dephosphorylates the costimulatory receptor CD28[80] thereby dampening TCR stimulation. Additionally, PD-1 also signals through the Ras/MAPK and PI3K/AKT/mTOR pathways to alter metabolic, nutrient sensing, survival, and cell growth of lymphocytes[81]; induce basic leucine zipper ATF-like transcription factor (BATF)-mediated inhibitory transcriptional changes[82]; and influence T cell motility[83]. Although the functional significance of these alternative signaling mechanisms in disease are unclear, PD-1 blockade certainly has efficacy in the clinic to treat cancer.

PD-1 blockade reverses T cell exhaustion during chronic viral infection and in cancer. T cell exhaustion was first described during chronic viral infection with LCMV clone 13 in mice[84] and describes a dysfunctional state of CD8$^+$ T cells due to persistent antigen exposure and inflammation[85]. It is marked by a transcriptional profile distinct from effector or memory T cells[75], progressive loss of cytotoxicity, cytokine production, and proliferative potential[86], and high expression of T cell inhibitory markers such as PD-1[84,85]. In addition to being found during chronic viral infections, exhausted T cells are also found in cancer[87] and is one proposed way that T cells are unable to eliminate tumors[88]. Importantly, in both chronic infection and cancer, a subset of exhausted CD8$^+$ T cells can be reinvigorated with PD-1 blockade, restoring their effector function[75,89].

PD-L1 is a ligand for PD-1 and is expressed by many cell types within the host and

integral to PD-1-dependent control of immunopathology and autoimmunity[85]. PD-L1 was first identified on antigen presenting cells in peripheral blood[79], but is also expressed by other hematopoietic and non-hematopoietic cells within the host[70,90–92]. Loss of the hosts ability to signal through this axis potentiates the development of autoimmunity in mice[93]. In models of experimental autoimmune encephalomyelitis (EAE), loss of host PD-L1 greatly exacerbates onset and severity of disease[94,95], a phenotype largely due to PD-L1 expression by $CD11c^+$ DCs[96]. Consistently, hematopoieitc PD-L1 dampens $CD8^+$ T cell activation and expansion during chronic viral infection[76,79,94]. Host PD-L1 is also crucial for protection from immunopathology. PD-$L1^{-/-}$ mice infected with chronic clone 13 LCMV die due to immunopathology and fatal circulatory failure[76,84], a phenotype attributed to the non-hematopoietic compartment of PD-L1 that prevents T cell mediated killing of infected endothelial cells[76,92]. Non-hematopoietic PD-L1 also contributes to dampening chronic inflammatory responses in the small intestine[97], limiting lymphocyte infiltration into the cornea in chronic dry eye disease[98], limiting infiltration in a model of multiple sclerosis[99], the pathology of stroke[100–102], and in autoimmune diabetes[103]. Altogether this indicates that both hematopoietic and non-hematopoietic sources of PD-L1 contribute to inhibiting T cell behavior and therefore together cooperatively protect the host from autoimmunity and immunopathology.

Immunotherapy targeting PD-L1 has seen unprecedented results in treating many types of cancer in the clinic, however, it does not work in all patients. It was originally hypothesized that α-PD-L1 blockade interferes with PD-L1 expression by tumor cells during adaptive immune resistance preventing T cell mediated killing. As such, PD-L1 expression by tumor cells is one criteria for treatment of non-small cell lung cancer[104,105], however, tumor cell PD-L1 expression does not perfectly stratify patient response to therapy, and often PD-$L1^-$ patients do respond[41,74,106]. This indicates that other non-tumor sources of PD-L1 must contribute to suppressing antitumor immunity. The field however, is slow to acknowledge this, seemingly ignoring the fact that other sources of PD-L1 suppress immune responses that cause autoimmunity and prevent immunopathology. While tumor cell PD-L1 can prevent direct killing by tumor specific $CD8^+$ T cells[73], mouse mod-

els also demonstrate roles for host PD-L1 in dampening antitumor immunity[73,90,107], indicating that the role of host PD-L1 may be context dependent. A complete understanding of the underlying biology of host PD-L1 on the antitumor immune responses is essential to to improve α-PD-L1 therapy in the clinic and identify biomarkers of all patients that will respond.

Hypothesis: PD-L1 expression by lymphatic and blood endothelial barriers impacts immune cell infiltration and behavior in skin

Immune checkpoint therapy targetting PD-1 or PD-L1 often fails in the clinic, with the best response rate of 60% when combined with α-CTLA4 therapy[40]. Patients who do not respond to therapy have three types of immune landscapes within their tumors: nonfunctional immune infiltrate, immune cell excluded, and immunological deserts[108]. With the assumption that these tumors possess mutations sufficient to generate adaptive immune responses[34], then the cause of these immune landscapes is reduced to two basic principles: 1) that T cells are unable to get into the tumor and find their target; or 2) they get to their target, but are dysfunctional or inhibited locally and unable to kill their target. As discussed below, the endothelial cell barriers in tissues, and tumors, direct local T cell recruitment to, and migration and retention within the local tissue or tumor microenvironment (TME). Thus tumor infiltrating lymphocytes must come into physical contact with BECs or lymphatic endothelial cells (LECs) as they enter or leave the TME, respectively. This represents a required physical contact between T cells and endothelial cells, however, the ramifications of such an encounter on T cell behavior is unclear. Interestingly, both LECs and BECs express PD-L1 in LNs[70,109,110] and can upregulate and express it in tumors[70,91,111]. This indicates as T cells cross endothelial barriers in tumors they may simultaneously receive a PD-L1 inhibitory signal. However, PD-L1 expression by cells other than tumor or myeloid cells is the TME is often disregarded as functionally relevant. Here I hypothesize the contrary, that PD-L1 expression on LECs and BECs shapes the T cell landscape within the TME and therefore represents a novel component of the TME that inhibits T cell accumulation and behavior within tumors.

Lymphatic Endothelium as a Selective Barrier in Immunity

Lymphatic vessels can no longer be considered passive conduits through which stuff drains, rather they respond to local environmental cues and are essential for immune responses. Historically, lymphatic vessels were considered passive conduits that continuously drain tissues, much the same way a sewer system works, thus the more lymphatic vessels there are the more drainage that occurs. In tumors, this was most commonly associated with metastasis; tumors with higher lymphatic vessel density (LVD) have increased LN metastasis, and therefore poorer prognosis[112,113]. Recently however, it has been appreciated that the level of LVD in a tumor also correlates with the level of immune cell infiltration in tumors[55], and therefore the presence of lymphatic vessels may be beneficial. However, all of these studies relied on manipulation of lymphatic vessels along their lymphangiogenic axis (i.e. eliminating LVs completely or over expressing the growth factor VEGF-C). Whether preexisting lymphatic networks may change their function *independent* of lymphangiogenesis to modulate peripheral immune responses is incompletely understood and represents an exciting area to be explored.

BASIC FUNCTIONS OF LYMPHATIC VESSELS

The lymphatic system is composed of a unidirectional vasculature that connects peripheral tissues to secondary lymphoid organs and is crucial for maintaining tissue fluid homeostasis[114], initiating adaptive immune responses[115], and lipid transport[116] (Figure 1.2 A). In the skin, initial lymphatic capillaries reside in the dermis as a plexus or network of blind ended, highly permeable capillaries with a discontinuous basement membrane and converge into precollecting, and eventually collecting lymphatic vessels in the hypodermis[115,117]. Collecting lymphatic vessels, unlike capillaries, are much less permeable, possess a complete continuous basement membrane, and are surrounded by smooth muscle cells that contract and, with help from unidirectional valves, propel afferent lymph fluid towards LNs[114,117]. Disruption of fluid transport properties of lymphatic vessels results in accumulation of fluid in tissues, called lymphedemia, that leads to progressive fibrosis, adipose deposition, and inflammation[118]. Traditionally, fluid transport by lym-

phatic vessels was considered to be a passive process similar to a sewer system. However, we now know that this is not the case. Active restructuring of lymphatic capillaries during inflammatory challenge alters fluid[53] and lipid[119] transport properties (preventing particulate dissemination to LNs), but still facilitates DC migration to LNs to prime adaptive immunity[53]. Whether peripheral lymphatic vessels respond to other environmental signals and have consequences on immune responses is unclear.

Lymphatic vessels connect peripheral tissues to LNs and provide a route for communication between the outside pathological environment and the internal adaptive immune response (Figure 1.2 B). Typically they remain in an inactive or quiescent state, continuously transporting self antigens and DCs to LNs during normal tissue turnover[117,120], however upon inflammatory stimuli, lymphatic vessels readily change their fluid transport properties[53] and mobilize DC towards lymphatic capillaries[53,57,58,121]. During inflammation, LECs increase production of CCL21 which directs $CCR7^+$ DC migration[54] towards lymphatic vessels[122]. LEC expression of LYVE1[123] and ICAM[124] are required for DC docking and crawling within lymphatic capillaries, respectively. Subsequently, LECs not only provide a route required for adaptive immune priming in LNs[53,55], but also can impact DC migration by changing expression of molecules required for trafficking. Altogether, the lymphatic vasculature is a selective barrier that regulates DC trafficking thereby shaping the immune response.

LYMPHATIC VESSELS FACILITATE LYMPHOCYTE EGRESS FROM TISSUE

In addition to providing the route for DC migration to LNs, lymphatic vessels also provide an exit route for T cells from tissue. Following entry into and surveillance of tissue, at least a subset of T cells continue on and egress out through lymphatic vessels (Figure 1.2 C). Parabiosis experiments demonstrate that most endogenous memory T cells in peripheral tissue reach equilibrium with migratory blood-borne donor T cells indicating rapid turnover in peripheral tissue[125] (with the notable exception of tissue resident memory lymphocytes[126]). In sheep, where lymph can be readily sampled, afferent lymph contains 10^6 cells/ml[127]. Furthermore, the number of leukocytes in lymph increase by as much as 100-fold in response acute and chronic inflammatory signals[128], indicating tissue egress

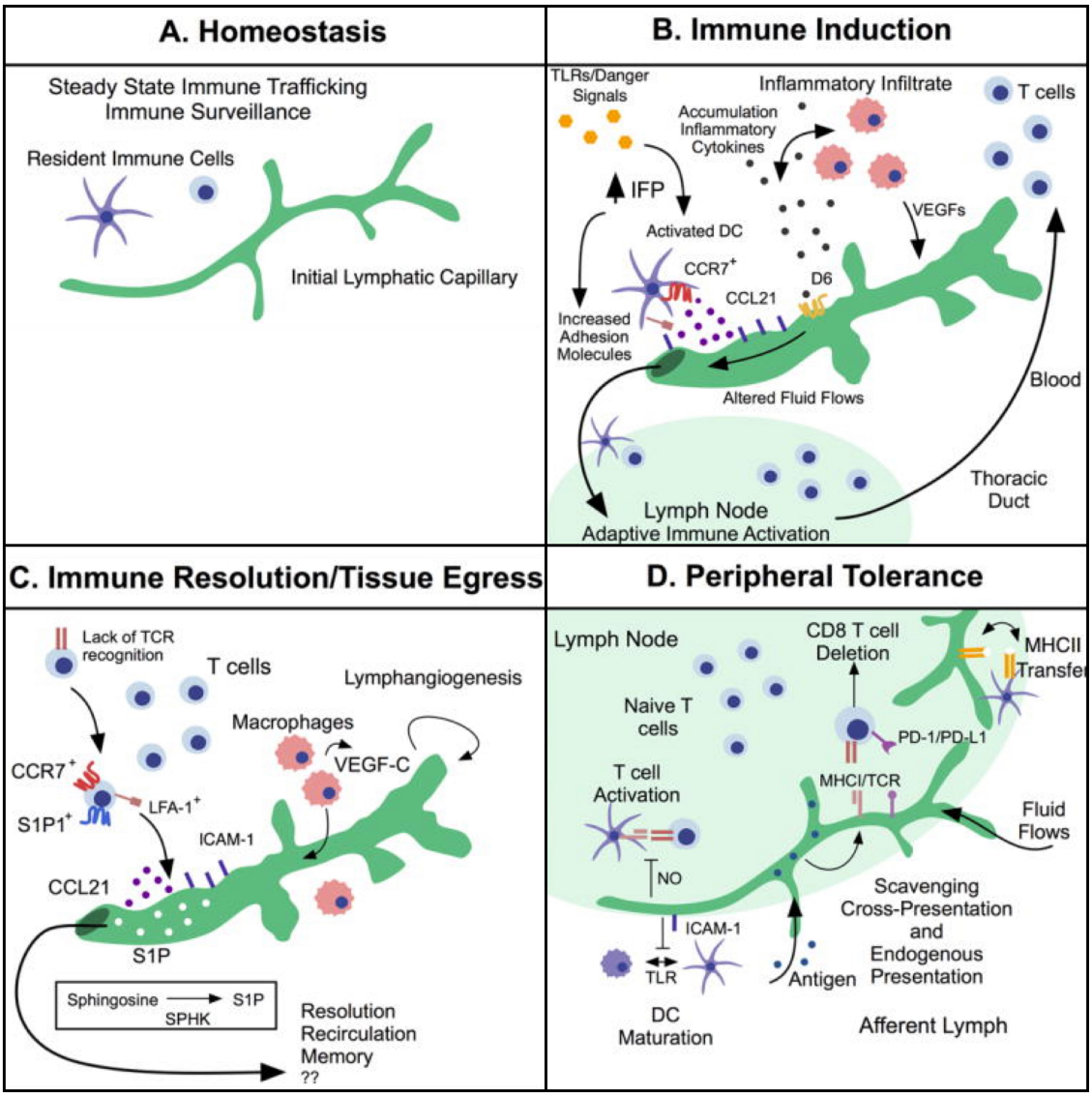

Figure 1.2: Lymphatic vessels, inflammation, and immunity (A) homeostatic lymphatic capillaries support immune surveillance through steady-state homing of resident immune cells, including DCs and some subsets of memory T cells. (B) Local inflammation and damage activate a series of danger signaling as well as increased IFPs that activate initial lymphatic capillaries, resulting in remodeling (either proliferative or nonproliferative), upregulation of adhesion molecules, and enhanced expression of the homing chemokines (e.g. CCL21) . Altered adhesions and CCL21 coordinate to facilitate entry of activated CCR7$^+$ DCs into afferent lymphatic vessels and migration toward draining LNs where they interact with and activate naïve T cells. The decoy receptor D6 ensures proper presentation of homeostatic chemokines by LECs by scavenging inflammatory chemokines to specifically facilitate mature over immature DC migration. Changes in lymphatic flows that result from altered signaling in both initial capillaries and collecting vessels may influence accumulation of inflammatory cytokines that help to perpetuate local inflammation leading to infiltration and accumulation of leukocytes in tissue, which further drive lymphatic remodeling. (C) Although important for immune induction, evidence also indicates that lymphatic capillaries importantly regulate resolution of local inflammation and immunity through leukocyte egress and chemokine sequestration. Both macrophages and some T cells exit peripheral tissue through draining lymphatic capillaries using CCL21 and sphingosine kinase (SPHK) conversion of sphingosine into sphingosine-1-phosphate (S1P) as signals for their exit, all produced by initial lymphatic vessels. Cellular exit is required for resolution of disease. ICAM1, intracellular adhesion molecule 1; LFA1, lymphocyte function associated antigen 1. (D) Novel immunomodulatory roles of LECs have been described, largely in the context of lymphoid organs. LECs inhibit both antigen-dependent and independent T-cell activation through production of nitric oxide (NO) and nonspecific inhibition of DCT-cell interactions. Inflamed LECs inhibit maturation of DCs through ICAM1 and receive peptide-loaded MHCII complexes from mature DCs. In addition, LECs promiscuously present endogenous and scavenge exogenous antigen for cross-presentation on MHCI molecules and direct deletion of antigen-specific CD8$^+$ T cells. Adapted from Lund et al. *Cancer Discovery* 2016.

is influenced by context. Whether the cellular component of afferent lymph is simply a reflection of the tissue it drains (e.g. passive, random transport) or rather represents a

subset of tissue lymphocytes (e.g. active, selective transport) remains largely unknown.

To facilitate tissue exit, lymphatic vessels express an array of chemokines in a context-dependent manner. LECs constitutively express CCL21[122,129] and further increase expression during chronic lung inflammation[130] and acute inflammation in skin, but not treatment with complete Freund's adjuvent (CFA)[131]. TNFα stimulation of LECs causes release of CCL21 stores[132] and *de novo* production of CCL21[132] as well as a host of other chemokines including CCL20, CXCL5, CCL5, CXCL2, CX_3CL1, and CCL2[133]. Additionally, *in vitro* analysis indicates that lipoteichoic acid, a component of gram-positive bacterial cell walls, induces TLR2-dependent expression of CXCL1, CXCL3, CXCL6, and CXCL8[134]. *In vivo* analysis of mRNA from LECs in inflamed skin confirms these *in vitro* results, and also identified several other chemokines expressed by LECs, including the $CD8^+$ T cell-homing chemokines CXCL9 and CXCL10[131], altogether indicating that the chemokine repertoire produced by LECs in peripheral tissue is context dependent. Consequently, how this diverse repertoire of chemokines produced by inflamed LECs regulates lymphocyte egress from tissue remains a largely open question.

LECs also increase expression of the T cell adhesion molecules in response to local inflammation and interstitial fluid flows. Intracellular adhesion molecule 1 (ICAM-1), vascular cell adhesion protein 1 (VCAM-1), and E-selectin are expressed on the LEC surface rapidly following peripheral challenge *in vivo*[53,131,133] and following stimulation *in vitro*[135]. LFA-1 is necessary for naïve T cell egress from inflamed skin[124] and inhibition of common lymphatic endothelial and vascular endothelial receptor-1 (CLEVER-1) and macrophage mannose receptor prevent T cell migration through afferent lymphatic vessels to draining LNs[136,137]. The requirement for integrins in LEC transendothelial migration in inflamed tissue may mirror the differential integrin requirement for DCs. While DCs in skin squeeze through overlapping, button-like junctions in naïve lymphatic capillaries[138], transmigration across inflamed vessels requires integrin-mediated adhesion[135]. Interestingly, cutaneous viral infection[53] and tracheal bacterial infection[139] induces lymphatic capillary remodeling of naïve button-like junctions to tight, zipper-junctions, typically found in deeper collecting vessels. Similarly, forced zippering, through VEGF-A sig-

naling on intestinal lymphatic vessels called lacteals, prevented chylomicron uptake and protected against diet-induced obesity[119]. These reversible changes may generate a less permeable endothelium and thus determine the integrin dependence of cellular transport. The functional relevance of lymphocyte egress at steady-state, during inflammation and in tumors remains to be determined, and in particular whether lymphocytes exit tissue to mediate immune resolution or rather enter LNs for re-stimulation by professional APCs remains an open and interesting question.

IMMUNOSUPPRESSIVE FUNCTIONS OF LN RESIDENT LECS

Although a main function of lymphatic vessels is to be conduit and selective barrier for leukocyte trafficking during immune responses, LECs that comprise the LN are unique in that they also possess tolerogenic properties (Figure 1.2 D). Similar to thymic epithelium responsible for eliminating self-reactive T cells during lymphocyte development[44], LECs express peripheral tissue-restricted antigens (PTAs), albeit a different, AIRE-independent mechanism[110,140,141]. For example, LN resident LECs, and to a much lesser extent peripheral LECs in the diaphragm, express the mRNA for the melanocyte/melanoma-specific protein, tyrosinase[110]. Transfer of naive transgenic FH $CD8^+$ T cells, whose TCR is specific for the Tyr_{369} peptide presented on a human/mouse hybrid MHCI molecule, AAD (called Tyr^+ mice)[142], proliferate initially, express high levels of PD-1, and then get deleted in LNs[109,110,140]. This promotes tolerance to tyrosinase antigen that is lost with α-PD-L1 blockade or in chimeric mice lacking non-hematopoietic PD-L1[109]. Although it was not directly demonstrated that LECs are the cell responsible for deletion of tyr-specific T cells *in vivo* it is credited to them for a few reasons. First, LN resident LECs express several PTAs and they are the only LN stromal cell that expresses tyrosinase[110,140]. Second, LN resident LECs lack expression of proper costimulatory molecules (e.g. CD80 and CD86) and express high levels PD-L1[109], though other LN stromal populations also express PD-L1, but to a lesser extent[109]. Third, Tyr_{369}-pulsed LECs were the only LN stromal cell that induce FH $CD8^+$ T cell proliferation *ex vivo*[140]. Lastly, β-galactosidase (β-gal)-specific $CD8^+$ T cells are deleted in a PD-L1-dependent manner when transferred into mice who transgenically express β-gal under a lymphatic-specific

Prox-1 promoter[143]. It is assumed that this function of LECs is restricted to LN resident LECs, however, whether peripheral LECs have similar functions with effector T cells remains an interesting idea to be explored.

In addition to inducing $CD8^+$ T cell tolerance to PTAs[110,140], LECs also suppress non-self T cells. LECs in LNs, through a process called scavenging, take up exogenous antigens draining in LNs, and to a similar extent as cross-presenting DCs[144]. Presentation of antigen this way, and probably in combination with lack of proper costimulation[109], induces dysfunctional T cell activation marked by increased expression of exhaustion markers, decreased IFNγ and IL-2 production, and rapid apoptosis following proliferation[144,145]. This may be important for tolerance to peripheral antigens that are continually draining tissues during normal tissue turnover. However, LECs can cross present tumor-derived antigens and induce dysfunctional antitumor $CD8^+$ T cell responses[145]. While this presumably occurs through direct presentation of MHCI-restricted antigens directly to $CD8^+$ T cells, LECs can also indirectly inhibit T cell activation, independent of direct cell contact[146]. IFNγ and TNFα produced by recently activated T cells induces LEC nitric oxide synthase 2 (NOS2) upregulation and subsequent production of nitric oxide (NO) that feeds back and inhibits T cell proliferation *in vitro*[146]. Though LECs suppress naive $CD8^+$ T cells in LNs, whether they also scavenge and cross-present exogenous antigens to effector $CD8^+$ T cells and whether this has immunological consequences in the periphery is unknown.

Similar to their contribution to maintaining $CD8^+$ T cell tolerance, LN LECs are also able to suppress $CD4^+$ T cells too, albeit different mechanisms. LECs in LNs constitutiviely express MHCII, the MHC that interacts with $CD4^+$ T cells[109], and when pulsed with peptide, induce $CD4^+$ T cell proliferation *ex vivo*[143]. Although they express MHCII and upregulate it in response to IFNγ[147], they lack the machinery to process antigens and load them onto MHCII themselves[143], indicating that their ability to induce $CD4^+$ T cell tolerance must occur independent of their own ability to express and present PTAs on MHCII. Instead, they pass PTAs to DCs who present them to $CD4^+$ T cells and induce anergy[143], perhaps because DC adhesion to LECs leads to decreased costimulatory

molecule expression by DCs[148]. Interestingly, LECs can also acquire peptide-MHCII complexes (pMHCII) from DCs[147] and $CD4^+$ T cells preexposed to LECs that have DC-derived pMHCII complexes, fail to respond to restimulation after LEC coculture, indicating that LECs inhibit $CD4^+$ T cells[147]. Perhaps, LECs pass PTAs to DCs, who load them onto MHCII molecules and then pass them back to LECs, and together, they maintain CD4 tolerance, although this is only speculative. It is assumed that these interactions would occur in LNs of mice and thus are characteristics of LN resident, but not peripheral LECs, however, it was recently reported that DCs interact with T cells in afferent lymphatic vessels during skin inflammation[149], indicating the potential for all three cell types to interact together outside of secondary lymphoid organs. Whether LECs in peripheral tissues interact with DCs in these ways or posses any of these features to mediate local $CD8^+$ or $CD4^+$ effector T cell function and how these may be altered in the TME are interesting questions moving forward.

Vascular Endothelium as a Selective Barrier of Immunity

Inflamed endothelial cells provide signal two for tissue infiltration

Though activated effector and memory T cells acquire the machinery necessary for homing to inflamed tissue in response to TCR and inflammatory stimuli in circulation and lymphoid organs[150], they do not enter tissues haphazardly, rather, activated ECs that line post capillary venules in tissue provide the critical signal 2 necessary for infiltration. Lymphocytes home to sites of inflammation following a cascade of adhesive and signaling events mediated by sequential ligation and activation of selectins, integrins, and chemokines on ECs. EC activation and expression of these necessary adhesive molecules occurs only at sites of inflammation, thus ensuring specific infiltration of inflamed tissue[66] and sparing normal, uninflamed tissues from unnecessary lymphocyte infiltration, such that ECs act as key determinants for the anatomic tissue distribution of stimulated lymphocytes (Figure 1.3).

At steady-state, low levels of lymphocyte adhesion molecule expression[151,152] is main-

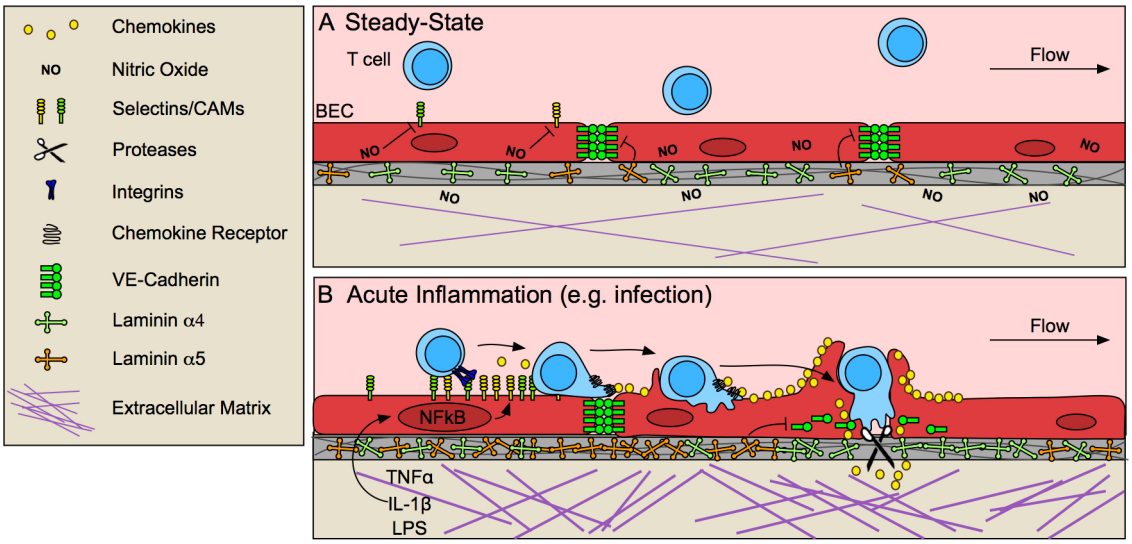

Figure 1.3: BECs control T cell entry into inflamed tissue (A) The vascular endothelium limits T cell infiltration at steady-state by low expression of selectins and cell adhesion molecules (CAMs), and stabilized endothelial cell-cell junctions, due in part to tonic nitric oxide (NO) signaling and laminin α5-mediated VE-cadherin stabilization. (B) In response to pathological challenge and inflammatory stimulus (e.g. TNFα, IL-1β, LPS), BECs (BECs) become activated and increase expression of selectins, CAMs and chemokines, which promote lymphocyte adhesion and migration to sites permissible for transmigration. In some cases, BECs form a transmigratory cup that provides a perpendicular scaffold to direct T cell transmigration. Inflammatory remodeling of the basement membrane contributes to lymphocyte access through destabilization of VE-cadherin at endothelial junctions and by generating low-density sites permissive to lymphocyte migration. Lane and Lund, *Frontiers in Immunology* 2018

tained by tonic NO signaling[153] and lack of inflammatory stimuli. In response to challenge, tissue-resident macrophages, mast cells, and damaged fibroblasts[154] produce tumor necrosis factor α (TNFα) and interleukin-1 (IL-1)[155,156], which are sufficient to activate local but not systemic ECs[157]. Activation of nuclear factor-κB (NF-κB) in ECs by these inflammatory stimuli upregulates P- and E-selectins, ICAM-1,VCAM-1, and chemokines, and EC-specific loss of NF-κB is sufficient to prevent lymphocyte infiltration into tissue[156]. Selectins bind to carbohydrate moieties on glycoproteins expressed by effector and memory T cells[150]. Selectin binding initiates T cell rolling along the inflamed endothelium[158], allowing for subsequent chemokine detection. Chemokines produced by ECs then direct actin-dependent spreading, polarization, and lateral migration of arrested lymphocytes across the endothelial surface, presumably to identify sites permissive to transmigration, marked by clustered cell adhesion molecule (CAM) expression. High-affinity adhesive interactions between ICAM-1 and VCAM-1 and their respective integrins (LFA-1/αLβ2 and VLA-4/α4β1 integrin) ultimately lead to lymphocyte arrest[155].

While the endothelium rapidly responds to inflammatory cues to recruit circulating lymphocytes, it may also inhibit T cell adhesion and migration under certain conditions. T

cells have decreased adhesion to inflamed ECs co-cultured with dermal fibroblasts, but not fibroblasts isolated from synovial joints of rheumatoid arthritis patients[159], indicating that fibroblasts help to maintain the endothelial barrier to lymphocyte infiltration in healthy tissue while their dysfunction may promote disease. PEPITEM, a small peptide released from adiponectin-stimulated B cells, binds to cadherin-15 on ECs and triggers production and release of sphingosine 1 phosphate (S1P), which reduces T cell trafficking across endothelium[160], and low expression of adiponectin receptor on B cells is associated with chronic lymphocyte infiltration in diseases such as type 1 diabetes, rheumatoid arthritis, and aging[160].

Upon adhesion to inflamed endothelium, lymphocytes next traverse through the endothelial barrier. Endothelial cells actively support and guide lymphocytes to sites permissive to transmigration while still maintaining barrier integrity via integrin-dependent mechanisms of actin remodeling[161]. At sites of transmigration, ICAM-1/LFA-1 and VCAM-1/VLA-4 clustering forms an immunological synapse-like interaction between ECs and T cells[162], concentrating adhesion molecules into a ring structure[163]. ECs often extend microvilli symmetrically around T cells to form a transmigratory cup[164] which further strengthens adhesion and provides a perpendicular scaffold to promote transmigration[162]. Ultimately, T cells pass through the endothelium in one of two ways, either between ECs at intercellular junctions (paracellular route), or directly through individual ECs (transcellular route). Transcellular migration seems to be initiated by invadosome-like protrusions on lymphocytes[165]. Paracellular migration, on the other hand, requires EC-mediated destabilization of vascular endothelial cadherin (VE-cadherin) at endothelial cell-cell junctions[166] and is further mediated by integrins, CAMs, and other adhesion molecules such as PECAM-1, JAM-1, and CD99[155].

Destabilization of VE-cadherin at EC cell-cell junctions seems to be necessary for lymphocyte transmigration[167]. ECs expressing a mutant form of VE-cadherin that is not endocytosed and therefore retained at cell-cell junctions, prevents lymphocyte recruitment to inflamed skin[166]. Blockade of VE-cadherin stabilizing integrins, $\beta 1$ and $\beta 3$[167] or dephosphorylation of tyrosine 731 by SHP-2 targets VE-cadherin for endocytosis and

subsequently increases neutrophil transmigration *in vitro*[168]. Interestingly, lymphocyte binding to ECs induces SHP-2-mediated VE-cadherin destabilization[168], indicating that lymphocyte adhesion may prime ECs to be permissive of transmigration. VE-cadherin is also cleaved by a disintegrin and metalloproteinase 10 (ADAM10) and tetrospanin 5 and 17, expressed by inflamed ECs, and EC-specific loss of ADAM-10 delays T cell, but not neutrophil or B cell, transmigration *in vitro*[169]. Interestingly, proteolytically active leukocytes, such as neutrophils, may mediate cleavage necessary for lymphocyte transmigration in the absence of EC proteolysis[169]. Thus, even if not intrinsically proteolytic, leukocyte protease activity may positively promote lymphocyte transmigration across inflamed endothelium *in vivo*.

ANTIGEN-DEPENDENCE OF T CELL RECRUITMENT AND EXTRAVASATION

Peripheral effector[66] and memory T cells[170] are recruited to inflamed tissue in an antigen-independent manner, indicating that local presentation of cognate antigen is not necessary for tissue infiltration. The antigen-independence of T cell recruitment is exemplified by recent studies that demonstrate abundant bystander, pathogen-specific T cells, in solid tumors[171]. Interestingly, however, homing of insulin-specific $CD8^+$ T cells to pancreatic islets, but not other tissues, is reduced with loss of major histocompatibility complex class I (MHC-I) *in vivo*[172] and antigen-loaded MHC-I presented on lumenal surfaces of the blood-brain barrier was functionally required for antigen-specific T cell trafficking to the brain[173]. These observations have led to the hypothesis that antigen presentation by ECs may amplify antigen-specific T cell recruitment in certain tissues and disease states. ECs dynamically express MHC-I and MHC-II during inflammatory processes and possess antigen-processing machinery necessary for cross-presentation of exogenous antigens[174]. Human ECs scavenge and cross-present the type I diabetes islet autoantigen GAD65 on MHC-II and this enhances the transmigration of antigen-specific T cells *in vitro*[175]. Further *in vitro* evidence supports both inhibitory[176] and promotional[177,178] roles for EC antigen presentation in lymphocyte trafficking, indicating that antigen presented by ECs may provide context dependent go or stop signals that tune T cell infiltration.

Interestingly, ECs express a variety of T cell costimulatory and coinhibitory molecules[162],

and as such, may represent semi-professional APCs strategically placed to interact with activated effector and memory T cell populations. In addition to tuning transmigration, data from various tissues indicate that ECs may employ their repertoire of immune checkpoints and APC-like function to mediate peripheral tolerance and modify T cell behavior as they transmigrate or arrest at the vascular interface. For example, liver sinusoidal endothelial cells scavenge and cross-present food-borne antigens and induce tolerance through T cell adhesion and sequestration in the liver[179,180], and tumor-associated LECs cross-present exogenous antigens[144,145] and maintain peripheral tolerance to self-antigens in LNs[109,140] dependent on constitutive expression of PD-L1[109]. The relative significance of EC antigen presentation *in vivo*, however, is likely both tissue and disease specific. Further testing using EC-specific knockdown strategies is needed to determine the functional relevance of EC antigen-processing and presentation *in vivo*.

OVERCOMING THE BASEMENT MEMBRANE

The final, and rate-limiting step in lymphocyte extravasation is crossing the basement membrane[181]. The basement membrane is a 20-200nm thick dense proteinaceous substrate composed of laminins, collagen type IV, and sulfated proteoglycans[182], that separates the vascular endothelium from extracellular matrix (ECM) in the tissue parenchyma. Laminins and collagen IV produced by ECs self-assemble into a dense sheet that is crosslinked by perlecans and nidogen and contains 2-5 μm-in-diameter pore-like regions of low protein density[183], presumed sites of lymphocyte passage. Basement membrane composition differs between developmental stage, vessel type, and activation state of the endothelium[182], with particular variability of laminin isoforms. Laminins are composed of alpha, beta, and gamma chains (e.g. laminin α4, β1, γ1 is denoted as laminin 411), and presence in basement membrane is context and location dependent. In the central nervous system (CNS), laminin α4 is ubiquitous[184], while laminin α5 expression is patchy and irregular[185], but both are increased upon inflammation[182,186]. In murine EAE extravasation occurs predominantly at sites of low laminin α5 density[167,186] and laminin α5 is sufficient to inhibit T cell transmigration in a dose-dependent manner *in vitro*[185]. Additionally, laminin α4-deficient mice increase expression of laminin α5 in the CNS leading

to decreased T cell migration across the blood brain barrier in EAE[185], suggesting that the composition of laminins in the basement membrane may selectively regulate T cell transmigration.

The mechanisms by which different laminin isoforms regulate T cell transmigration are unclear. Laminin $\alpha 5$ binds to integrin $\beta 1$ and $\beta 3$ on ECs and stabilizes VE-cadherin at EC junctions[167]. However, activated lymphocytes also express integrin $\beta 1$[155], and it is possible that laminin $\alpha 5$ may signal directly to infiltrating lymphocytes and instruct transmigration, although this has not been investigated. Regardless of how T cells get across the EC layer, the basement membrane is a dense, proteinaceous barrier that they must penetrate to complete diapedesis. Neutrophils express elastase to remodel regions of low basement membrane density allowing for their tissue infiltration[187], however, the specific mechanisms of lymphocyte migration through the basement membrane is unclear. The small size and pliability of lymphocytes and their nuclei may permit movement through the 2-5 μm pore-like regions of the basement membrane. However, T cell intrinsic loss of granzyme B (GrzB), which degrades both collagenous and non-collagenous ECMs[188,189], reduces extravasation *in vivo*[189], indicating proteolysis may be required for basement membrane penetration. Further studies are needed to evaluate the contribution of the basement membrane to selective lymphocyte extravasation in acute and chronically inflamed tissues, and in tumors.

Types of Immune landscapes in TME

Current efforts to define biomarkers that are predictive of response to immune checkpoint blockade reveal an array of factors from myeloid cells to the microbiome, that affect patient response. Multiple studies across tumor types now indicate that the presence of T cells within tumor nests is predictive of response to therapy[190]. As a consequence, non-responding tumors typically exhibit T cell infiltrates that are described by three main patterns: (1) non-functional immune responses, possessing an intratumoral but seemingly ineffective infiltrate; (2) tissue excluded T cell infiltrates, possessing a T cell infiltrate that is restricted to the tumor periphery; and (3) immunological deserts, completely lacking T

cell infiltrate both in the tumor nests and in adjacent stroma[108]. The underlying biology that regulates these patterns of T cell infiltration is clearly multifactorial – some of the contributing factors from the perspective of the blood and lymphatic endothelium are discussed below (Figure 1.4).

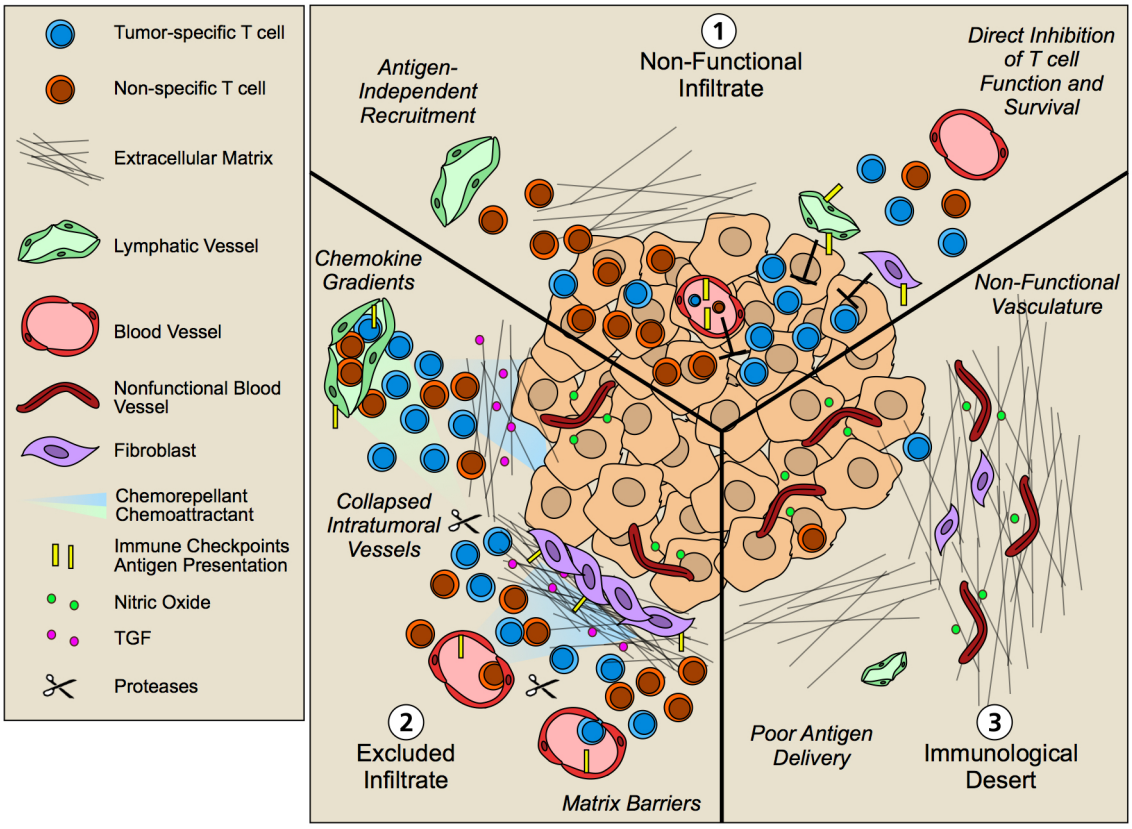

Figure 1.4: Non-hematopoietic cell contribution to the tumor immune landscapes The geographic distribution of T cells within intratumoral and peritumoral regions is both predictive of overall survival and response to immunotherapy. Patients that fail to respond to immunotherapy often exhibit three patterns of T cell infiltrate that are governed by an array of mechanisms including contributions from the tumor cells and infiltrating hematopoietic cells. Non-hematopoetic cells, however, additionally contribute to the infiltration, retention, and function of T lymphocytes in TMEs. (1) Non-functional infiltrate: possessing an intratumoral but seemingly ineffective infiltrate. Antigen-independent recruitment of both effector and memory T cells subsets by vascular endothelium generates a diverse repertoire of T cells both relevant and irrelevant for tumor killing. Upon tissue entry, non-hematopoietic cells further exert multiple mechanisms of immune suppression, including expression of immune checkpoints such as PD-L1 and FasL that limit local T cell function. (2) Excluded infiltrate: possessing a T cell infiltrate that is restricted to the tumor periphery. Establishment of matrix barriers, collapsed intratumoral vessels, poor expression of adhesion molecules, and collaborating chemoattractant and chemorepellant gradients likely all contribute to the exclusion of T cells at the periphery of tumor nests such that inhibition of these features may improve infiltration. (3) Immunological desert: Completely lacking a T cell infiltrate in both tumor nests and stroma. Impaired lymphatic transport may result in poor antigen delivery to LNs and thus poor priming. However, even in the presence of an activated systemic T cell pool, non-functional vessels driven by the angiogenic and desmoplastic TME may prevent local infiltration leading to lesion-specific differences in immune infiltrates. Lane and Lund, *Frontiers in Immunology* 2018

NONFUNCTIONAL T CELL INFILTRATE

Non-functional immune infiltrates[108], refers to tumors containing intratumoral lymphocytes in both pre- and post-therapy biopsies that do not contribute to significant clinical response. Importantly, methods to evaluate intratumoral T cell populations largely quantify changes in bulk T cell populations (CD4 or CD8), and even when enriched for markers

of previous antigen exposure (CD45RO) or effector function (GrzB) likely still quantify a heterogenous pool of effector, central memory, and exhausted T cells that represent a range of antigen specificities both relevant and irrelevant to the tumor. Rapid recruitment of effector and memory T cells is antigen-independent[66,170], and bystander, viral-specific T cells (e.g. HCMV or EBV-specific) are abundant in human tumor tissue[171]. Thus, efforts to specifically quantify tumor-reactive T cell clones may be more predictive than bulk T cell populations. Consistent with this hypothesis, CD39 was recently identified as a marker to distinguish tumor antigen-specific $CD8^+$ T cells from bystander T cells across multiple tumor types[171,191] and stratification of patients based on frequency of $CD39^+CD103^+$ double positive $CD8^+$ T cells associated with increased overall survival in head and neck cancer patients[191]. Thus, because of the promiscuity of T cell infiltration across the vascular endothelium, the presence of bulk T cells in TMEs may be insufficient to indicate response. Even when tumors are well infiltrated with antigen-specific T cells, however, multiple additional mechanisms suppress their local effector function mediated by tumor, hematopoietic[192], and non-hematopoietic stromal cells.

Aberrant tumor angiogenesis and disrupted fluid flows in TMEs generate hypoxia and increased interstitial fluid pressures in solid tumors[46,114] that influence T cell function. Hypoxia induces Warburg effect by cancer cells, leading to increased acidification and lactate production, both of which inhibit cytotoxic activity of lymphocytes *in vivo*[193,194]. Furthermore, increased interstitial fluid flow in the TME activates fibroblasts leading to TGF-β production[114] and ECM contraction. ECM contraction together with shear stress activates stromal stores of latent TGF-β[195], which attenuates $CD8^+$ T cell cytotoxicity[196] making them nonresponsive to TCR signaling[197]. Thus the disrupted fluid mechanics within tumor tissue may itself participate in the regulation of local T cell function.

Furthermore, non-hematopoietic cells likely exert direct effects on T cells within TMEs. As discussed previously, LECs in LNs display specific immunological properties that function to maintain peripheral tolerance at steady state, and while we have drawn parallels between the structural role of LN stromal cells and non-hematopoietic cells in peripheral, non-lymphoid tissues, it remains less clear whether peripheral non-

hematopoietic cells also acquire immunomodulatory properties characteristic of LN stroma. In tumors LECs are also capable of scavenging tumor-associated antigens and cross-presenting them on MHC-I[145], however, whether LEC antigen presentation functionally contributes to T cell responses in the periphery remains unknown. Thus, tumors may coopt normal non-hematopoietic-based mechanisms of tissue protection for immune escape.

EXCLUDED T CELL INFILTRATE

T cell exclusion, in which T cells are absent from tumor nests and rather retained in adjacent, surrounding stroma[108,198] is a significant barrier to response to therapy. One leading hypothesis is that tissue desmoplasia, the aberrant synthesis, alignment, and crosslinking of ECM proteins by fibroblasts in TMEs[199,200], creates a physical barrier that prevents T cell invasion. Pancreatic ductal adenocarcinoma (PDAC) is particularly fibrotic and breast carcinomas exhibit stiff collagen fibers in parallel alignment tangential to tumor borders that correlate with poor prognosis[201,202]. Furthermore, dynamic intravital imaging reveals T cell migration along collagen fibers and vessels in tumors[203,204], consistent with their preferred amoeboid-like mode of migration described in non-malignant matrices. Thus it has been proposed that the orientation and density of matrix fibers prevents T cell infiltration into tumor parenchyma[203].

In addition to the effects of desmoplasia on T cell exclusion, angiogenic growth factors such as vascular endothelial growth factor A (VEGF-A), angiopoietin, basic fibroblast growth factor (bFGF), and endothelin-1[205,206] attenuate inflammatory-mediated endothelial activation and thus intratumoral vessels exhibit reduced expression of adhesion molecules that would mediate lymphocyte extravasation, such as ICAM, VCAM, and E-selectin[207,208]. For example, bFGF inhibits TNFα/IL-1α-mediated expression of ICAM, VCAM, and E-selectin *in vitro*[209], and VEGF-A disrupts their clustering, therefore decreasing T cell adhesion to ECs[152]. Endothelin signaling on ECs increases NO production and subsequent downregulation of adhesion molecules, thus blockade of the receptor increases T cell adhesion and infiltration into tumors[208]. Angiogenic signaling from tumor cells also induces FasL expression on tumor associated ECs that limits tumor infiltrating

$CD8^+$ T cells, presumably through direct killing as demonstrated *in vitro*[210,211]. Consequently, factors that drive the angiogenic switch in tumors simultaneously establishes immunological barriers to limit immune surveillance and facilitates immune escape.

While anti-angiogenic therapy focused on destruction of tumor-associated vessels largely failed in most solid tumor types, adaptation of these strategies utilizing lower, normalizing doses to restore perfusion and adhesion molecule expression has proved more productive[212]. Dual angiopoietin and VEGF-A blockade leads to increased T cell accumulation and function in several tumor models and synergizes with anti-PD-1 therapy[91]. Furthermore, combination of anti-VEGFR2 and anti-PD-L1 antibodies induced lymphotoxin-dependent emergence of high endothelial venule-like vessels[213], which were necessary for response and are associated with better overall outcome in patients[214,215]. Interestingly, in mouse models, responders to immune checkpoint blockade exhibited rapid reperfusion of intratumoral vessels indicating that intratumoral vascular function may be required for T cell effector function and additionally that checkpoint blockade may directly affect endothelial cells[216]. Thus, normalizing the angiogenic tumor vasculature may improve local T cell recruitment generating microenvironments primed to be responsive to immunotherapy. Interestingly, poorly adhesive, angiogenic vessels appear to be largely restricted to intratumoral regions, where they exhibit reduced adhesive properties and elevated expression of immune checkpoints[208]. While this geographic vessel heterogeneity may limit infiltration directly into the tumor proper, it still allows infiltration into adjacent stroma perhaps contributing to the dense rings of $CD8^+$ T cells observed around tumor nests.

Additionally, antitumor effector and memory T cells restricted to peritumoral stroma may be unable to locate target tumor cells due to disrupted chemokine signals. High expression of the T cell attracting chemokines CXCL9, CXCL10, CXCL12, and CCL5 correlates positively with $CD8^+$ T cell infiltration across several tumor types[217–219], indicating that if the tumors express the proper chemokines, T cells can get there. Chemokines, however, can be post-translationally modified by proteolytic cleavage, glycosylation, nitration, or deamination which results in dramatically altered activity[198]. For example,

when CCL2 is nitrated by reactive nitrogen species in the TME T cell infiltration into tumors is hindered and rather, remain excluded from the tumor mass[220]. In addition to the absence of chemoattractants, secretion of chemokines that serve as chemorepellants may protect tumor nests from T cell infiltration. In a mouse model of PDAC, fibroblast activating protein (FAP)-expressing CAFs produce CXCL12 that coats tumor cells and prevents $CXCR4^+$ $CD8^+$ T cells from infiltrating tumor nests and controlling the tumor[221]. Administration of AMD3100 (CXCR4 inhibitor) increased T cell infiltration into tumor nests, and synergized with α-PD-L1 therapy to reduce tumor growth[221]. Thus competing chemokine gradients, initiated and maintained by multiple cell types within the TME, determine lymphocyte positioning and subsequent function.

IMMUNOLOGICAL DESERT

Finally, immunological deserts are defined as those TMEs completely lacking T cell infiltrates within tumor nests and in adjacent stroma. Low somatic mutational burden and tumor immunogenicity is likely a significant driver of failed T cell responses in these tumors. However, even in the presence of immunogenic epitopes, lymphatic transport and poor DC migration may limit anti-tumor T cell priming in lymphoid organs and thus prevent systemic T cell expansion. In fact, tumors induced or implanted in mice lacking dermal lymphatic vessels fail to activate and accumulate anti-tumor T cell responses[55,222] and lymphatic vessel density correlates with T cell infiltration in colorectal cancer and melanoma patients[223,224]. Conversely, overexpression of lymphangiogenic growth factors enhances intratumoral inflammation and response to various immunotherapies[145,225], indicating that lymphatic transport plays an important role in both adaptive immune priming and setting up an inflammatory TME. Thus, the non-hematopoietic stroma may dictate the systemic expansion of anti-tumor immunity and thereby restrict the pool of T cells available for tumor recruitment. Still, downstream of T cell priming, analysis of T cells in synchronous metastases reveals heterogeneous distribution of the existing systemic repertoire[226] indicating additional mechanisms of control. Furthermore, even in the absence of *de novo*, tumor-specific T cell priming, recruitment of pre-existing memory populations should lead to intratumoral accumulation of T cells. Thus, additional factors must limit

extravasation and tumor residence of bulk T cell populations. Tissue-specific vascular heterogeneity or dysfunction (stromal and intratumoral) may limit T cell infiltration in a lesion-specific manner and thus contribute to immunological deserts in some and not all metastatic lesions.

Chapter 2:

IFNγ-Activated Dermal Lymphatic Vessels Inhibit Cytotoxic T cells in Melanoma and Inflamed Skin

Published manuscript:

R. S. Lane, J. Femel, A. P. Breazeale, C. P. Loo, G. Thibault, A. Kaempf, M. Mori, T. Tsujikawa, Y. H. Chang, and A. W. Lund. "IFNγ-activated dermal lymphatic vessels inhibit cytotoxic t cell in melanoma and inflamed skin." *Journal of Experimental Medicine*, 2018.

Introduction

Lymphatic vessels compose a hierarchical vasculature that facilitates the unidirectional transport of fluid, and cells from peripheral, blind-ended capillaries through collecting vessels to lymphatic sinuses in secondary lymphoid organs[117]. Lymphatic vessels transport antigen and dendritic cells (DC) to lymph nodes (LN) to prime naïve T cells following peripheral tissue viral infection[53,57,58], and remain the main route of DC migration and *de novo* immune priming in tumors[54,55]. Consistent with the role for lymphatic vessels in *de novo* adaptive immunity, lymphatic vessel density (LVD) in primary tumors of colorectal patients positively correlates with intratumoral $CD8^+$ T cell infiltrates[223,224], and similarly work in mouse models demonstrates a causal relationship between tumor-associated lymphangiogenesis and intratumoral inflammation[55,145,222,225] leading to improved response to immunotherapy[225]. Thus, lymphatic transport shapes inflammatory and immune microenvironments in solid tumors[227].

Rather than acting as passive conduits, however, lymphatic capillaries are responsive to their inflamed tissue microenvironment[131] and remodeled in infected, inflamed, and

neoplastic tissue[115]. In infected skin, type I Interferon (IFN) remodels lymphatic capillaries and rapidly shuts down fluid transport leading to viral sequestration[53]; sustained inflammation following *Yersinia pseudotuberculosis* infection induces collecting lymphatic vessel leakage leading to insufficient DC migration to LNs and poor immunity[228]; and lymphatic transport is elevated from tumors early, prior to metastatic seeding[229], but decreases with tumor progression[230]. Furthermore, lymphatic endothelial cells (LEC) are activated by inflammatory cytokines and elevated interstitial fluid flows, increasing expression of chemokines and adhesion molecules necessary for DC trafficking[133,135]. Consequently, peripheral lymphatic capillaries tune their transport function (fluid and cellular) in response to inflammatory cues with functional consequences for tissue inflammation and immunity.

Interestingly, beyond their bulk transport properties, LECs that compose lymphatic sinuses in LNs exhibit unique, intrinsic immunological activity that can both facilitate and suppress adaptive immune responses. In vaccine models, LN LECs scavenge and archive antigen to support future memory responses[231], while in tumor draining LNs, LECs, rather, cross-present scavenged tumor antigens leading to dysfunctional T cell priming[144,145]. Furthermore, at steady state, LECs constitutively express the co-inhibitory molecule programmed death-ligand 1 (PD-L1) and maintain $CD8^+$ T cell tolerance through Aire-independent, promiscuous expression of peripheral tissue antigens[109,140], and inhibit T cell proliferation through production of nitric oxide[146]. Thus, LN LECs are thought to be critical players in the maintenance of peripheral tolerance to self-antigen specifically within the unique microenvironment of LNs at steady state[109,110,140,143,146]. Whether the LECs that compose lymphatic capillaries in peripheral, non-lymphoid tissues acquire similar functionality, however, is unclear. Two reports indicate that tissue inflammation induces PD-L1 expression on LECs in skin[131] and orthotopic, implanted tumors[111], suggesting that peripheral LECs may acquire similar immunological function. The functional relevance of peripheral LEC PD-L1 expression *in vivo*, however, remains unknown.

Tumors employ multiple mechanisms to evade host immunity including the expression of co-inhibitory molecules, such as PD-L1, that limit T cell effector function in tumor

microenvironments. Melanoma exhibits robust responses to immune checkpoint blockade as a result of significant CTL infiltrates that secrete IFNγ and activate expression of PD-L1 in tumors[232]. This phenomenon, termed adaptive immune resistance[71], protects tumor cells from CTL-mediated killing through PD-L1-dependent inhibition of T cell receptor (TCR) signaling[73]. In addition to PD-L1 expression by tumor cells, however, recent work highlights the role of host hematopoietic cells in PD-L1-dependent T cell exhaustion in mouse[90,107] and human studies[108], indicating that tumor microenvironments contribute to CTL exhaustion. Importantly, in non-malignant settings expression of PD-L1 by host cells serves to protect tissue from excessive immune-mediated damage and mediate return to homeostasis[76,92] and non-hematopoietic cells play a key tissue-protective role in chronic inflammation[97] and chronic viral infection[76,92]. The functional significance of a non-hematopoietic PD-L1 source in tumors, however, has not been demonstrated.

Herein we demonstrate that peripheral lymphatic vessels are exquisite sensors of interstitial IFNγ in tumor and inflamed microenvironments, and initiate immune suppressive programs that functionally limit the further accumulation of CTLs. At least one component of this response is expression of PD-L1 and we demonstrate that non-hematopoietic cells contribute to local, PD-L1-dependent, effector $CD8^+$ T cell control. Importantly, we demonstrate that when lacking IFNγR, peripheral lymphatic vessels fail to express PD-L1 in response to CTL infiltration and as a consequence CTL function in tumor microenvironments is improved. Thus, using both acute cutaneous viral models and multiple tumor models, we demonstrate that lymphatic vessels balance protective $CD8^+$ effector T cell immunity and immunopathology and identify the tumor-associated lymphatic vasculature as a critical component of tumor microenvironment-mediated control of effector, anti-tumor immunity.

Results

Non-hematopoietic PD-L1 limits the accumulation of cytotoxic $CD8^+$ T cells in melanoma

Immune checkpoint blockade, including antibodies targeted against PD-L1, is achieving unprecedented clinical responses[108,233,234]. The toxicity associated with treatments,

however, necessitates the identification of predictive biomarkers that would target a patient population most likely to respond. Though patients with PD-L1^{pos} tumor cells are enriched for responders, PD-L1^{neg} patients also respond[41,235], indicating that additional cellular players and potentially other anatomical locations contribute to patient response and should be explored further. Recent work highlights the role of host, and in particular hematopoietic, PD-L1 expression in tumor-associated T cell exhaustion in mice[90,107], and stratification of patient response in humans[108]; however, whether non-hematopoietic, non-tumor sources of PD-L1 additionally contribute to intratumoral mechanisms of T cell control remains unexplored. Importantly, non-hematopoietic expression of PD-L1 contributes to immunopathology during chronic viral infection[76] and DSS-induced colitis[97], and PD-L1 expression by LN LECs maintains peripheral tolerance at steady state[109]. We therefore asked whether PD-L1 expressed by non-tumor, non-hematopoietic stromal cells functionally inhibits CD8$^+$ T cell responses within tumor microenvironments. To ask this question we generated PD-L1$^{-/-}$ bone marrow chimeras by lethal irradiation of WT or PD-L1$^{-/-}$ mice and reconstitution with either WT or PD-L1$^{-/-}$ bon marrow (reconstitution >80%, Figure 2.1A). B16F10 tumors were implanted in reconstituted mice and analyzed at endpoint. While there was no significant change in tumor growth compared to controls (Figure 2.1B), consistent with the poor sensitivity of B16F10 tumors to single agent PD-L1 blockade[236], both hematopoietic and non-hematopoietic chimeras accumulated more activated CD44$^+$ CD8$^+$ T cells (Figure 2.1C), with increased expression of the effector molecule PD-1 (Figure 2.1D) and the core-2 O-linked glycosylation motif required for effector trafficking (1B11, Figure 2.1E)[237], demonstrating that PD-L1 expressed by both tumor-infiltrating leukocytes and, tumor-resident, non-hematopoietic stromal cells limits effector CD8$^+$ T cell-accumulation in tumor microenvironments.

Importantly, however, CD8$^+$ T cells in tDLNs (Figure 2.2A & B) and spleens (Figure 2.1F & G) exhibited a more activated phenotype with elevated PD-1 and 1B11 in hematopoietic, but not non-hematopoietic chimeras, indicating that some of the intratumoral effect observed in hematopoietic chimeras may result from recruitment of activated systemic populations rather than release of intratumoral immune suppression. Consistent

with these data and a role for hematopoietic PD-L1 in priming[76], CD103$^+$ migratory and CD8α^+ resident cross-presenting DCs expressed higher levels of PD-L1 in tDLNs as compared to contralateral, non-draining controls (Figure 2.2C), while no change was observed in constitutive expression by non-hematopoietic LN stromal cells (Figure 2.2D). Thus, to specifically determine the relative contribution of non-hematopoietic and hematopoietic PD-L1 within tumor microenvironments, independent of expanded systemic pools, we transferred *ex vivo* activated (CD44$^+$PD-1$^+$), effector OT-I TCR-Tg CD8$^+$ T cells whose TCR is MHC class-I restricted to the immunodominant peptide (H2K^b-OVA$_{257\text{-}264}$) of ovalbumin (OVA), into tumor-bearing chimeras. Increased B16F10.OVA tumor control was observed following adoptive transfer in both chimeras (Figure 2.1H & I), indicating that both hematopoietic and non-hematopoietic PD-L1 limits T cell-mediated tumor control locally.

Given the poor responsiveness of the B16F10 model to single agent PD-L1 therapy, we sought to confirm the role of non-hematopoietic cells in a PD-L1 sensitive murine melanoma model. YUMM1.7 cells were generated from genetically engineered murine melanomas (*Braf^{V600E};Pten$^{-/-}$;Cdkn2a$^{-/-}$*) and subsequently treated with three rounds of UVB radiation to generate YUMMER1.7 cells that exhibit increased somatic mutation burden, sensitivity to single agent immune checkpoint blockade[238,239], and regress in PD-L1$^{-/-}$ mice (Figure 2.2E). We implanted YUMMER1.7 cells into wildtype and non-hematopoietic PD-L1 chimeras to determine whether loss of stromal non-hematopoietic PD-L1 was sufficient to increase tumor control. While YUMMER1.7 tumors grew out in W-W mice, tumors entered stasis 10 days post implantation in mice lacking non-hematopoietic PD-L1 (Figure 2.1J). Interestingly, since tumors regress in full PD-L1$^{-/-}$ mice (Figure 2.2E), these are consistent with the hypothesis of synergistic, or at least additive effects of hematopoietic and non-hematopoietic PD-L1 in mediating intratumoral T cell exhaustion. As such, in addition to the known role for hematopoietic PD-L1[90,107], PD-L1 expression by non-hematopoietic stromal cells contributes to functional suppression of CD8$^+$ T cell accumulation within tumor microenvironments and subsequent tumor control. Furthermore, these data taken together indicate that the functional relevance of

non-hematopoietic PD-L1 expression is revealed in the presence of potent, anti-tumor immunity.

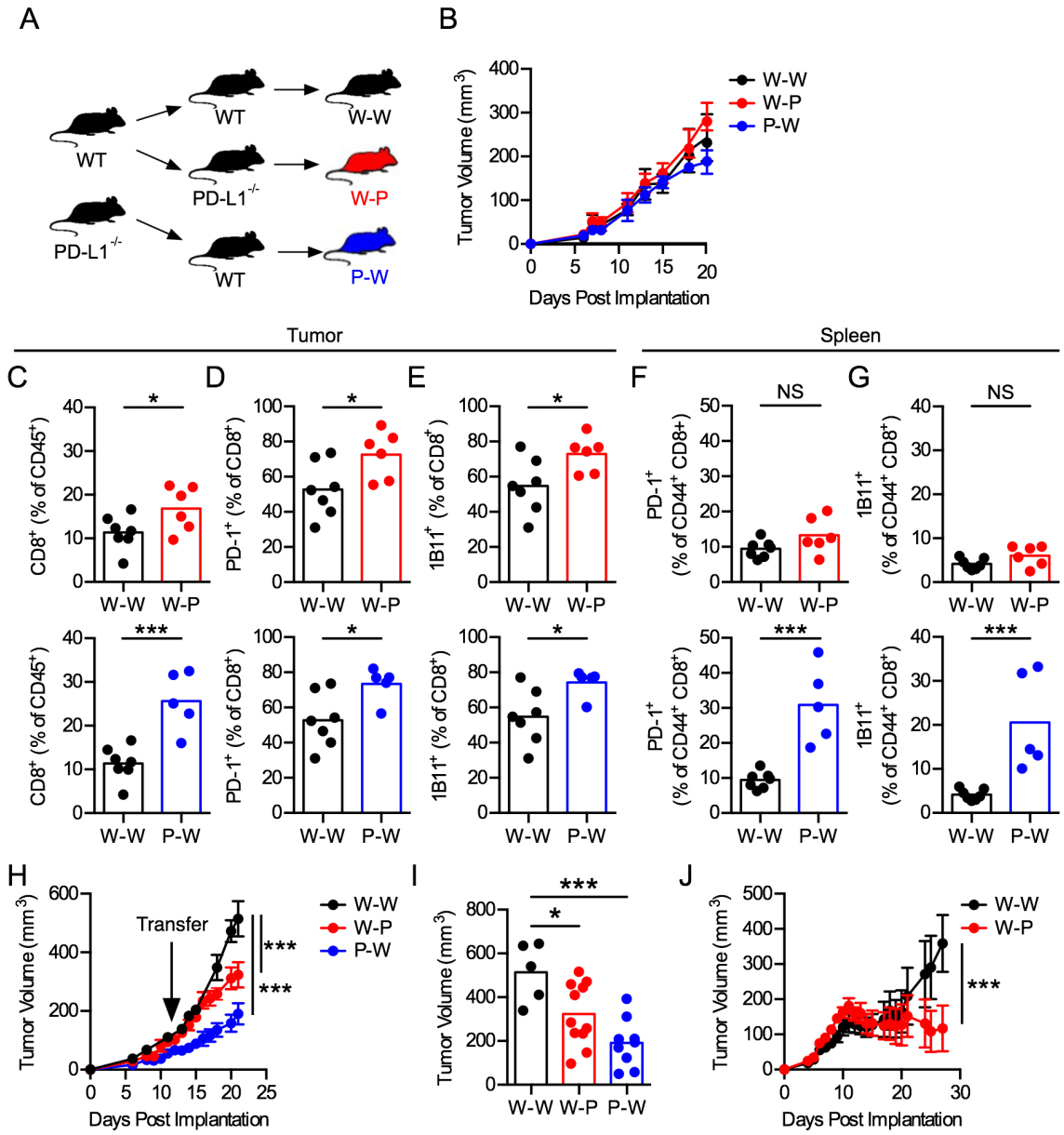

Figure 2.1: Non-hematopoietic expression of PD-L1 in peripheral tumors limits local cytotoxic T cell function. (A) Lethally irradiated WT or PD-L1$^{-/-}$ mice were reconstituted with WT or PD-L1$^{-/-}$ bone marrow generating WT into WT (W-W, black, controls), WT into PD-L1$^{-/-}$ (W-P, red, non-hematopoietic PD-L1$^{-/-}$), and PD-L1$^{-/-}$ into WT (P-W, blue, hematopoietic PD-L1$^{-/-}$) chimeric mice. (B) B16F10.OVA tumor growth in PD-L1$^{-/-}$ bone marrow chimeric mice. Average tumor volume ± SEM, n>8. (C-G) W-P (top) or P-W (bottom) PD-L1$^{-/-}$ chimeras compared to W-W controls. (C) Intratumoral CD8$^+$ T cells (%CD45). (D & E) PD-1 (D) and 1B11 (E) expression by intratumoral CD8$^+$ T cells. (F & G) PD-1 (F) and 1B11 (G) expression by CD8$^+$ T cells in spleens. (H & I) In vivo generated effector OT-I TCR-tg CD8$^+$ T cells were transferred into B16F10.OVA-tumor bearing PD-L1 chimeric mice. Tumor growth (H) and final volume (I) of PD-L1$^{-/-}$ chimeric mice. Average tumor volume ± SEM, n≥ 5. (J) YUMMER1.7 tumor growth in W-W and W-P PD-L1$^{-/-}$ chimeric mice. Average tumor volume ± SEM, n=5. Each point represents one mouse, bars indicate the mean. One-way ANOVA corrected for multiple comparisons (C-I). One-way ANOVA corrected for multiple comparisons (B, H and I) or students T test (J) performed on average slope and variance of individual tumor growth curves. $*p<0.05$, $***p<0.001$.

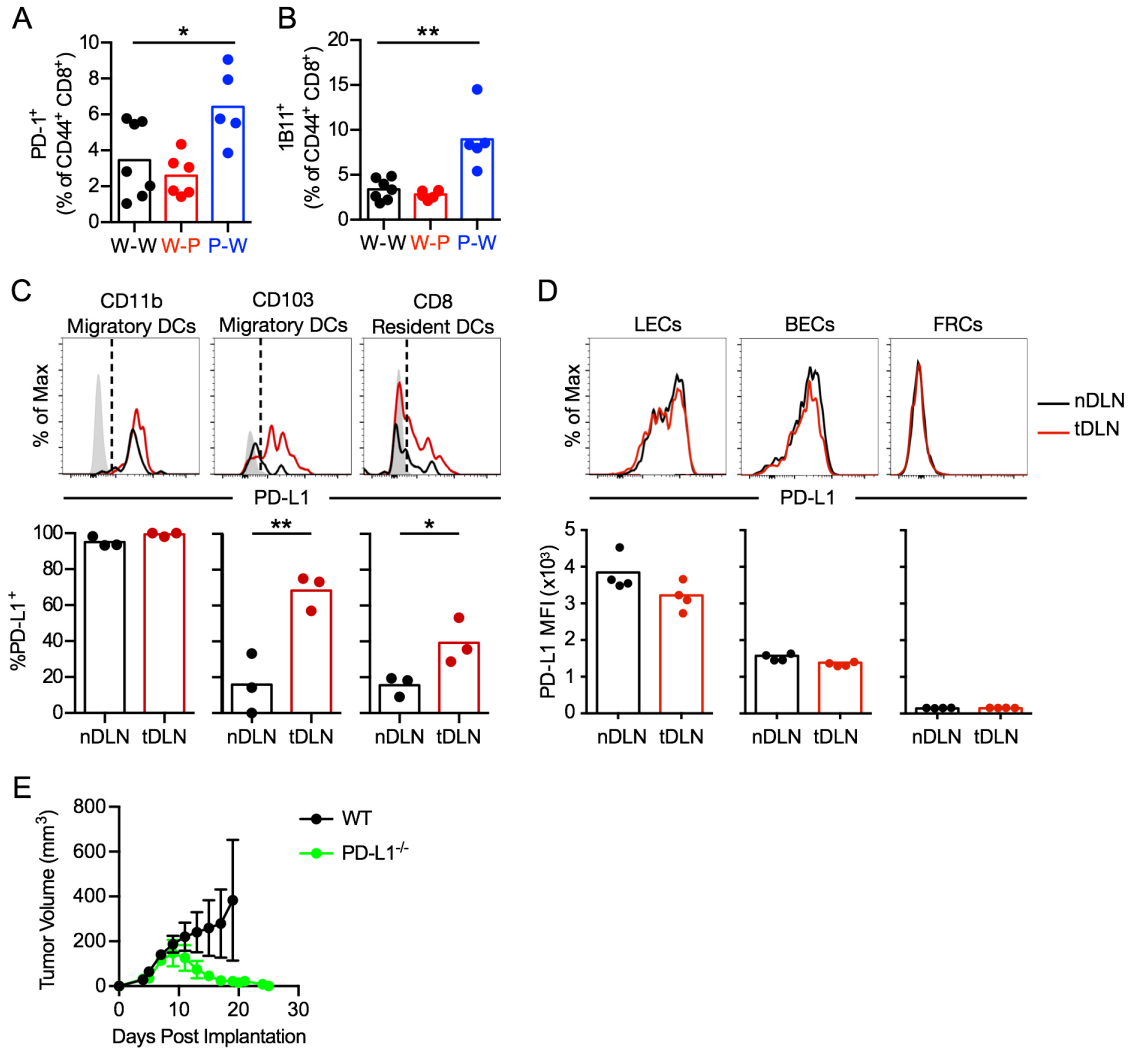

Figure 2.2: Hematopoietic, but not non-hematopoietic PD-L1 mediates peripheral expansion of CD8⁺ T cells following tumor implantation. (A & B) PD-1 (A) and 1B11 (B) expression by CD8⁺ T cells in B16F10.OVA tumor draining lymph nodes of PD-L1$^{-/-}$ bone marrow chimeric mice. (C & D) Representative histograms (top) and quantification (bottom) of PD-L1 expression by migratory and resident dendritic cells (C), CD11c⁺MHCIIhiCD11b⁺, CD11c⁺MHCIIhiCD11b-CD103⁺, CD11c⁺MHCII^{int}CD8α⁺; and non-hematopoietic stromal cells (D), CD45⁻CD31⁺gp38⁺ LECs, CD45⁻CD31⁺gp38⁺ BECS, and CD45⁻CD31⁻gp38⁺ fibroblastic reticular cells (FRC) cells in tumor draining (tDLN) and non-draining lymph nodes (nDLN). Each point represents one mouse, and bars indicate the mean. (E) YUMMER 1.7 Tumor growth in WT (black) and PD-L1$^{-/-}$ (green) mice. Shaded histogram represents isotype staining control. One-way ANOVA corrected for multiple comparisons (A & B). Students t-test (C-E) $*p<0.05$, $**p<0.01$

Lymphatic and blood endothelial cells express PD-L1 in primary murine melanomas and inflamed skin

Given the functional significance of the non-hematopoietic stroma in PD-L1-mediated T cell suppression, we investigated non-hematopoietic PD-L1 expression in various tumor microenvironments. We generated single cell suspensions from naïve skin, B16F10, MC38, YUMM1.7, and YUMMER1.7 tumors and identified CD45⁻CD31⁺ tumor-associated LECs (gp38⁺), blood endothelial cells (BECs; gp38⁻), and a CD45⁻CD31⁻gp38⁺ stromal population by flow cytometry (Figure 2.3A). Tumor-associated LECs (Figure 2.3B) and BECs (Figure 2.3C) were the highest PD-L1 expressers across tumor models, while

gp38$^+$ stromal cells (Figure 2.3D) were largely negative with the exception of YUMMER1.7 tumors. Interestingly, BECs constitutively express PD-L1 in skin, while LEC expression was dependent upon tumor context and demonstrated variable expression as a function of their local microenvironment (Figure 2.3B & C). Notably, highest expression for all cell types was observed in PD-L1-sensitive YUMMER1.7 tumors. We next asked whether PD-L1 expression by LECs was unique to tumors or rather a tissue-based response to local inflammation. Using three different models of cutaneous inflammation, cutaneous infection with Vaccinia Virus (VacV, scarification), delayed-type hypersensitivity (DTH, DNFB sensitization), and imiquimod-induced psoriasis, we evaluated LEC PD-L1 expression at sites local and distal to inflammatory challenge. In all models, inflammation enhanced expression of PD-L1 by LECs in affected (Figure 2.3E), but not contralateral (Figure 2.4A) skin as compared to naïve, while BECs upregulate PD-L1 at both sites of challenge and in contralateral, uninflamed skin (Figure 2.4B & C). Thus, while PD-L1 was expressed by BECs under all conditions systemically, LECs demonstrated the highest specificity to local microenvironments and exhibit significantly different levels of PD-L1 expression in checkpoint sensitive and insensitive tumors.

Dermal LEC PD-L1 is induced by interstitial, antigen-sepcific CD8$^+$ T cell immunity

Given the observation that LEC PD-L1 expression was tuned in tumor microenvironments correlating with increasing CD8$^+$ T cell infiltration (Figure 2.4D), we hypothesized that LECs may be directly responsive to infiltrating antigen-specific CD8$^+$ T cells. Due to the robust induction of PD-L1 on LECs in VacV infected skin 7 days post infection (Figure 2.3E), we used this model for kinetic analysis of EC PD-L1. Flow cytometric analysis of dermal endothelial populations in infected ears at days 0, 3, 7, and 10 post infection revealed peak LEC (100-fold) and BEC (2.5-fold) PD-L1 expression 7 days post infection (Figure 2.5A), concomitant with dermal infiltration of antiviral CD8$^+$ T cells[53,240]. Depletion of both CD4$^+$ and CD8$^+$ T cells during the first 7 days of infection significantly reduced, but did not eliminate PD-L1 expression by LECs (Figure 2.5B), indicating that T cells are sufficient, but perhaps not necessary to induce LEC PD-L1 expression. This LEC

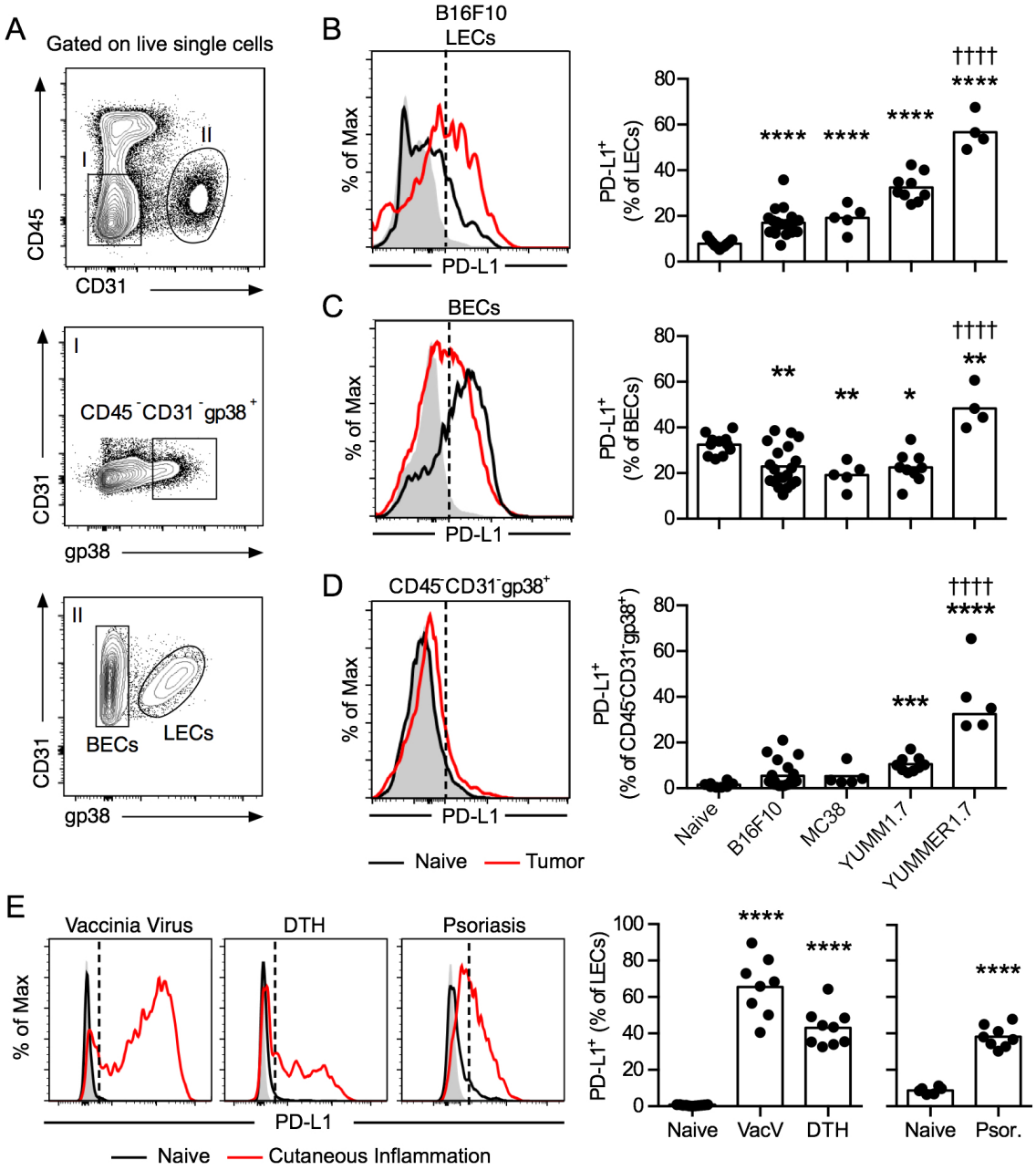

Figure 2.3: Cutaneous lymphatic endothelial cells express PD-L1 in inflamed and malignant skin. (A) Gating scheme for lymphatic endothelial cells (LEC; CD45⁻CD31⁺gp38⁺), blood endothelial cells (BEC; CD45⁻CD31⁺gp38-), and stromal cells (CD45⁻CD31⁻gp38⁺) from tumors. (B-D) Representative histogram (B16F10; left) and quantification (right) of PD-L1 expression by LECs (B), BECs (C), and stromal cells (D) in naïve skin, B16F10 melanoma, MC38 colorectal adenocarcinoma, YUMM1.7, and YUMMER1.7 melanoma tumors implanted in the skin of mice. (E) Representative histograms (left) and quantification (right) of PD-L1 expression by cutaneous LECs in inflamed skin challenged with Vaccinia virus (VacV), delayed-type hypersensitivity (DTH), or imiquimod-induced psoriasis (Psor) compared to skin of naive mouse (ear or back skin). Each point represents one mouse, bars indicate the mean. Gray histogram represents isotype staining control, dotted line indicates positive gate. One-way ANOVA corrected for multiple comparisons. ∗p<0.05, ∗∗p<0.01, ∗∗∗p<0.001, ∗∗∗∗p<0.0001 (compared to naïve skin). †††† p<0.0001 (compared to B16F10).

adaptation to infiltrating immunity is reminiscent of mechanisms of adaptive immune resistance described in tumors[71], therefore we hypothesized that boosted T cell infiltration into tumor microenvironments with low PD-L1 expression would switch on analogous programs of LEC-mediated immune resistance.

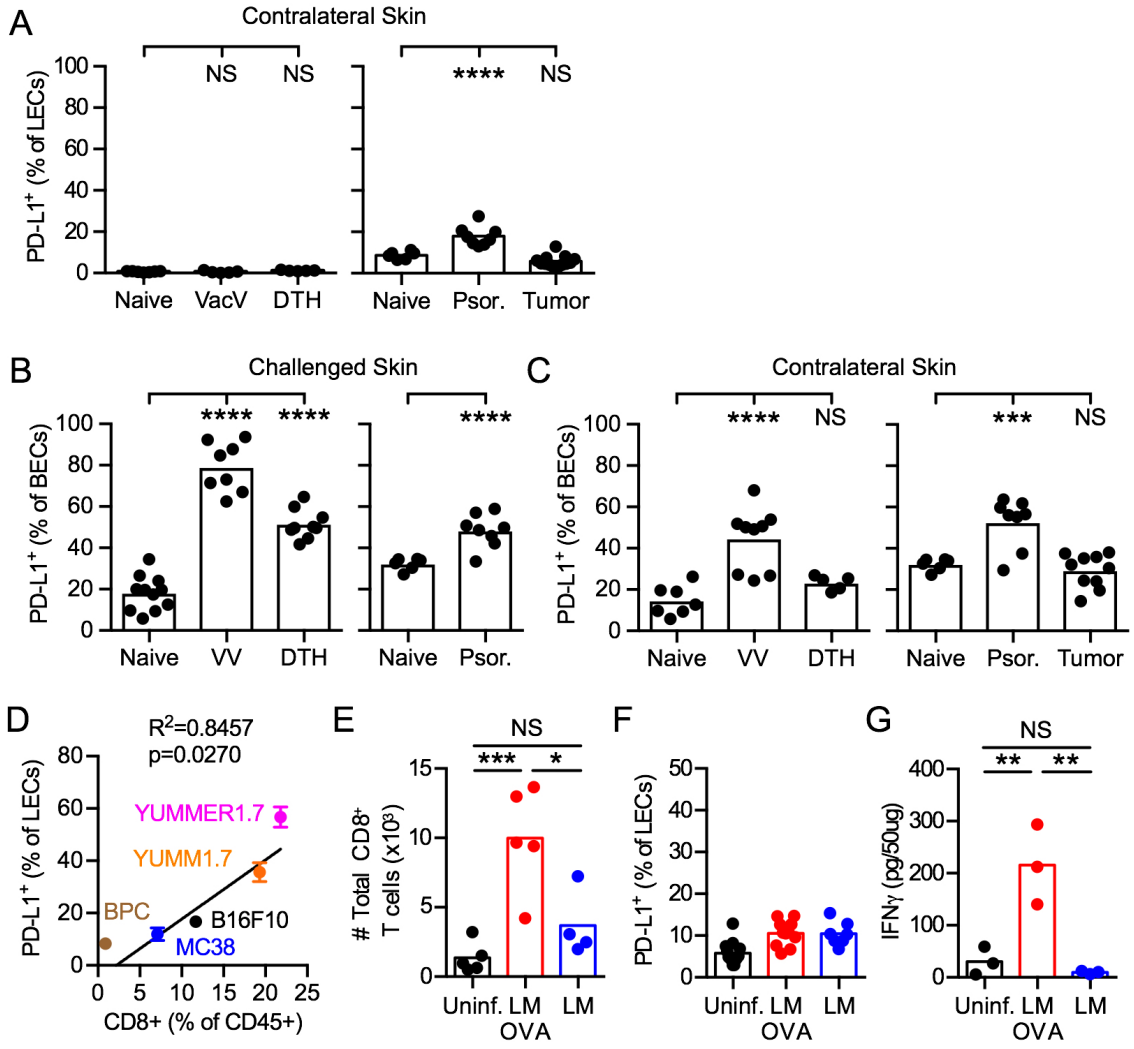

Figure 2.4: LEC PD-L1 expression in contralateral skin. (A) PD-L1 expression by LECs at sites distal to cutaneous challenge with Vaccinia virus (VV), delayed-type hypersensitivity (DTH), imiquimod-induced psoriasis (Psor), or B16F10 melanoma, compared to skin of naive mouse. (B & C) PD-L1 expression by inflamed (B) or contralateral (C) skin of mice challenged with Vaccinia virus (VV), delayed-type hypersensitivity (DTH), imiquimod-induced psoriasis (Psor), or B16F10 melanoma. (D) Correlation between $CD8^+$ T cell infiltration and tumor associated LEC PD-L1 expression across various tumor models indicated on graph. (E) Total $CD8^+$ T cells in B16F10.OVA tumors of mice vaccinated with LM, LM-OVA, or no vaccination. (F) PD-L1 expression by cutaneous LECs in skin contralateral to B16F10.OVA tumors of mice vaccinated with LM, LM-OVA, or no vaccination. (G) IFNγ, measured by ELISA, in tumor lysates from B16F10.OVA tumors of mice vaccinated with LM, LM-OVA, or no vaccination. Each dot represents one mouse, bars represent mean. One-way ANOVA corrected for multiple comparisons (A-G). Pearson correlation (D). $*p<0.05$, $**p<0.01$, $***p<0.001$, $****p<0.0001$.

To boost a tumor-specific $CD8^+$ T cell response and directly interrogate its effect on LECs we utilized a vaccination strategy (attenuated *Listeria monocytogenes*; LM) that induced either non-specific (LM) or specific (LM-OVA) $CD8^+$ T cell immunity against the model tumor antigen, OVA. As expected, vaccination with LM-OVA slowed B16F10.OVA tumor growth compared to LM-infected or uninfected mice (Figure 2.5C) and boosted the number of total tumor-infiltrating (Figure 2.4E) and H2-K^b-restricted, $OVA_{257\text{-}264}$(SIINFEKL)-specific $CD8^+$ T cells (Figure 2.5D). Specific upregulation of PD-L1 by LECs in

tumor microenvironments (Figure 2.5E), and not contralateral skin (Figure 2.4F), and when using LM expressing OVA and not without, is consistent with a requirement for local antigen recognition. It is likely that antigen recognition is both required for the continued accumulation of these antigen-specific cells at the tumor site and elevated IFNγ. To further test this hypothesis, we adoptively transferred *in vitro* activated effector OT-I TCR-Tg $CD8^+$ T cells into tumor-bearing mice. Analysis of tumor-associated LECs four days later revealed elevated expression of PD-L1 with transfer relative to steady-state tumors (Figure 2.5F), indicating local antigen-recognition by $CD8^+$ T cells was sufficient to activate regional LECs.

Accumulation of antigen-specific T cells and local TCR activation boosts IFNγ concentrations in tumors (Figure 2.4G), which activates PD-L1 expression through the JAK-STAT pathway[241]. Neutralization of IFNγ either during the first 7 days of viral infection (Figure 2.5G) or 2 weeks of tumor growth (Figure 2.5H) resulted in reduced levels of LEC PD-L1. To investigate whether effector T cells directly activate LECs and induce PD-L1 expression via secretion of IFNγ, naïve or *in vitro* activated $CD8^+$ T cells were cultured overnight with murine immortalized LECs (iLECs) in the presence or absence of a semipermeable transwell membrane and IFNγ blocking antibody. *In vitro* activated, but not naïve, $CD8^+$ T cells induced PD-L1 expression on LECs dependent on IFNγ and independent of direct cell-cell contract (Figure 2.5I). Further, IFNγ was sufficient to induce PD-L1 expression in *ex vivo* murine LECs in a STAT1 and IFNγR-dependent manner (Figure 2.5J) and also in primary human LECs (Figure 2.5K). Consequently, LECs are sensitive to cytotoxic immunity and express PD-L1 in response to IFNγ and local antigen recognition by infiltrating T cells.

IFNγ-signaling in lymphatic vessels limits cutaneous anti-viral immunity

We hypothesized that the IFNγ-responsiveness of cutaneous lymphatic vessels might represent a tissue-resident mechanism of immune control that functions to balance protective immunity with immunopathology such that the accumulation of cytotoxic T cells switches on compensatory mechanisms of immune resolution. To disrupt this crosstalk,

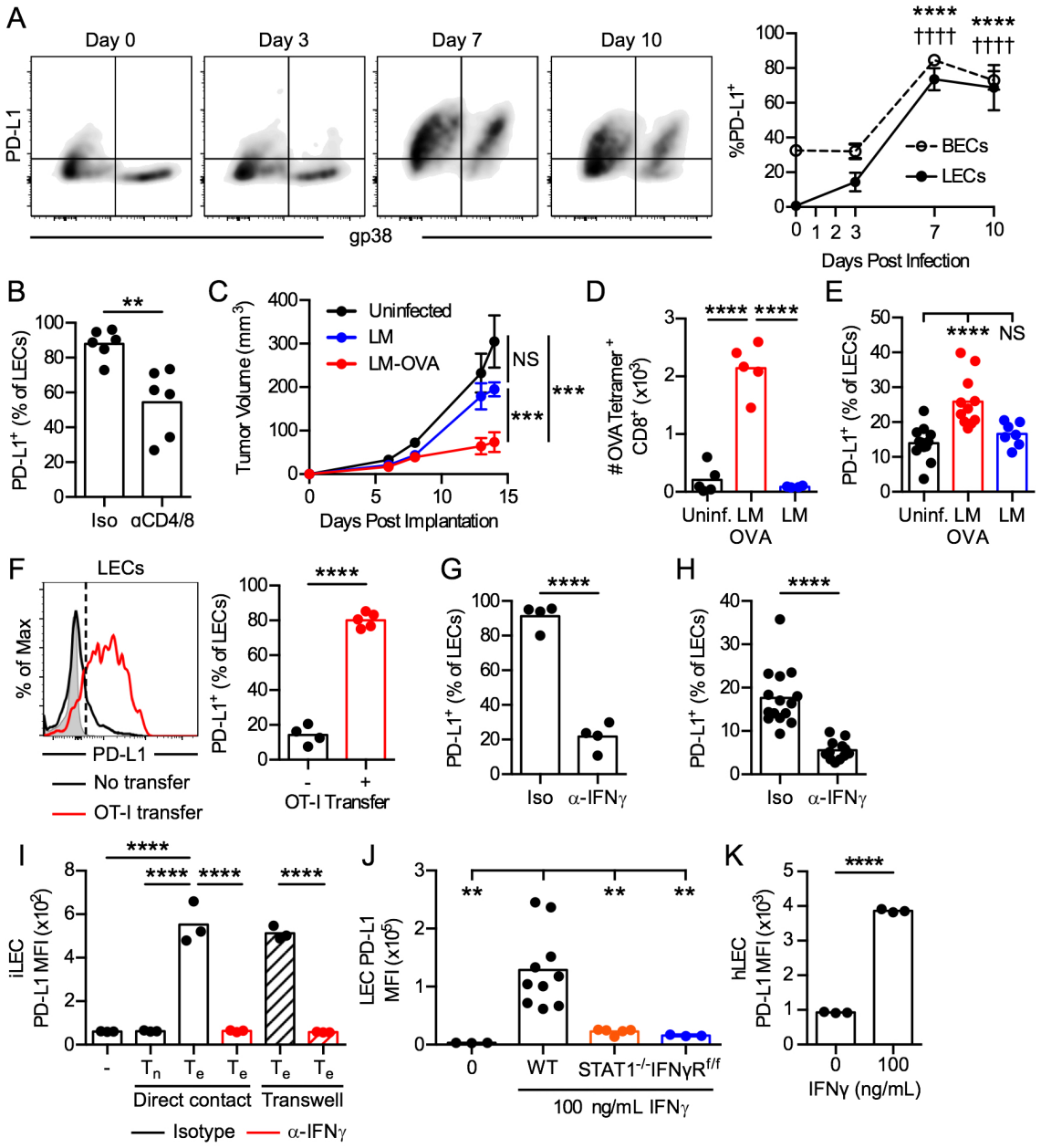

Figure 2.5: T cells induce IFNγ-dependent PD-L1 expression in cutaneous LECs. (A) Representative flow plots (left, gated on $CD31^+CD45^-$) and quantification (right) of PD-L1 expression by lymphatic endothelial cells (LEC; $CD45^-CD31^+gp38^+$) and blood endothelial cells (BEC; $CD45^-CD31^+gp38$-) in skin following VacV infection. Mean ± SEM, n≥3. (B) PD-L1 expression by cutaneous LECs 7 days post VacV infection in mice treated with αCD4/8 depleting antibodies or isotype control. (C-E) B16F10.OVA-tumor bearing mice were vaccinated with attenuated (ActA deficient) *Listeria monocytogenes*, expressing OVA (LM-OVA) or not (LM), day 4 post tumor implantation. (C) B16F10.OVA growth curves. (D) Number of H2-K^b-restricted, $OVA^{257-264}$(SIINFEKL)-specific $CD8^+$ T cells in tumors. (E) PD-L1 expression by tumor-associated LECs. (F) Representative histograms (left) and quantification (right) of PD-L1 expression by tumor-associated LECs in B16F10-OVA tumor-bearing mice receiving, or not, *in vitro*-activated OT-I TCR-Tg $CD8^+$ T cells adoptively transferred 10 days post implantation. (G) PD-L1 expression by cutaneous LECs on day 7 post VacV infection and (H) B16F10 tumor-associated LECs in mice receiving IFNγ-neutralizing antibody or isotype control. (I) PD-L1 expression by immortalized LECs (iLECs) following culture with naïve (T_n) or *in vitro*-activated, effector $CD8^+$ T cells (T_e), treated with αIFNγ or isotype control, and separated by semipermeable transwell membranes. Representative of 3 independent experiments. (J) PD-L1 expression by textitex vivo harvested LECs from WT, $STAT1^{-/-}$, or $IFN\gamma R^{\Delta LYVE1}$ mice (textit$IFN\gamma R^{f/f}$) following 100ng/ml IFNγ stimulation. (K) PD-L1 expression by primary human dermal LECs following IFNγ stimulation. Shaded histogram represents isotype staining control, dotted line indicates positive gate. Each point represents one mouse, bars indicate mean. Students t-test (B, F, G, H, & K), one-way ANOVA corrected for multiple comparisons (A, D, E, I, & J). One-way ANOVA corrected for multiple comparisons performed on average slope and variance of individual tumor growth curves (C). ∗p<0.05, ∗∗p<0.01, ∗∗∗p<0.001, ∗∗∗∗p<0.0001. (A) ∗∗∗∗(BECs) & ††††(LECs) p<0.0001 relative to time 0.

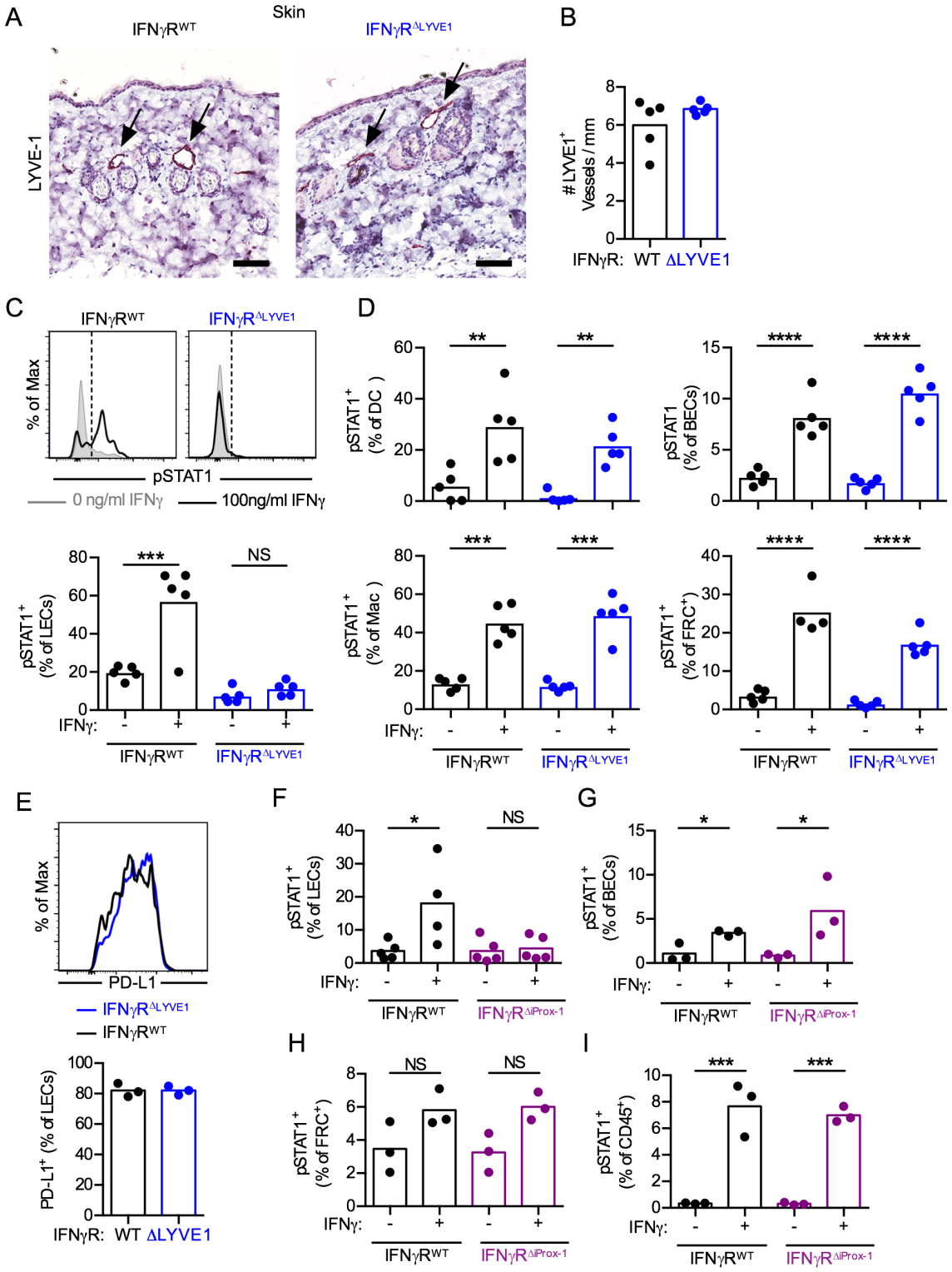

Figure 2.6: LEC-specific loss of IFNγR. (A & B) Representative images (A) and quantification (B) of lymphatic vessel density in naïve skin of IFNγR$^{\Delta LYVE1}$ mice or littermate controls. (C) Representative histograms (top) and quantification (bottom) of STAT1 phosphorylation (pSTAT1) following IFNγ stimulation of *ex vivo* lymphatic endothelial cells (LEC; CD45$^-$CD31$^+$gp38$^+$) harvested from IFNγR$^{\Delta LYVE1}$ mice or littermate controls. (D) Quantification of STAT1 phosphorylation (pSTAT1) following IFNγ stimulation of *ex vivo* dendritic cells (DC; CD11c$^+$MHCII$^+$), macrophages (Mac; CD11c$^-$CD11b$^+$F4/80$^+$), blood endothelial cells (BEC; CD45$^-$CD31$^+$gp38-), and fibroblastic reticular cells (FRC; CD45$^-$CD31$^-$gp38$^+$) harvested from IFNγR$^{\Delta LYVE1}$ mice or littermate controls. (E) PD-L1 expression by LECs in naïve LNs of IFNγR$^{\Delta LYVE1}$ mice or littermate controls. (F-I) Quantification of pSTAT1 following *ex vivo* IFNγ stimulation of LEC (F), BEC (G), FRC (H), and CD45$^+$ cells (I) harvested from IFNγR$^{\Delta iProx\text{-}1}$ mice or littermate controls. Each point represents one mouse, bars indicate mean. Shaded histogram represents isotype staining control. One-way ANOVA corrected for multiple comparisons. $**p<0.01$, $***p<0.001$, $****p<0.0001$.

we generated mice whose LECs were insensitive to IFNγ by crossing IFNγR$^{f/f}$ mice with mice expressing Cre recombinase under control of the lymphatic-specific, lymphatic vessel endothelial hyaluronan receptor 1 (LYVE1) promoter (IFNγR$^{\Delta LYVE1}$). At steady state, we found no gross change in cutaneous lymphatic vessel structure and density (Figure 2.6A & B) and LN LECs harvested from IFNγR$^{\Delta LYVE1}$ mice failed to phosphorylate STAT1 (Figure 2.6C) following IFNγ stimulation demonstrating the efficiency of the Cre. Macrophages and DCs, as well as other LN stromal cells, including BECs and fibroblastic reticular cells (FRCs) maintained their ability to phosphorylate STAT1 following IFNγ stimulation (Figure 2.6D), indicating specificity of the Cre. Importantly, constitutive PD-L1 expression by LN LECs remained unchanged (Figure 2.6E). Interestingly, though previous work indicated that IFNγ was required to limit nodal lymphangiogenesis, we found no gross differences in LN LYVE1$^+$ lymphatic structures at steady state (Figure 2.7A & B), or when draining implanted melanomas (Figure 2.7C) or VacV infected skin (Figure 2.7D).

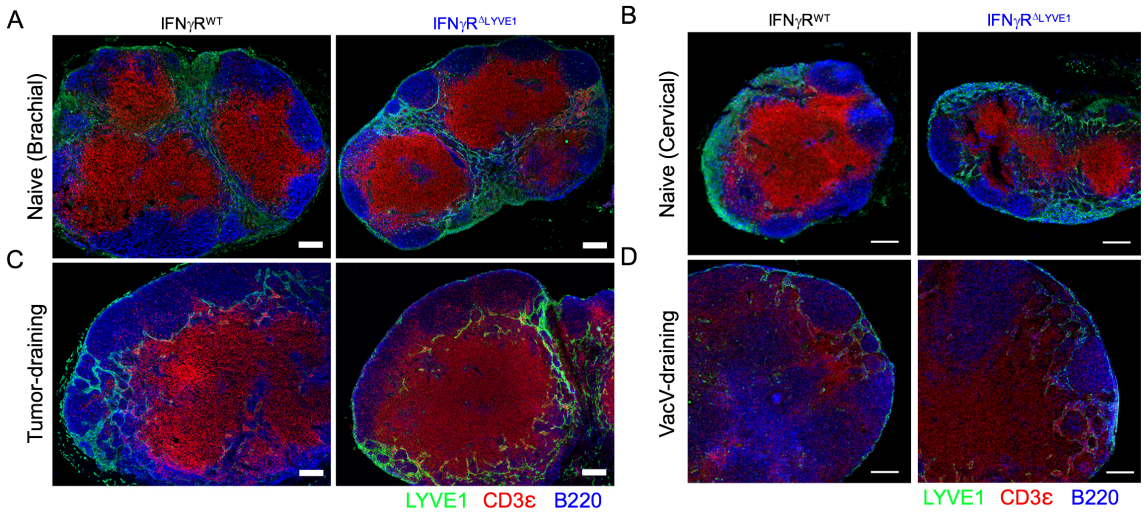

Figure 2.7: Loss of IFNγ signaling on LECs does not affect LN lymphangiogenesis. (A & B) Representative images of brachial (A) and cervical (B) lymph nodes (LN) of naïve IFNγR$^{\Delta LYVE1}$ mice or littermate controls. (C) Representative images of tumor draining LN of IFNγR$^{\Delta LYVE1}$ mice or littermate controls (brachial). (D) Representative images of vaccinia infected (VacV) draining LN from IFNγR$^{\Delta LYVE1}$ mice or littermate controls (cervical). Lymphatic vessels (green, LYVE1), B cells (blue, B220), and T cells (red, CD3ε). Scale bar = 100 μm.

We therefore utilized this model to ask whether loss of IFNγ-sensitivity by peripheral lymphatic vessels (IFNγR$^{\Delta LYVE1}$) impacted pathology associated with infection and accumulation of anti-viral immunity. Importantly, LEC IFNγR was required for *in vivo* expression of PD-L1 7 days post infection (Figure 2.9A), while no change was observed

in expression by BECs or CD45$^+$ leukocytes (Figure 2.8A & B). Loss of IFNγR resulted in a reduction of LYVE1$^+$ but not podoplanin$^+$ structures in infected skin (Figure 2.9B-D). As LYVE1 can be variably expressed on lymphatic vessels and internalized in regions of active inflammation, these data seem to indicate regional differences in lymphatic vessel activation rather than changes in overall density.

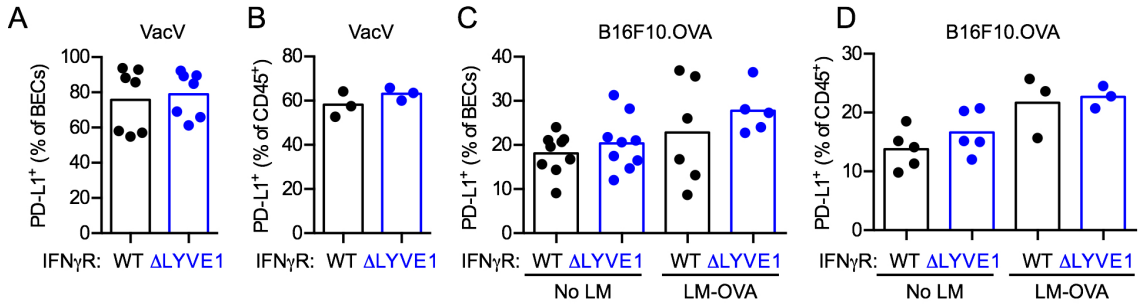

Figure 2.8: PD-L1 expression in challenged skin of IFNγR$^{\Delta LYVE1}$ mice. (A & B) PD-L1 expression by blood endothelial cell (BEC; CD45$^-$CD31$^+$gp38-) (A) and CD45$^+$ cells (B) in skin of IFNγR$^{\Delta LYVE1}$ mice or littermate controls, 7 days post vaccinia (VacV) infection. (C & D) PD-L1 expression by tumor associated BECs (C) and CD45$^+$ cells (D) in B16F10.OVA tumors of IFNγR$^{\Delta LYVE1}$ mice or littermate controls receiving LM-OVA vaccination on day 4 post implantation or not. Each point represents one mouse, bars indicate mean. Students T-test (A & B) or One-way ANOVA corrected for multiple comparisons (C & D).

Notably, 7 and 10 days post infection we observed elevated pathology (Figure 2.9E) in infected ears of IFNγR$^{\Delta LYVE1}$ mice as determined by overall ear thickness (Figure 2.9F) and significant increases in both epidermal (Figure 2.9G) and dermal thickness (Figure 2.9H). Total numbers of CD45$^+$ leukocytes in infected ears was significantly elevated 7 days post infection (Figure 2.9I) while the accumulation of CD45$^+$ leukocytes in skin as determined by IHC only trended up at day 10 (Figure 2.9J). We did not observe increased F4/80$^+$ macrophage (Figure 2.9K) or mast cell (Figure 2.9L) accumulation in ears 10 days post infection that might explain these changes, but rather saw significant increases in CD4$^+$ and CD8$^+$ T cell infiltration at day 7 (Figure 2.9M and N). To determine whether IFNγ signaling on LECs negatively regulated antigen-specific CD8$^+$ T cell priming, we evaluated CD8$^+$ T cells specific for the immunodominant epitope, H2-K^b restricted, B8R$_{20\text{-}27}$(TSYKFESV) in draining LNs. 7 days post infection, the peak of T cell expansion, we observed no difference in priming (Figure 2.9O), consistent with normal expression of PD-L1 in lymphoid organs (Figure 2.6E). Within infected tissue, however, there was a two-fold enrichment for B8R$_{20\text{-}27}$-specific CD8$^+$ T cells in ears of IFNγR$^{\Delta LYVE1}$ mice compared to littermate controls (Figure 2.9P). It is noteworthy, that

the 2-fold enrichment in antigen-specific T cells doubles an already impressive number of T cells within a single infected ear from $10x10^4$ to $20x10^4$. While we did not observe accelerated viral control (Figure 2.9Q) as the existing response is already effective at mediating viral clearance, this data taken all together indicates that IFNγ-dependent adaptation of LECs to skin-infiltrating cytotoxic T cells and expression of PD-L1 functionally limits T cell accumulation that may dampen the pathological response (as determined by dermal and epidermal thickening) in tissue.

CD8$^+$ T cells are correlated with and proximal to the lymphatic vasculature in primary human melanoma

For IFNγ and PD-L1-dependent crosstalk between peritumoral lymphatic vessels and tumor-infiltrating CD8$^+$ T cells to be functionally relevant, T cells must be proximal to lymphatic vessels in inflamed tissue microenvironments. Immunofluorescence analysis of CD3ε^+ T cell infiltrates in VacV-infected skin revealed both perilymphatic and intralumenal T cells in infected skin (data not shown), and our previous work demonstrated colocalization of T cells and lymphatic vessels in murine tumors[145]. We therefore sought to evaluate the correlation between cytotoxic T cells and lymphatic vessels and their spatial proximity in human primary melanomas. We first employed a previously established lymphatic score (LS; based on transcript levels of VEGFC, PDPN, LYVE1)[55] to stratify patients from publicly available cutaneous melanoma gene expression data sets of the Broad Institute The Cancer Genome Atlas (TCGA). Across both primary and metastatic cutaneous melanoma samples, LS positively correlated with expression of gene transcripts associated with CTLs either as individual transcripts (Figure 2.10A) or a composite score (Figure 2.10B). Samples stratified as LS^{hi} exhibited a statistically significant increase in this T cell inflammation score (Figure 2.10C), a type II interferon score (Figure 2.10D), and expression of *CD274* (PD-L1, Figure 2.10E) and *IDO1* (Figure 2.10F), as compared to LS^{lo} patients, indicating that patients enriched for high expression of lymphatic-associated genes were also enriched for more T cell inflammation and compensatory mechanisms of immune suppression. Importantly, though we found a correlation between LS and T cell inflammation, the strength of the relationship is not sufficient

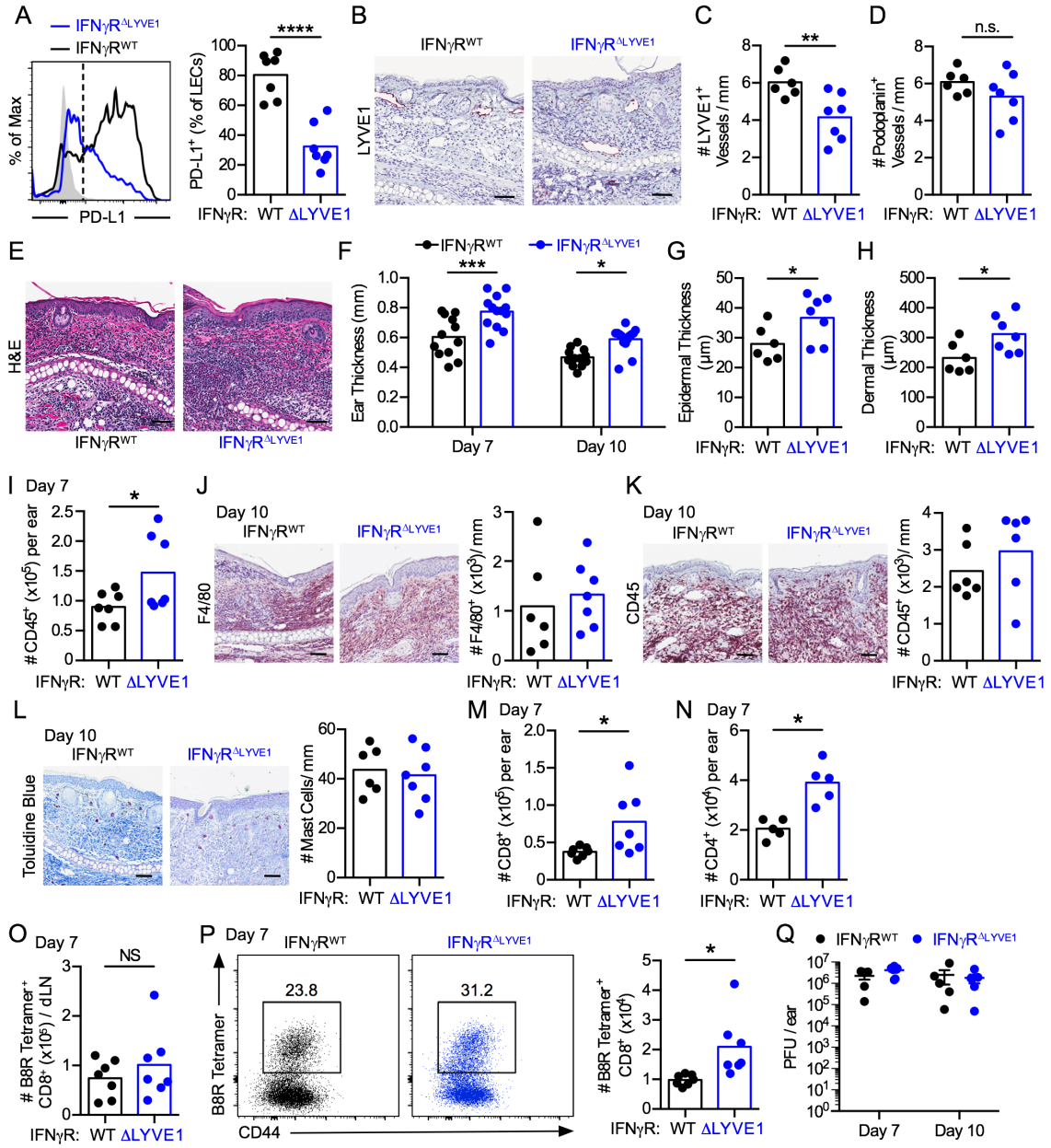

Figure 2.9: IFNγ signaling in cutaneous LECs limits anti-viral immunity, but prevents immunopathology. (A) Representative histogram (left) and quantification (right) of PD-L1 expression by cutaneous LECs 7 days post vaccinia (VacV) infection in IFNγR$^{\Delta LYVE1}$ mice or littermate controls. (B-D) Representative images (B) and quantification of LYVE1$^+$ (C) and podoplanin$^+$ (D) lymphatic vessels in ears of IFNγR$^{\Delta LYVE1}$ mice or littermate controls on day 10 post VacV infection. (E-H) Representative histology (E, H&E) and quantification of total ear thickness by calipers (F), epidermal thickness (G), and dermal thickness (H) on day 10 post VacV infection in IFNγR$^{\Delta LYVE1}$ mice or littermate controls. (I) Number of total CD45$^+$ leukocytes in ears of IFNγR$^{\Delta LYVE1}$ mice or littermate controls on day 7 post infection. (J-L) Representative IHC images and quantification ofCD45$^+$ leukocytes (J), F4/80$^+$ Macrophages (K) and mast cells (L, toluidine blue) in ears of IFNγR$^{\Delta LYVE1}$ mice or littermate controls on day 10 post VacV infection. (K) Representative IHC images (left) and quantification (right) of CD45$^+$ cells in ears on day 10 post VacV infection in IFNγR$^{\Delta LYVE1}$ mice or littermate controls. (L-N) Quantification of total CD8$^+$ T cells (M), and CD4$^+$ T cells (N) in infected skin on day 7 post VacV infection of IFNγR$^{\Delta LYVE1}$ mice or littermate controls. (O) Total number of H2-K^b-restricted B8R-specific CD8$^+$ T cells in draining lymph nodes (dLN) 7 days post VacV infection. (P) Representative plots (left; gated on CD45$^+$CD8$^+$) and quantification (right) of virus-specific H2-K^b-restricted B8R-specific CD8$^+$ T cells in ears of IFNγR$^{\Delta LYVE1}$ mice or littermate controls 7 days post VacV infection. (Q) Viral titers in IFNγR$^{\Delta LYVE1}$ mice or littermate controls on day 7 and 10 post VacV infection. Shaded histogram represents isotype staining control, dotted line indicates positive gate. Each point represents one mouse, bars indicate mean. Scale bar = 100μm. Students t-test (A-D & G-P), one-way ANOVA corrected for multiple comparisons (F & Q), $*p<0.05$, $**p<0.01$, $***p<0.001$, $****p<0.0001$.

to allow LS-dependent prediction of inflammation, not surprisingly then indicating that other factors contribute to the inflamed status of primary cutaneous melanoma.

To validate the observation that tumor-associated lymphatic vessels correlate with infiltrating T cells, we performed multiplexed immunohistochemistry (mIHC)[242] using formalin-fixed paraffin embedded (FFPE) human primary melanoma samples (Table 2.1). We simultaneously evaluated hematopoietic and non-hematopoietic components of tumor microenvironments (Figure 2.10G) and performed spatial proximity analysis to calculate distance from tumor borders. $CD8^+$ T cells (Figure 2.10H) and lymphatic vessels (Figure 2.10I) are restricted to the peritumoral stroma in primary melanoma samples, while blood vessels are evenly distributed between intra- and peri-tumoral regions (Figure 2.10J). The distance of each $CD8^+$ T cell to the nearest blood vessel, lymphatic vessel, and tumor cell revealed proximity of all cellular components within the tumor periphery, with $CD8^+$ T cells quantitatively closest to blood vessels (Figure 2.10K) but with a significant population of T cells proximal to lymphatic vessels (Figure 2.10L). Importantly, and consistent with our transcriptional analysis, peritumoral LVD positively correlated with peritumoral $CD8^+$ T cell density (Figure 2.10M), establishing a correlation between lymphangiogenic tumor microenvironments and T cell infiltration in human melanoma.

Loss of IFNγ signaling on LECs drives $CD8^+$ T cell-dependent tumor control and survival

Mechanisms of immune resolution are often coopted by tumors to mediate their immune escape. The enhanced CTL accumulation in virally infected skin (Figure 2.9) and proximity of tumor-infiltrating $CD8^+$ T cells and tumor-associated lymphatic vessels (Figure 2.10) raised the possibility of lymphatic vessel-dependent T cell suppression in melanoma. While loss of non-hematopoietic PD-L1 was functionally significant in bone marrow chimera experiments (Figure 2.1), we next asked whether LEC-specific adaptive immune resistance mediated by IFNγ and PD-L1 was relevant in tumor settings. We first implanted PD-L1 insensitive B16F10[236] and YUMM1.7[239] tumors into $IFN\gamma R^{WT}$ and $IFN\gamma R^{\Delta LYVE1}$ mice. In these models, where PD-L1 blockade is ineffective, there was no change in PD-L1 expressed by tumor-associated LECs in $IFN\gamma R^{\Delta LYVE1}$ mice compared to littermate controls (Figure 2.11A & B) and subsequently tumor growth was unaffected (Figure 2.11C & D). Our bone marrow chimera experiments indicated that the functional

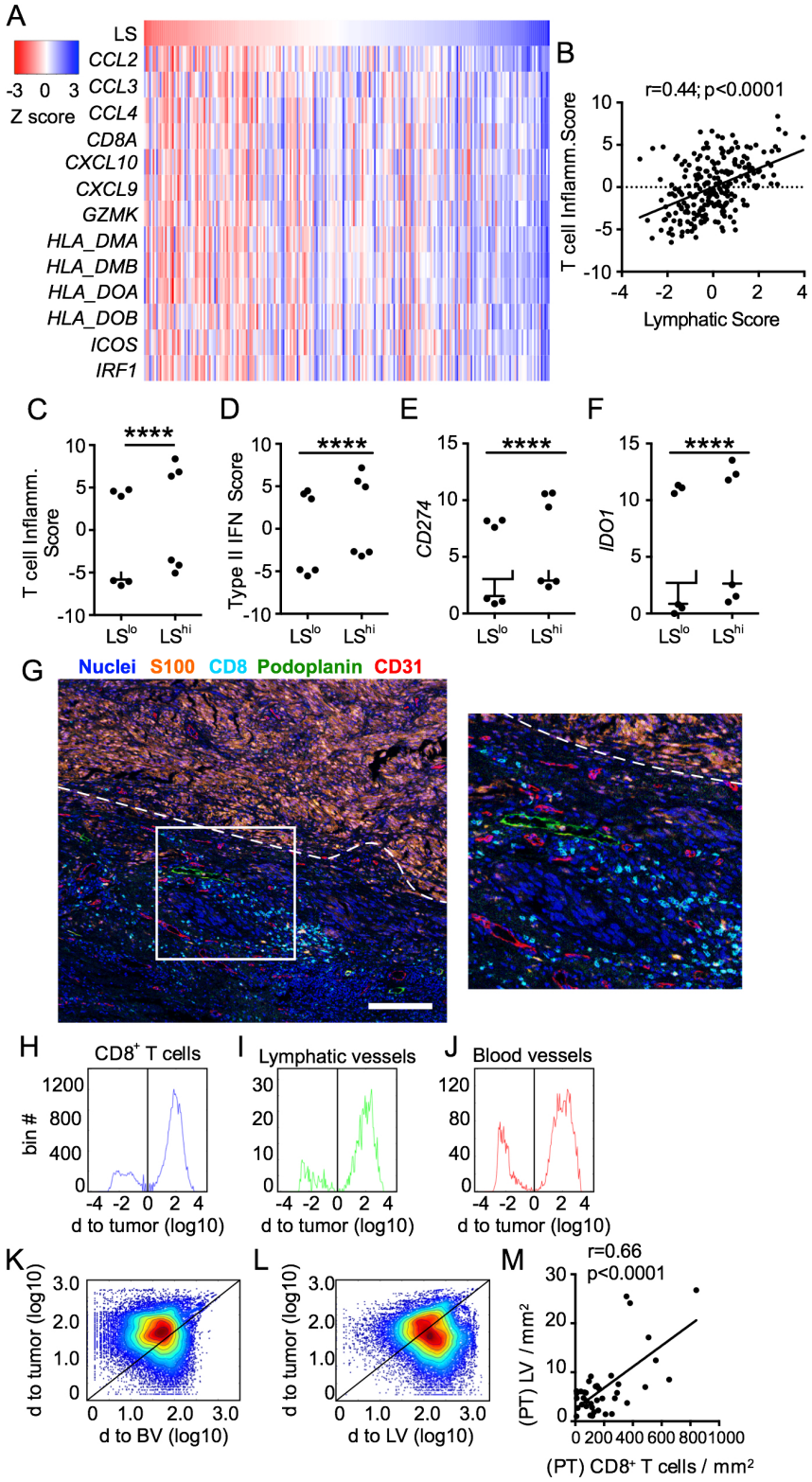

Figure 2.10: Tumor-associated lymphatic vessels correlate with and are proximal to T cell infiltrates in human primary melanoma. (A) Heatmap clustering of genes associated with T cell inflammation and Lymphatic Score (*VEGFC*, *PDPN*, *LYVE1*) across 231 primary and metastatic (non-glabrous, non-lymphoid) patient samples from the Broad Institutes TCGA database. (B) Correlation between lymphatic and T cell inflammation scores. Pearsons correlation coefficient (r). (C-F) Stratification of lymphatic score into high (LS^{hi}; n=68) and low (LS^{lo}; n=71) cohorts stratifies T cell inflammation score (C), type II IFN score (D), *CD274* expression (E), and *IDO* expression (F) melanoma samples. Box plots, whiskers indicate 5-95th percentile with outliers. Students t-test, $****$ p<0.0001. (G) Digital overlay of pseudo-colored single stains from multiplexed immunohistochemistry of FFPE human primary melanomas. Representative image and inset. Hematoxylin, (nuclei, blue); S100 (orange); CD8 (cyan); D2-40 (podoplanin, green); CD31 (red). Scale bar = 200μm. (H-J) Distribution of $CD8^+$ T cell (H), D2-40$^+$ lymphatic vessel (I), and $CD31^+$ blood vessel (J) distance from $S100^+$ tumor border. (K & L) Scatter plots represent shortest distance from $CD8^+$ cells to $S100^+$ tumor border versus $CD31^+$ vessels (K) and D2-40$^+$ lymphatic vessels (L). (M) Correlation between peritumoral (PT) lymphatic vessel density and PT $CD8^+$ T cell density, compiled data across n=17 samples and 40 regions of interest.

significance of LEC/T cell crosstalk might be revealed in the setting of more robust pre-existing anti-tumor immunity, similar to PD-L1 blockade. Therefore, we looked at the response to LM-OVA vaccination in IFNγR^{WT} and IFNγR$^{\Delta LYVE1}$ B16F10-bearing mice. Importantly, LM-OVA primed equivalent systemic OVA-specific responses in both mice (Figure 2.11E), however, LECs failed to activate and upregulate PD-L1 in IFNγR$^{\Delta LYVE1}$ mice (Figure 2.11F), while PD-L1 expression on leukocyte and BECs was unchanged (Figure 2.8C & D). Coincident with a failure to upregulate PD-L1 expression on tumor-associated LECs, we observed improved tumor control with smaller tumors at endpoint (Figure 2.11G) and two-fold enrichment of activated, intratumoral tumor-specific CD8$^+$ T cells (Figure 2.11H). Thus, antigen-specific T cells activate compensatory LEC-specific and IFNγR-dependent mechanisms of local immune control.

While this data demonstrates that following a therapeutic boost in anti-tumor immunity, intratumoral T cell activity is limited by IFNγ signaling on lymphatic vessels, we were interested in determining whether lymphatic vessel-dependent T cell control might be functional in the absence of vaccination. We therefore implanted the immune checkpoint sensitive YUMMER1.7 cells into IFNγR^{WT} and IFNγR$^{\Delta LYVE1}$ mice. Tumor-associated LECs extracted from YUMMER1.7 tumors in IFNγR$^{\Delta LYVE1}$ mice revealed that lymphatic vessels failed to upregulate PD-L1 (Figure 2.11I), with no observed change in either lymphatic or blood vessel density (Figure 2.11J-L). Analysis of YUMMER1.7 growth in IFNγR^{WT} and IFNγR$^{\Delta LYVE1}$ mice revealed significant tumor control initiated ten days post implantation, consistent with an adaptive immune response, leading to extended overall survival dependent on CD8$^+$ T cells (Figure 2.11M & N). We confirmed lymphatic vessel specificity of our result using an inducible Prox1:Cre-ERT2 (IFNγR$^{\Delta iProx\text{-}1}$). *Ex vivo* functional analysis confirmed the specificity and efficiency of the *Prox1* inducible Cre (Figure 2.6F-I). Consistent with our results in IFNγR$^{\Delta LYVE1}$, YUMMER1.7 tumors implanted into IFNγR$^{\Delta iProx\text{-}1}$ were controlled relative to Cre negative mice, again initiating ten days post implantation, leading to significantly improved overall survival (Figure 2.11O & P). Thus, using two independent systems we demonstrate that disruption of IFNγ-signaling on tumor-associated lymphatic vessels relieves local

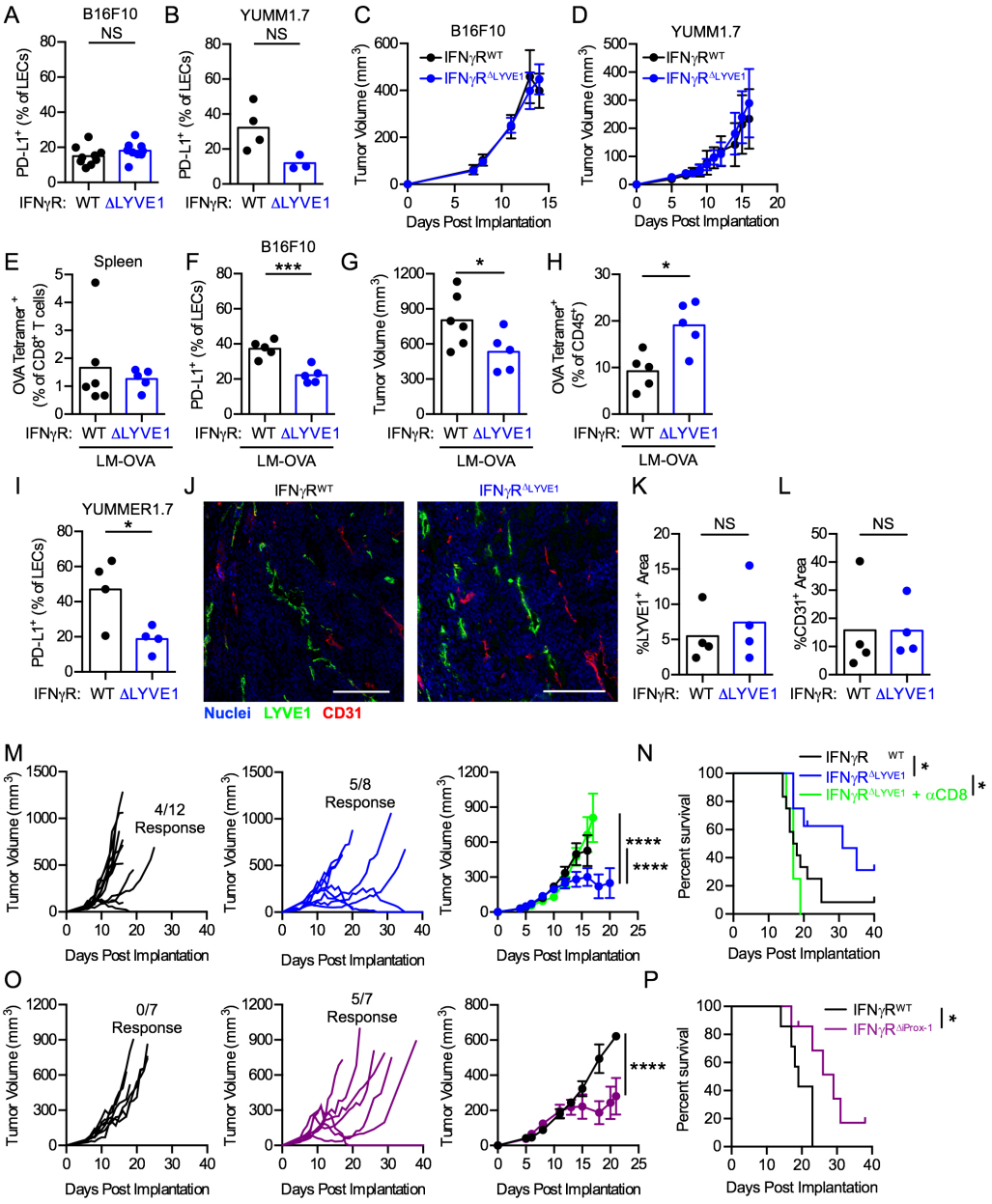

Figure 2.11: Disrupting IFNγ-mediated LEC crosstalk with T cells enhances CD8$^+$ T cell dependent melanoma control. (A & B) Quantification of tumor-associated LEC PD-L1 expression in B16F10 (A) and YUMM1.7 (B) tumors implanted into IFNγR$^{\Delta LYVE1}$ mice or littermate controls. (C & D) B16F10 (C) and YUMM1.7 (D) tumor growth in IFNγR$^{\Delta LYVE1}$ mice or littermate controls. (E) H2-K^b-restricted OVA-specific CD8$^+$ T cells in spleens of B16F10.OVA tumor bearing IFNγR$^{\Delta LYVE1}$ mice or littermate controls vaccinated with LM-OVA. (F) PD-L1 expression by LECs in B16F10.OVA tumors of IFNγR$^{\Delta LYVE1}$ mice or littermate controls vaccinated with LM-OVA. (G) Final B16F10.OVA tumor volumes IFNγR$^{\Delta LYVE1}$ mice or littermate controls vaccinated with LM-OVA. (H) H2-K^b-restricted OVA-specific tumor infiltrating CD8$^+$ T cells from tumors of mice in G. (I) PD-L1 expression by LECs in YUMMER1.7 tumors implanted into IFNγR$^{\Delta LYVE1}$ mice or littermate controls. (J-L) Representative immunofluorescence images and quantification (K & L) of lymphatic vessels (green, LYVE1, K), blood vessels (red, CD31, L) in YUMMER1.7 tumors implanted into IFNγR$^{\Delta LYVE1}$ mice or littermate controls. Scale bar = 200 μm. (M & N) YUMMER1.7 tumor growth (M) and survival (N) of IFNγR$^{\Delta LYVE1}$ mice (blue), IFNγR$^{\Delta LYVE1}$ mice treated with CD8-depleting antibody (green), or littermate controls (black). (O & P) YUMMER1.7 tumor growth (O) and survival (P) of IFNγR$^{\Delta iProx\text{-}1}$ mice (purple) or littermate controls (black). Each point represents one mouse, bars indicate mean. Students t-test (A, B, & E-I). One-way ANOVA corrected for multiple comparisons (M) or students T test (C, D, & O) performed on average slope and variance of individual tumor growth curves Mantel-Cox test used for comparison of survival (N & P) $*p<0.05$, $***p<0.001$, $****p<0.0001$.

immune suppression driving persistent and durable tumor-specific CD8$^+$ T cell responses with similar kinetics to that observed in non-hematopoietic PD-L1 chimeras (Figure 2.1J).

These data support the hypothesis that the tumor-associated lymphatic vasculature induces IFNγ-dependent adaptive immune resistance with direct consequences for local, cytotoxic immunity *in vivo*. Taken together with our results in viral infection, we suggest that IFNγ-mediated activation of the lymphatic endothelium is a tissue-resident protective response limiting tissue damage that is coopted in tumor microenvironments for immune escape.

Discussion

Tissues balance immune activation and immune suppression to mediate rapid response to pathogenic challenge while simultaneously preventing immunopathology and autoimmunity. At environmental barriers, such as skin, the balance between protection and tolerance is even more critical[243] and tumors that arise coopt mechanisms of tolerance to mediate their immune escape. The tissue-specific mechanisms that mediate the balance between immunity and tolerance, and specifically the relative contribution of circulating leukocytes and resident stromal cells, remains an open question.

While hematopoietic cells employ multiple mechanisms to suppress cytotoxic T cell accumulation and function in tumor microenvironments, this report demonstrates that non-hematopoietic LECs also regulate immune microenvironments in melanoma. While lymphatic vessel transport is required for *de novo* priming and expansion of antigen-specific immunity[53,55], we show that lymphatic vessel adaptation to infiltrating cytotoxic $CD8^+$ T cells induces compensatory, suppressive mechanisms that limit local effector function. We find that endothelial adaptation is mediated by IFNγ and part of a broader skin-intrinsic program activated across cutaneous pathologies, including acute viral infection, psoriasis, and delayed type hypersensitivity. IFNγ-sensing by cutaneous LECs activates PD-L1 expression, which we demonstrate is functional within non-hematopoietic stromal cells in tumors. Importantly, LEC-specific loss of IFNγR, and therefore inhibition of the ability for lymphatic vessels to adapt to CTLs, results in elevated pathology following cutaneous infection and improved tumor control.

Interestingly, T cells and IFNγ are implicated as negative regulators of LN lymphatic

sinus development and inflammation-induced LN lymphangiogenesis[244]. Our analyses did not reveal significant changes in gross lymphatic vessel density in either LNs or skin in IFNγR$^{\Delta LYVE1}$ mice, perhaps indicating that T cell-mediated control of lymphangiogenesis is IFNγ-independent. Interestingly, recent work demonstrates that type I rather than type II IFNs regulate contraction of LN lymphangiogenesis and that type I IFN-induced PD-L1 expression in a subset of LN LECs protects these cells from apoptosis[245]. The molecular mechanisms downstream of type I IFN and PD-L1 that mediate LEC survival, however, remain unclear. Notably loss of IFNγR on LECs did not affect constitutive PD-L1 expression in LNs and as such we saw no changes in LN lymphatic structures at steady state or during active inflammation and no changes in peripheral T cell priming. Similarly, in skin, we saw no difference in lymphatic vessel density, however, it is important to note that lymphatic vessels in highly inflamed regions of infected IFNγR$^{\Delta LYVE1}$ skin, but not adjacent normal, were negative for LYVE1. Inflamed lymphatic vessels were identified instead by their expression of podoplanin, thus leading to a reduction in LYVE1$^+$ but not podoplanin$^+$ structures in IFNγR$^{\Delta LYVE1}$ infected skin. Inflammation induces internalization of LYVE1[246] and thus loss of expression on LYVE1$^+$ structures may be a readout of local inflammation. Additionally, however, it is possible that loss of LYVE1 on peripheral lymphatic vessels is IFNγR-dependent and given the role of LYVE1 in DC transendothelial migration[123] this may be intriguing to investigate in the future.

IFNγ may be a common mechanism governing tissue homeostasis, immune resolution, and tumor immune evasion. Migratory DCs respond to IFNγ at steady state and inhibit T cell priming as a mechanism of peripheral tolerance and tumors recall this homeostatic program to prevent robust anti-tumor immune activity[247]. Our data further demonstrates that IFNγ-mediated crosstalk between the tumor-associated lymphatic vasculature and infiltrating CTLs has a negative impact on anti-tumor immunity. Thus, while IFNγ is critical for effector function within tumor microenvironments[248], it may additionally signal to initiate programs of resolution and evasion where multiple cell types, both hematopoietic and non-hematopoietic, contribute. These mechanisms compete with cytotoxic activity in tumors and may partially explain the poor clinical utility of IFNγ

treatment in the clinic where it was found to induce T cell suppression[249,250]. Importantly, while T cells are sufficient to activate IFNγ-dependent mechanisms of immune suppression, they are not necessary and other IFNγ secreting cells, such as NK cells, may also contribute.

One component of IFNγ-driven immune evasion in tumors, termed adaptive immune resistance[71], is the expression of the immune checkpoint PD-L1. Several recent reports specifically demonstrate that loss of PD-L1 by either tumor cells or the host into which those cells are implanted results in improved tumor control[73,90,107], providing strong evidence that PD-L1 expressed by the tumor microenvironment is relevant for therapy. These studies, however, did not interrogate the role of non-hematopoietic, non-tumor PD-L1 expression, leaving this question open. Similar to our data, the functional significance of loss of PD-L1 on one or more cellular components within the tumor microenvironment is highly dependent upon the model chosen[73], indicating multiple, overlapping mechanisms that mediate immune escape. That the functional relevance of lymphatic vessel IFNγR was revealed only in immunogenic tumor models (YUMMER1.7) and when T cell-activating therapies (LM and adoptive T cell transfer) were administered to poorly immunogenic tumors (B16F10 and YUMM1.7) supports the model of adaptive immune resistance whereby infiltrating CTLs activate multiple mechanisms of local immune suppression (e.g. IDO, regulatory T cells etc) that ultimately feedback and limit their function. Importantly, growth of a variety of melanoma cell lines in mice whose lymphatic vessels lack IFNγR directly mirrors their sensitivity to PD-L1 blockade *in vivo*. Furthermore, while these adaptive mechanisms of suppression are activated in the presence of potent immunity, alternative mechanisms of tumor suppression are dominant in progressing, poorly immunogenic tumors. Notably, myeloid-targeted therapy effectively mobilized anti-tumor CTLs in checkpoint-insensitive YUMM1.7 tumors[251–253].

Our data importantly extends previously reported roles for non-hematopoietic PD-L1 in infection[76,92] and sterile inflammation[97] to tumor microenvironments. During chronic *lymphocytic choriomeningitis* (LCMV) infection non-hematopoietic PD-L1 delays viral clearance, but prevents overt immmunopathology[76], where loss of PD-L1 on infected en-

dothelium leads to barrier breakdown and fatal circulatory failure[92]. LCMV importantly infects vascular endothelium and as such PD-L1 protects endothelial cells from cytotoxic killing. Here we demonstrate that loss of IFNγR and thus PD-L1 expression on LECs during acute viral infection increased VacV-specific $CD8^+$ T cell accumulation in skin leading to enhanced local pathology though viral clearance was unaffected. Importantly, LECs are not directly infected in this model[53], however, it is unknown whether antigen-presentation is necessary for the observed PD-L1 dependent T cell control. In tumors, both tumor and myeloid cells express PD-L1 and their simultaneous presentation of antigen may also be required for PD-L1-dependent inhibition of $CD8^+$ T cell effector function[73]. While LECs are capable of scavenging and cross-presenting antigen to $CD8^+$ T cells *in vitro*[144] and in vivo[145], and inhibition of PD-L1 on antigen-pulsed LECs *in vitro* enhances $CD8^+$ T cell priming[111], whether tumor-specific antigen presentation is required for effector $CD8^+$ T cell control mediated by LEC PD-L1 *in vivo* remains unclear.

Alternatively, PD-L1 may function on non-hematopoietic cells to regulate lymphocyte migration across barrier tissues, both endothelial and epithelial. PD-L1 expressed on BECs inhibits transmigration in multiple sclerosis[99]; loss of PD-L1 on corneal epithelium results in pathological $CD8^+$ T cell infiltration and chronic dry eye disease[98]; and PD-1 on islet-specific $CD4^+$ T cells impairs pancreatic infiltration and diabetes onset in mice[103]. Furthermore, normalizing doses of anti-angiogenesis therapy induced PD-L1 expression by tumor-associated blood vessels leading to a synergistic response with PD-1 blockade and improved CTL infiltration into tumor parenchyma[91]. Whether PD-L1 expressed on endothelial cells specifically regulates T cell transendothelial migration in the absence of simultaneous antigen presentation remains to be carefully studied *in vivo*.

Herein, we provide two lines of evidence to support *in vivo* functionality of non-hematopoietic, LEC PD-L1. First, we generate bone marrow chimeras that lack PD-L1 expression on hematopoietic and non-hematopoietic cells to demonstrate that non-hematopoietic PD-L1 expression, in addition to expression by hematopoietic cells, influences intratumoral T cell activity. Second, we eliminate induction of PD-L1 expression in a cell-specific manner by preventing LEC response to IFNγ. Using two lymphatic-specific

Cre recombinases, we demonstrate that loss of IFNγ-sensitivity specifically in lymphatic vessels unleashes $CD8^+$ T cell immunity within tumor microenvironments leading to persistent tumor control. Furthermore, using the immunogenic melanoma cell line, YUMMER1.7, we demonstrate that both loss of non-hematopoietic PD-L1 and loss of lymphatic vessel IFNγR exhibit similar patterns of tumor control, which initiate following T cell accumulation in tumors approximately 10 days post implantation. It is still possible, however, that a broader program of IFNγ-dependent immune suppressive mechanisms contribute to the observed effects seen following lymphatic vessel-specific IFNγR deletion and thus further exploration of the cellular and molecular mechanisms regulated by IFNγ on peripheral lymphatic vessels is warranted.

Importantly, we observed systemic expansion of effector immunity in both PD-$L1^{-/-}$ mice and those treated with antibodies blocking PD-L1. Loss of PD-L1 in the hematopoietic compartment was sufficient for systemic effects indicating that hematopoietic PD-L1 may function to limit T cell priming or expansion in response to tumor antigen presentation in dLNs, as is also seen in LCMV Clone 13 infection[76]. Consistent with the hypothesis that new lymphocyte recruitment contributes to PD-L1-based therapies, administration of the small molecule FTY720, to prevent LN egress, inhibits α-PD-L1 therapy in tumor models[90]. We observe elevated PD-L1 expression on migratory, cross-presenting $CD103^+$ DCs required for antigen-specific T cell priming in LNs draining murine melanoma[54], while non-hematopoietic PD-L1 expression in LNs stromal cells[109] remains unchanged. Thus, our data, together with recently published work, indicates distinct roles and anatomical sites of action for hematopoietic and non-hematopoietic PD-L1 in the host response to tumors.

Finally, our data expands our model of lymphatic vessel contribution to anti-tumor immunity[115]. VEGF-C-driven tumor associated lymphangiogenesis is correlated with increased intratumoral inflammation and immune suppression in progressing tumors[145], but also generates tumor microenvironments more amenable to immunotherapeutic intervention[225]. It is interesting to speculate that the suppressive mechanism elucidated here may explain the improved response to immune checkpoint blockade in lymphangiogenic tu-

mors[225]. While lymphatic vessels promote the recruitment and accumulation of T cell inflammation in tumor microenvironments, we show that their activation in this context generates negative feedback that if inhibited revives peripheral immune responses. As such lymphatic vessels may be necessary for positive response to immune checkpoint blockade. Furthermore, and consistent with previous work demonstrating that lymphatic vessel density stratifies tumors with elevated TIL[55,223,224], we demonstrate that the lymphangiogenic tumor stroma in primary human melanoma accumulates significant $CD8^+$ T cell infiltrates. It is important to note that our samples exhibited a dominant excluded infiltrate phenotype and thus our specific correlation with peritumoral infiltrates. Whether changes in lymphatic vessel density only predict peritumoral rather than intratumoral accumulation remains to be evaluated in larger cohorts. A broader range of T cell involvement in melanoma, however, is captured by TCGA analysis, which indicates correlation between lymphatic-specific genes and T cell inflammation across all tumors, though the geographic distribution of T cells is lost.

Our cumulative work now demonstrates that while the existing lymphatic vasculature is required for de novo T cell priming[53,55], the remodeled, inflamed peripheral lymphatic vasculature sequesters and inhibits effector immunity directly in peripheral tissue leading to tumor progression and contributing to locoregional metastasis[254,255]. Ultimately, though therapies targeting the suppressive tumor microenvironment can rescue anti-tumor immunity, tissues ultimately activate multiple compensatory mechanisms to limit effector T cell immunity, driving return to homeostasis and immune escape.

Taken altogether, the lymphatic vasculature, as a part of the non-hematopoietic tumor stroma, is an active barrier to the effector arm of anti-tumor immune responses. The lymphatic vasculature activates programs of adaptive immune resistance following accumulation of interstitial antigen-specific immunity thus acting as a tissue-resident, immunological switch that balances immune function and damage. We propose that tissues provide a physical scaffold within which immune responses must exert their effector function and therefore are important regulators of local responses. It is interesting to speculate how, as this tissue microenvironment is altered by pathological state, environmental challenge, or

age, regional immunity may be similarly altered. Consideration of these tissue-specific effects may provide critical insight into the heterogeneous responses observed across tissue and tumor sites[226] and may provide unique biomarkers of therapeutic response, and consequently new local targets for clinical intervention.

Baseline Characteristic in Cohort at Inclusion	
Number of patients	17
Age, years	
Median (range)	55 (27-98%)
Primary Site	
Trunk	8 (47.1%)
Upper Limb	6 (35.3%)
Lower Limb	2 (11.8%)
Other and Face	1 (5.9%)
Tumor size , mm	
Median (range)	1.7 (1.0-6.9)
TNM[a] staging	
1A 1	(5.9%)
1B 8	(47.1%)
2A 3	(17.6%)
2B 3	(17.6%)
2C 2	(11.8%)
Lymphovascular Invasion	
Not Present	7 (41.2%)
Unknown/Indeterminate	10 (58.8%)
Metastasis	
No Regional LN[b]	17 (100%)
Distal Metastasis	0 (0%)
Ulceration	
ulcerated	6 (35.3%)
non-ulcerated	11 (64.7%)
Mitoses	
present	7 (41.2%)
absent	3 (17.6%)
N/A	7 (41.2%)
Clark Level	
I 0	(0%)
II 0	(0%)
III 2	(11.8%)
IV 2	(11.8%)
Unknown	13 (76.5%)

Table 2.1: Baseline characteristics of primary melanoma cohort at inclusion [a]TNM Classification of Malignant Tumors (TMN); [b]Lymph node (LN)

Chapter 3:

PD-L1 Blockade Increases Leukocyte Accumulation in Non-Inflamed Skin

Introduction

Immune checkpoint blockade targeting programmed cell death receptor 1 (PD-1) or its ligand (PD-L1) has been successful in the clinic to treat metastatic cancer, however, treatment is often limited by off target immune related adverse events (irAEs). IrAEs are often low grade and include manifestations like rash and pruritus[256–258] that require little intervention. However, more serious irAEs, such as colitis and pneumanitis, can be life threatening, requiring treatment discontinuation in 7-17% of patients[259,260]. This number increases to 40% of patients when PD-1 and CTLA4 immune checkpoint blockades are combined[41,259,260]. Importantly, irAEs requiring treatment discontinuation may signify a clinical response by the tumor[261], therefore, decoupling irAEs from the antitumor effects of immune checkpoint blockade may allow elimination or prevention of irAEs *without* treatment discontinuation. Uncovering the mechanisms that contribute to α-PD-L1-mediated irAEs is the first step to decoupling the effects of irAEs from the beneficial antitumor function of treatment.

During α-PD-L1 therapy, the accumulation of T cells in non-tumor tissues contributes to irAE formation. Though effector and memory T cells express the adhesion molecules and chemokine receptors required for extravasation into tissues[66,170], they only infiltrate tissues marked by activated vascular endothelium[67]. Conversely, uninflamed endothelium prevents T cell entrance by not expressing the cell adhesion molecules required for extravasation. Loss of the selectivity of this barrier could result in increased lymphocyte dissemination and therefore increased probability that a self reactive T cell would en-

counter its antigen in a tissue that it would normally be restricted from. The accumulation of T cells in non-tumor tissues during α-PD-L1 therapy is associated with outbreaks of irAEs such as autoimmune vitiligo[262]. Therefore during α-PD-L1 therapy either tissues are becoming inflamed everywhere and allowing T cells to enter, or α-PD-L1 therapy is permitting unrestricted access into non-inflamed tissues such that self reactive T cells encounter their antigen and drive local reactivity.

Previously, I showed that tumor associated BECs express PD-L1 (Figure 2.3) and demonstrated, using PD-L1$^{-/-}$ bone marrow chimeras, that loss of non-hematopoietic PD-L1 increases CD8^{+} T cell accumulation in tumors without increasing systemic activation[70]. We also know that BECs express PD-L1 at steady-state in the skin of mice[70], however, it is unknown whether blockade of this source of PD-L1 contributes to increased T cell accumulation in non-tumor sites and irAE formation. One possible hypothesis is that non-hematopoietic PD-L1 limits T cell trafficking into or out of the tumor microenvironment. Here I test the hypothesis that BEC PD-L1 regulates leukocyte dissemination to distal, non-tumor tissues and when blocked during α-PD-L1 immunotherapy contributes to onset of irAE formation.

Results

BECs increase PD-L1 systemically during localized inflammation

We observed constitutive expression of PD-L1 in cutaneous BECs both at steady-state and in response to challenge (Figure 3.1 A & B). We induced cutaneous inflammation by intradermal tumor implantation, vaccinia virus (VacV) infection by scarification, delayed type hypersensitivity response, or immiquimod induced psoriasis and assessed BEC PD-L1 expression at the site of inflammation as well as in contralateral skin. This revealed that, unlike LECs whose PD-L1 expression is restricted to sites of inflammation, BECs increased PD-L1 expression in contralateral skin (Figure 3.1 C). IFNγ can induce PD-L1 expression on endothelial cells[70,111], therefore to test whether BEC PD-L1 increased in contralateral skin is IFNγ-dependent I infected mice with VacV and administered IFNγ-neutralizing antibody on day 3 and 6 post infection and then harvested contralateral skin

on day 7. Indeed IFNγ neutralization decreased BEC PD-L1 expression (Figure 3.1 D). Interestingly, it was not completely reduced, but was brought back down to the level of naive ear skin, indicating that the low level of PD-L1 in steady-state skin may be IFNγ-independent.

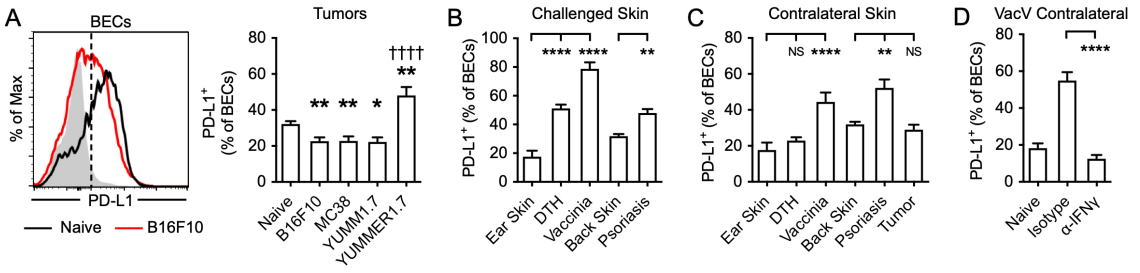

Figure 3.1: BEC PD-L1 is increased systemically during inflammation (A) Representative histogram (Isotype control, gray, naive skin, black, and B16F10 tumor, red) of BEC PD-L1 expression in B16F10 tumors and quantification of BEC PD-L1 expression in naive back skin and across indicated tumor models. (B & C) PD-L1 expression by BECs in inflamed (B) or contralateral (C) skin of mice challenged with Vaccinia virus (Vaccinia), delayed-type hypersensitivity (DTH), imiquimod-induced psoriasis (Psoriasis), or B16F10 melanoma (tumor). (D) BEC PD-L1 expression in skin contralateral to VacV infection in mice treated with α-IFNγ or IgG isotype control. One-way ANOVA corrected for multiple comparisons (A-C). Students T test (D). NS = not statistically significant $*p<0.05$, $**p<0.01$, $****p<0.0001$.†††† $p<0.0001$ (compared to B16F10)

A subset of postcapillary venule BECs actively express STAT1-dependent PD-L1 at steady-state in skin

Since cutaneous BECs express PD-L1 at steady state, and increase its expression in contralateral skin following infection (Figure 3.1), it is likely that this PD-L1 may be a target of α-PD-L1 blockade when given intravenously. Whether antibody blockade of BEC PD-L1 has a functional significance is unclear. One key EC barrier function includes regulating leukocyte transmigration. If BEC PD-L1 expression contributes to barrier selectivity, then we hypothesize that BECs would express PD-L1. Therefore we started by determining the extent to which PD-L1 is expressed by BECs in various tissues at steady-state. About 40% of BECs isolated from skin, small intestine, and heart express PD-L1 at steady-state in naive mice, while less than 10% of brain and lung ECs express PD-L1 (Figure 3.2 A). Since IFNs induce PD-L1 expression by LECs[70], we hypothesized that BEC PD-L1 at steady-state is maintained by tonic IFN signaling. STAT1 is required downstream of IFN receptors[263] and is necessary for IFNγ-inducible PD-L1 expression in LECs[70], therefore to test the hypothesis that BEC PD-L1 at steady-state is maintained by tonic IFN signaling we looked at PD-L1 expression in tissues from STAT1$^{-/-}$ mice. Indeed, PD-L1 expression was decreased in STAT1$^{-/-}$ mice compared to WT mice (Fig-

ure 3.2 B). Interestingly, there was no change in steady-state ICAM or P-selectin expression by BECs in tissues from STAT1$^{-/-}$ mice (Figure 3.2 C & D), indicating that steady-state PD-L1, but not adhesion molecule, expression is maintained by a STAT1-dependent signal. Cluster analysis performed on flow cytometry data of steady-state BECs isolated from mouse skin revealed subsets of cutaneous BECs and segregation of PD-L1^{+} and ICAM^{+}/P-selectin^{+} populations (Figure 3.2 E). Quantification of ICAM and P-selectin expression by PD-L1^{+} (P^{+}) and PD-L1^{-} (P^{-}) revealed that PD-L1^{-} BECs express more ICAM and P-selectin at steady-state in the skin of mice (Figure 3.2 F & G). Lymphocytes transmigrate through postcapillary venules[264], therefore we wanted to test whether PD-L1 is expressed by BECs that comprise postcapillary venules which can be identified by their expression of the glycoprotein endomucin[265]. PD-L1 expression is enriched on endomucin^{+} BECs compared to endomucin^{-} BECs in the skin of mice at steady-state (Figure 3.2 H). This also revealed that, as expected, ICAM and P-selectin expression are also enriched on the endomucin^{+} BECs comprising postcapillary venules and indicates that these are likely different capillary populations since PD-L1 and cell adhesion molecule expression is mutually exclusive (Figure 3.2 I & J). Altogether this demonstrates that a subset of postcapillary venules express STAT1-dependent PD-L1 at steady-state in the skin of mice. Whether postcapillary venule PD-L1 expression contributes to leukocyte accumulation in skin is unclear and an interesting question moving forward.

PD-L1 blockade does not change systemic immune response during Vaccinia virus infection

To test the effect of BEC PD-L1 on leukocyte trafficking into uninflamed skin we used used scarification with vaccinia virus (VacV) as a model to generate a systemic immune response that only homes to the infected skin, leaving uninflamed contralateral skin largely uninfiltrated[66]. Since BECs in contralateral skin express PD-L1(Figure 3.1 C) and elevate expression in response to distal challenge, this gives us a model to ask whether α-PD-L1 administration increases leukocyte infiltration to uninflamed skin. We first asked whether α-PD-L1 administration changed systemic immune responses during VacV infection. Mice were treated with α-PD-L1 and then infected with VacV by scarification on

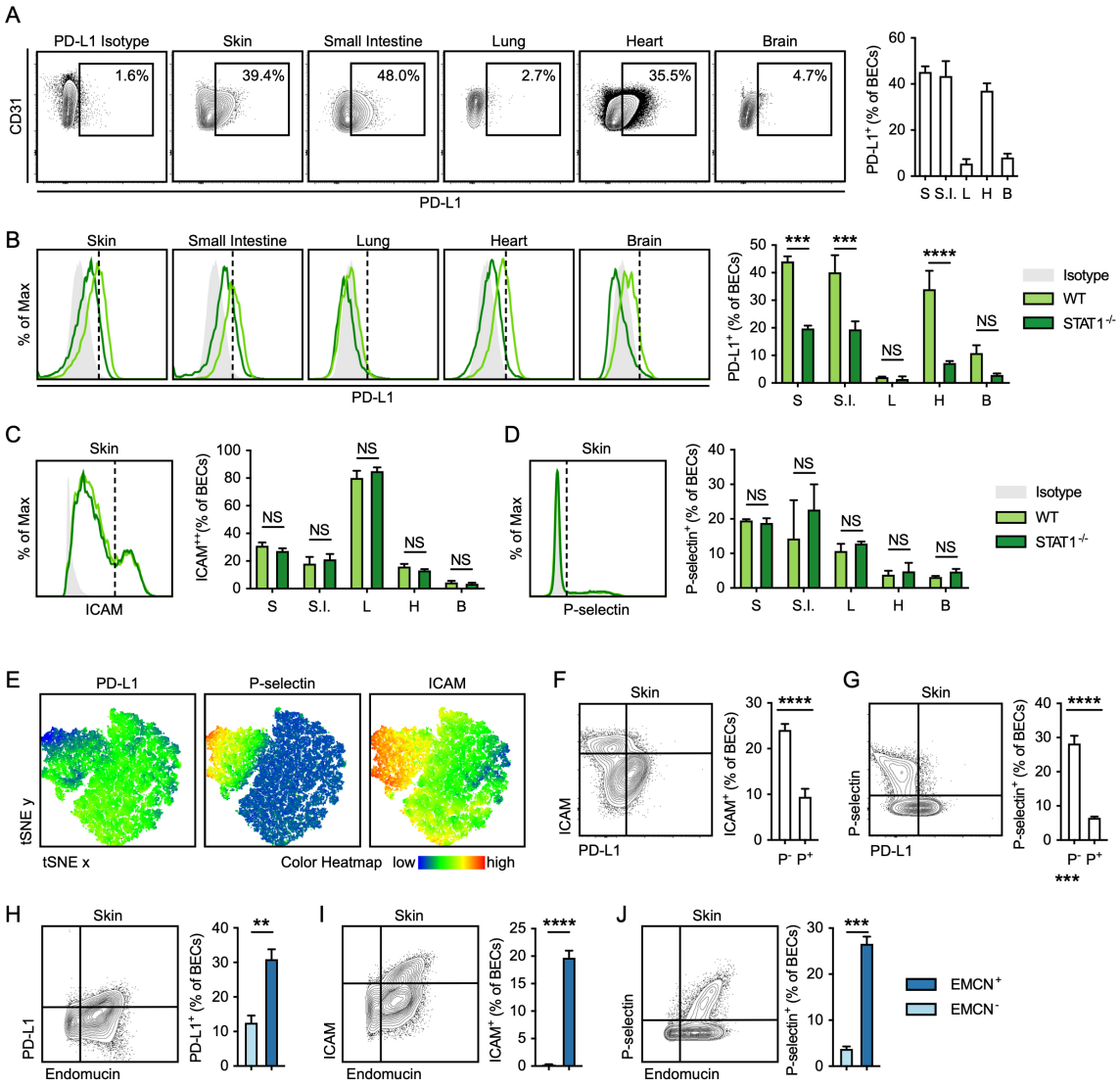

Figure 3.2: A subset of capillary BECs express STAT1 dependent PD-L1 at steady-state (A) Representative flow cytometry plots and quantification of PD-L1 expression by steady-state BECs harvested from skin (S), small intestine (S.I.), lung (L), heart (H), and brain (B) of mice. (B-D) Representative histograms and quantification of PD-L1 (B), ICAM (C), and P-selectin (D) expression on steady-state BECs harvested from skin (S), small intestine (S.I.), lung (L), heart (H), and brain (B) of WT (light green) or STAT1$^{-/-}$ mice (dark green). (E) Color heatmaps of PD-L1, ICAM, and P-selectin expression by cutaneous steady-state BECs follow cluster analysis. (F & G) Representative flow plots of ICAM (F) and P-selectin (G) expression and quantification of ICAM (F) and P-selectin (G) expression as a percent of PD-L1^{+} (P^{+}) and PD-L1^{-} (P^{-}) steady-state BECs in the skin of mice. (H-J) Representative flow plots and quantification of PD-L1 (H), ICAM (I), and P-selectin (J), expression as a percent of endomucin^{+} (dark blue) or endomucin^{-} (light blue) steady-state BECs in skin of mice. One-way ANOVA corrected for multiple comparisons (B-D). Students T test (F-J). NS = not statistically significant, $**p<0.01$, $***p<0.001$, $****p<0.0001$

the ear pinna and tissues harvested either 1 or 10 days post infection (schematic, Figure 3.3 A). Flow cytometry analysis (gating scheme, Figure 3.3 B) revealed that α-PD-L1 treatment did not change the number of systemic Ly6C^{hi} or Ly6C^{mid} monocytes, neutrophils, CD4^{+} T cells, CD8^{+} T cells, or MHC-I H2k^{b}-restricted B8R$_{20\text{-}27}$-specific CD8^{+} T cells specific at either 1 or 10 days post infection (Figure 3.3 C & D). Thus, we concluded that any changes we see in tissues likely stems from differences in trafficking.

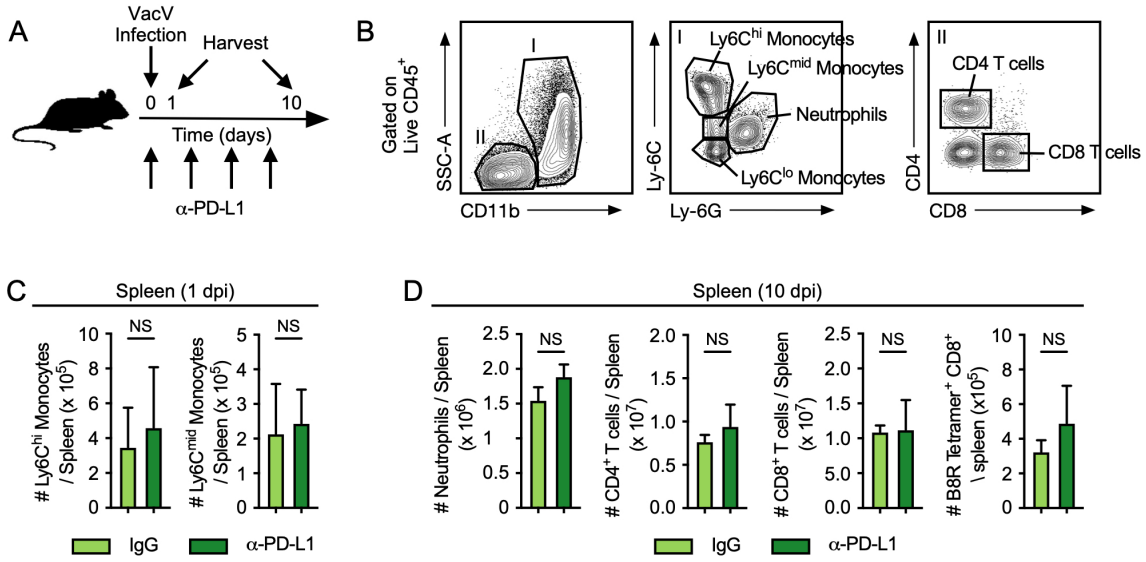

Figure 3.3: α-PD-L1 blockade does not effect the number of circulating leukocytes during vaccinia infection (A) Schematic: mice were infected by scarification with VacV on left ear pinna. Antibodies were administered every three days starting on day 0. Mice were euthanized and tissue collected on days 1 and 10 post infection. (B) Flow cytometry gating scheme for leukocyte populations indicated. (C) Quantification of total number of Ly6C^{hi} and Ly6C^{mid} monocytes in spleens of mice treated with α-PD-L1 (dark green) or rat IgG control (light green) 1 day post infection. (D) Quantification of total number of neutrophils, CD4$^+$ T cells, CD8$^+$ T cells, and B8R-specific CD8$^+$ T cells in spleens of mice treated with α-PD-L1 (dark green) or rat IgG control (light green) 10 days post infection. Students T test. NS = not statistically significant

PD-L1 blockade increases leukocyte accumulation in non-inflamed skin independent of PD-1

Next, to investigate the contribution of BEC PD-L1 on leukocyte trafficking to inflamed skin we treated mice with α-PD-L1 or rat IgG isotype control, infected with VacV, and harvested the infected and contralateral uninfected ears 1 day post infection. We noticed a two fold increase in accumulation of Ly6C^{mid} and Ly6C^{mid} immature monocytes in uninfected ears of mice treated with α-PD-L1 compared to isotype control (Figure 3.4 A). We also observed an increase in Ly6C^{mid} but not Ly6C^{hi} monocytes in infected ears of mice treated with α-PD-L1 (Figure 3.4 B). Importantly, this occurred despite no change in circulating monocyte populations (Figure 3.3 C). Interestingly, neither Ly6C^{mid} or Ly6C^{hi} monocytes expressed PD-1 in spleens, infected skin or contralateral skin (Figure 3.4 C). This raised the interesting possibility that PD-1 ligation by PD-L1 might not be required for increased monocyte accumulation in skin. Next to test whether PD-L1 blockade would also increase T cell accumulation in the skin we infected mice with VacV in one ear and treated with either α-PD-L1 or IgG isotype every three days and harvested on day 10 at the peak T cell response[53]. We noticed a 4-fold increase in neutrophils, and 2-fold increases in CD4$^+$ T cells, CD8$^+$ T cells, and B8R-specific CD8$^+$ T cells specific for the

immunodominant epitope of VacV in contralateral skin of mice treated with α-PD-L1 compared to isotype controls (Figure 3.4 D). Strikingly, we did not see any increase in these populations in the infected ear (Figure 3.4 E) or spleens (Figure 3.3 D) of mice treated with α-PD-L1. While there was little to no PD-1 expression on $CD4^+$ T cells, $CD8^+$ T cells or B8R-specific $CD8^+$ T cells in the spleen, all T cell subsets we analyzed expressed high levels of PD-1 in both infected and contralateral ears (Figure 3.4 F). Tissue infiltrating neutrophils remained PD-1 negative (Figure 3.4 F). To test the hypothesis that PD-L1 blockade increases leukocyte recruitment independent of PD-1 expression, mice were treated with α-PD-1 blocking antibody, then infected in one ear with VacV, and tissues harvested 1 day post infection. There was no change in $Ly6C^{mid}$ or $Ly6C^{hi}$ monocyte accumulation in contralateral or infected ears of mice receiving α-PD-1 blocking antibody (Figure 3.4 G & H). This indicates that α-PD-L1 blockade may promote leukocyte recruitment in non-inflamed skin independent of PD-1 ligation.

Discussion

Here I demonstrate that BECs express PD-L1 in inflamed tissue environments as well as in skin contralateral to inflammation . Further I show that steady-state BECs in skin, small intestine, and heart, but not in lungs or brain, express PD-L1 that is dependent on host STAT1 signaling. Interestingly, PD-L1 expression marks a subset of postcapillary venule BECs in the skin that is unique from those that constitutively express the adhesion molecules ICAM and P-selectin. PD-L1 blockade during VacV infection increases $Ly6C^{hi}$ and $Ly6C^{mid}$ monocyte accumulation in uninfected skin 1 day post infection. Extending PD-L1 blockade 10 days post infection led to increased neutrophil, $CD4^+$ T cells, $CD8^+$ T cells, and B8R-specific $CD8^+$ T cell accumulation in uninfected skin. Importantly, α-PD-L1 did not change the number of circulating $Ly6C^{hi}$ and $Ly6C^{mid}$ monocytes on day 1 post infection or neutrophil, $CD4^+$ T cells, $CD8^+$ T cells, and B8R-specific $CD8^+$ T cells on day 10 post infection, indicating that changes in tissue accumulation were not due to increased systemic populations. Monocytes that accumulated in uninfected or infected skin did not express high levels of PD-1 and PD-1 blockade did not recapitulate increased

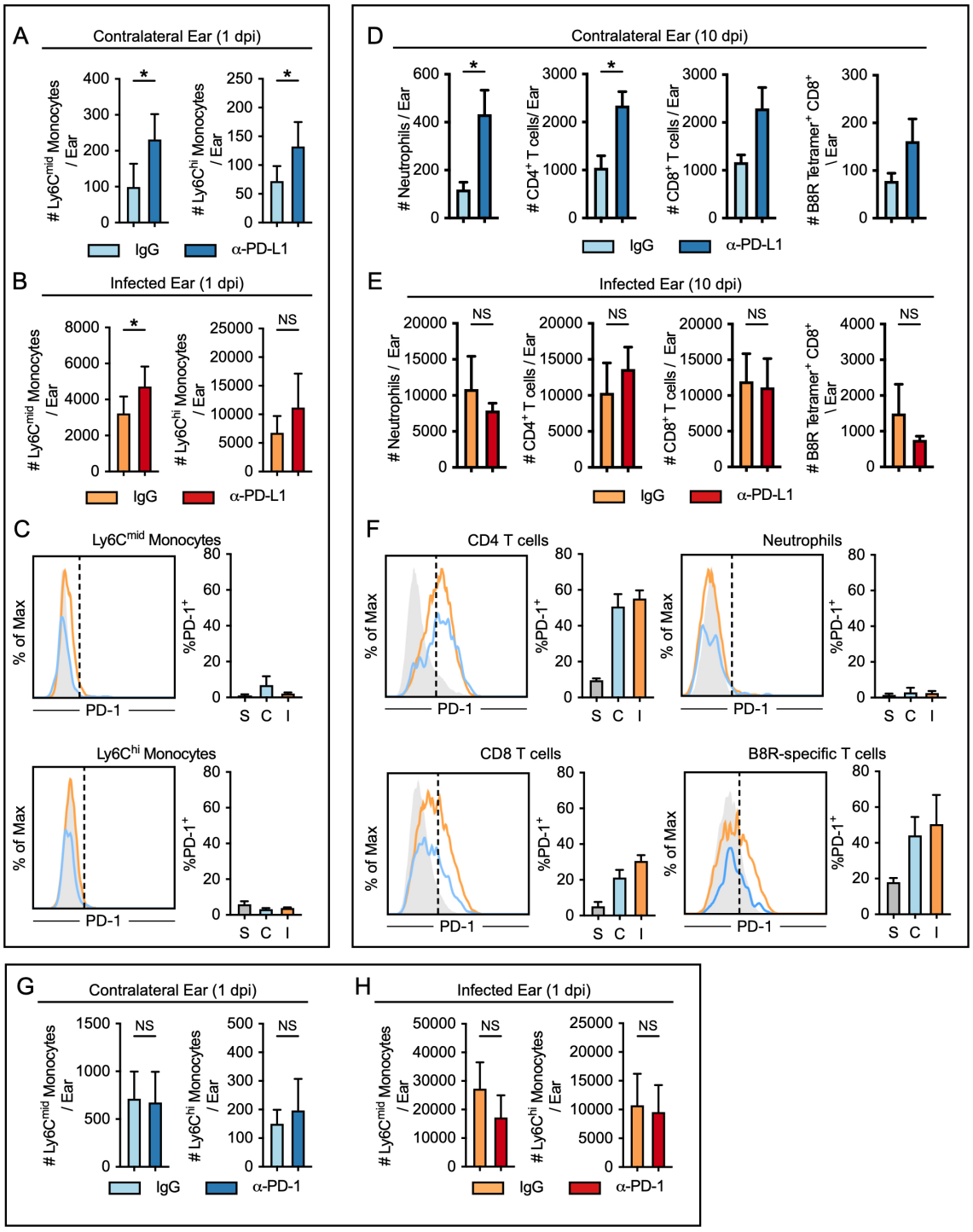

Figure 3.4: PD-L1, but not PD-1 blockade increases leukocytes in uninfected skin Mice were infected with VacV by scarification of the left ear pinna and treated with α-PD-L1, α-PD-1, or IgG every three days beginning on day0. (A & B) Quantification of total number of Ly6C^{hi} and Ly6C^{mid} monocytes in contralateral uninfected (A) or infected (B) ears of mice treated with α-PD-L1 or IgG 1 day post VacV infection. (C) Representative histograms and quantification of PD-1 expression by Ly6C^{mid} and Ly6C^{hi} monocytes isolated from spleens (gray), contralateral ear skin (blue) or infected ear skin (orange) 1 day post VacV infection. (D & E) Quantification of total number of Neutrophils, CD4$^+$ T cells, CD8$^+$ T cells, or B8R-specific CD8$^+$ T cells in contralateral, uninfected (D) or infected (E) ears on day 10 post infection of mice that were treated with α-PD-L1 or isotype control. (F) Representative histograms and quantification of PD-1 expression by Neutrophils, CD4$^+$ T cells, CD8$^+$ T cells, and B8R-specific CD8$^+$ T cells in spleens (gray), contralateral uninfected ear skin (blue), or infected ear skin (orange) on day 10 post infection. (G & H) Quantification of Ly6C^{hi} and Ly6C^{mid} monocytes in contralateral uninfected (G) or infected (H) ear skin on day 1 post infection of mice treated with α-PD-1 or IgG. Students T test. NS = not statistically significant, $*p<0.01$

monocyte accumulation seen with α-PD-L1 treatment, indicating that PD-L1 may impact leukocyte accumulation independent of PD-1.

Reduced PD-L1 expression on homeostatic BECs in STAT1$^{-/-}$ mice indicates that a STAT1-mediated signal is required for steady-state BEC PD-L1 it does not demonstrate that this signal is directly on BECs. A BEC-specific STAT1$^{-/-}$ transgenic mouse would determine whether STAT1 signaling within BECs is required or if there is another cell type mediating this response. Nonetheless, my work shows that PD-L1 marks a subset of capillary BECs that are distinct from those that express ICAM and P-selectin at steady-state. Whether PD-L1^{+} BECs are interspersed with ICAM^{+}/P-selectin^{+} BECs within the same capillary or whether each subtype represents its own individual capillary is unclear. How these two BEC subsets might differentially impact leukocyte entry into tissues remains an interesting question moving forward.

I also demonstrate that PD-L1 blockade during acute viral infection increases leukocyte recruitment into non-infected skin at early and late time points. Importantly, administration of α-PD-L1 during VacV infection did not change circulating monocyte, neutrophil, or T cell populations indicating that the systemic pool able to contribute to tissue infiltration in both groups was the same. Therefore, we interpret the increased monocyte, neutrophil, and T cell accumulation in tissues as a tissue-intrinsic phenomenon. Though this experimental design demonstrates increased accumulation of leukocytes, we have not determined whether this occurred due to increased leukocyte recruitment, increased proliferation, decreased apoptosis, or decreased tissue egress during α-PD-L1 blockade. The observation that α-PD-L1 increases Ly6C^{hi} and Ly6C^{mid} monocytes early, 1 day post infection, indicates that this increase might be from increased trafficking rather than the other mechanisms that might take longer. Importantly, α-PD-1 blockade did not replicate α-PD-L1-mediated increased monocyte accumulation 1 day post infection, indicating that the PD-L1 may inhibit monocyte accumulation independent of PD-1. Consistently, monocytes that accumulated within infected or non-infected skin express low levels of PD-1.

Altogether my data demonstrates that BECs in postcapillary venules express PD-L1, and when PD-L1, but not PD-1, is blocked, monocyte accumulation increases in non-

infected skin 1 day post infection. Though I lack the tools necessary to determine whether BEC PD-L1 contributes to monocyte accumulation in uninfected skin, it is possible that BEC PD-L1 limits leukocyte accumulation by preventing leukocyte recruitment *independent* of PD-1 expression. Whether BEC PD-L1 impacts leukocyte behavior independent of PD-1 is unknown. However, the intrinsic domain of PD-L1 in murine melanoma cells inhibits STAT3 tyrosine 705 (Y705) phosphorylation and is blocked using α-PD-L1 antibody[266]. Interestingly, VEGF-A and IL-6 also signal through STAT3 Y705 phosphorylation and destabilize VE-cadherin[267,268] – VE-cadherin destabilization is required for leukocyte transmigration across endothelial barriers[166–168]. Whether PD-L1 expression on BECs limits STAT3 Y705 phosphorylation in response to VEGF-A or IL-6 such that VE-cadherin is not destabilized is unknown. Therefore I hypothesize that PD-L1 expression on capillary BECs contributes limiting leukocyte transmigration by stabilizing VE-cadherin at EC cell-cell junctions.

Future Directions

To test the hypothesis that BEC PD-L1 expression stabilizes VE-cadherin at EC junctions I will use human dermal microvascular endothelial cells (HMVECs) *in vitro* and block PD-L1 by antibody and siRNA. The readouts for these experiments will be visualization of HMVEC cell-cell junctions using immunofluorescence microscopy (IF) and analysis of phosphorylation using western blotting (WB) and IF. If PD-L1 contributes to VE-cadherin stabilization, then I anticipate that antibody blockade or knockdown of PD-L1 will result in decreased concentration of VE-cadherin at cell junctions. VE-cadherin phosphorylation at Y658 signals it for endocytosis and degradation during destabilization[269], therefore I also anticipate that PD-L1 blockade or knockdown will increase levels of Y658 phosphorylation on VE-cadherin. It is possible that loss of PD-L1 will not increase VE-cadherin stability in HMVECs *in vitro* at steady-state, but would in a context that normally induces destabilization such as VEGF-A or IL-6 signaling[267,268]. Therefore I will perform the above experiments in the presence and absence of VEGF-A and IL-6. Additionally, I will perform a cytokine array on mouse serum following VacV infection to identify any other candidates that may contribute to endothelial stability. Any novel

candidates will also be assessed as mentioned above.

To test the hypothesis that BEC PD-L1 prevents leukocyte TEM I will use *in vitro* coculture systems with HMVECs and THP-1 (monocyte) and Jurkat (T cell) cell lines. Though I hypothesize that BEC PD-L1 limits transmigration through EC junction stabilization, adhesion, rolling and stopping are all steps required for leukocyte transmigration and may be impacted by BEC PD-L1. To test the role of BEC PD-L1 on leukocyte adhesion, rolling, and stopping, I will use flow chambers covered with PD-L1^{+} or PD-L1^{-} HMVECs and flow THP-1 or Jurkat cells over them and quantify the number of cells adhering, rolling and stopping. To test whether BEC PD-L1 limits leukocyte transmigration, I will seed HMVECs onto the upper chamber of a transwell insert and place THP-1 or Jurkat cells on top in the presence or absence of PD-L1 blocking antibody. I will then count the number of cells that have transmigrated across the HMVEC monolayer into the lower chamber and anticipate that if PD-L1 limits leukocyte transmigration then I will observe increased THP-1 or Jurkat cells in the lower well when HMVEC PD-L1 is blocked or knocked down.

Conclusion

Immunotherapy harnessing the patients own immune system is an exciting approach in the clinic to treat cancer, however, accompanying the clinical responses are treatment-limiting irAEs driven by the inappropriate accumulation of T cells in non-tumor tissues (e.g. skin, lung, gut). Distinguishing between the mechanisms that contribute to clinical response and those that contribute to irAE formation is critical moving forward to maintain cancer treatment while simultaneously preventing and eliminating irAE manifestations. Under normal conditions, circulating effector and memory T cell populations are restricted access to non-tumor sites, however during α-PD-L1 therapy they gain access and initiate irAE formation, indicating that a loss of barrier selectivity by the endothelium has occurred in these tissues. Understanding whether T cell accumulation in non-tumor tissue during α-PD-L1 therapy occurs due to systemic activation of endothelium allowing leukocyte entry everywhere, or whether α-PD-L1 permits otherwise restricted access across uninflamed endothelium into non-tumor tissues is important for developing irAE

treatments.

Chapter 4:

Discussion

Summary of Key Findings

My work establishes peripheral lymphatic vessels as key players in the resolution of local immunity. Initial experiments, either eliminating lymphatic vessels completely or over expressing the lymphangiogenic growth factor VEGF-C, demonstrated the requirement for lymphatic vessels to transport antigen to lymph nodes for T cell priming. My work demonstrates that preexisting lymphatic vessels, independent of lymphangiogenesis, turn off local immunity by limiting the number of T cells accumulating in the skin. This work establishes a new paradigm that peripheral, in addition to LN resident LECs, also directly suppress T cell responses. My work identifies peripheral lymphatic vessels as an immunological switch within the TME that inhibits T cell-mediated tumor control and opens the door to future mechanistic studies to identify novel targets for immunotherapy.

My research demonstrates that non-hematopoietic sources of PD-L1 within the TME suppress T cell-mediated control of tumors. Initial experiments supported the hypothesis that tumor cell PD-L1 expression prevents T cell mediated killing, however, we now know that hematopoietic sources of PD-L1 also contribute to T cell inhibition. My work establishes BEC and LEC PD-L1 as an additional, non-hematopoietic, source contributing to dampened antitumor immunity in the TME. Further, I provide evidence that PD-L1^{+} BATF3^{+} cross-presenting DCs limit antitumor T cell activation in lymph nodes, indicating that α-PD-L1 blockade may also release PD-L1-mediated inhibition *outside* of the TME. Careful dissection using, previously unavailable, PD-L1$^{\text{floxed}}$ mice[96] is needed to determine how each cell type contributes to PD-L1-mediated antitumor T cell suppression to identify additional therapeutical targets or biomarkers predicting patient responses to immune checkpoint blockade.

Future Perspectives and New Questions

A NEW UNDERSTANDING OF PERIPHERAL LYMPHATIC VESSELS

My thesis research provides the first *in vivo* evidence that peripheral LECs inhibit effector T cell function in skin. This extends our understanding for how LECs participate in immune suppression. Prior to my research, the working model was that LN LECs delete naive, self-reactive $CD8^+$ T cells[109,110,140,143]. When tyrosinase specific $CD8^+$ T cells are transferred into transgenic mice genetically engineered to present tyrosinase peptide, they get deleted in a non-hematopoietic PD-L1 dependent manner[109,140]. This is credited to LECs because LN LECs constitutively express both the self antigen tyrosinase[110,140] and PD-L1[109] and they are the only LN stromal cell that induces tyrosinase-specific $CD8^+$ T cell proliferation *ex vivo* when pulsed with Tyr_{369} peptide[110]. However, these observations are limited to *in vitro* coculture systems or *in vivo* models requiring forced antigen presentation. Therefore, the relative physiological contribution of LECs control over $CD8^+$ T cell responses *in vivo* remained unknown. Additionally, it was unclear whether peripheral LECs may also activate similar mechanisms to control effector T cell responses in a context-dependent manner. To fill this gap I used a genetic approach to delete the IFNγR on LECs using lymphatic-specific LYVE1 or Prox-1 cre mice crossed to IFNγR^{floxed} mice. My work now demonstrates that peripheral LECs respond to IFNγ during ongoing immune responses, express PD-L1, and inhibit effector T cell accumulation *in vivo*. We interpreted increased T cell accumulation in skin without increased $CD8^+$ T cell priming as evidence that loss of IFNγR on LN LECs did not contribute to the increased T cell accumulation in the skin. Thus, the new model of how LECs participate in immune suppression is that LN resident *and* peripheral LECs both inhibit $CD8^+$ T cells, but at different times during the immune response; LN LECs delete naive self-reactive $CD8^+$ T cells in LNs and, I show, peripheral LECs limit effector T cell accumulation in tissues and therefore promote immune resolution at the end of the immune response.

I demonstrated that peripheral LECs limit T cell accumulation in skin and tumors. However, the specific mechanisms by which loss of IFNγ signaling in LECs leads to increased T cell accumulation and enhanced T cell-mediated tumor control remain un-

known. Investigating the mechanisms contributing to this enhanced tumor control may identify new targets for immunotherapy. The number of T cells present within a tissue at any given time is dependent upon mechanisms of T cell trafficking, local T cell proliferation and local T cell apoptosis. We know that lymphatic vessels provide an exit route for T cells from peripheral tissues and tumors[68] and LECs induce proliferation and dysfunctional activation (marked, in part, by increased apoptosis) of T cells *in vitro*[110,111,145]. We also know that lymphatic vessels increase chemokine expression during inflammation[131] and I demonstrate that, in addition to PD-L1, they also increase MHC-II in response to IFNγ during inflammation (Figure 4.1). This indicates that inflammation increases both chemokine expression and the molecules at the interface of a potential LEC-T cell interaction. Whether LECs limit T cell accumulation dependent upon bulk trafficking properties or through direct interaction with T cells has implications in targeting them for therapeutic blockade in humans. To test the hypothesis that IFNγ-activated lymphatic vessels limit T cell accumulation by increasing T cell egress, I would adoptively transfer photoconvertible transgenic T cells into IFNγR$^{\Delta LYVE1}$ mice, implant tumors, and track T cell egress out of the tumors. To test the hypothesis that IFNγ-activated peripheral LECs suppress proliferation or increase apoptosis of T cells in local environments, I would assess proliferation markers and annexin V staining by T cells in tumors. The results of these initial experiments would likely inform me of the overarching mechanisms contributing to increased T cell accumulation in skin and provide the rationale for more detailed experiments to dissect the molecular pathways involved.

NON-HEMATOPOIETIC PD-L1 AND BEYOND

Here I show for the first time that non-hematopoietic PD-L1 contributes to inhibiting antitumor immunity. The current model for how α-PD-L1 works in patients is that it blocks PD-L1 expressed by tumor cells in the TME, thereby allowing cytotoxic CD8$^+$ T cells to kill the tumor. As such, PD-L1 expression by tumor cells is required for patients to qualify for α-PD-L1 therapy. However, PD-L1 expression by tumor cells does not stratify patient response to therapy[74,108]; often PD-L1$^+$ patients fail to respond and PD-L1$^-$ patients do respond to α-PD-L1 therapy. This suggests that other, non-tumor, sources of

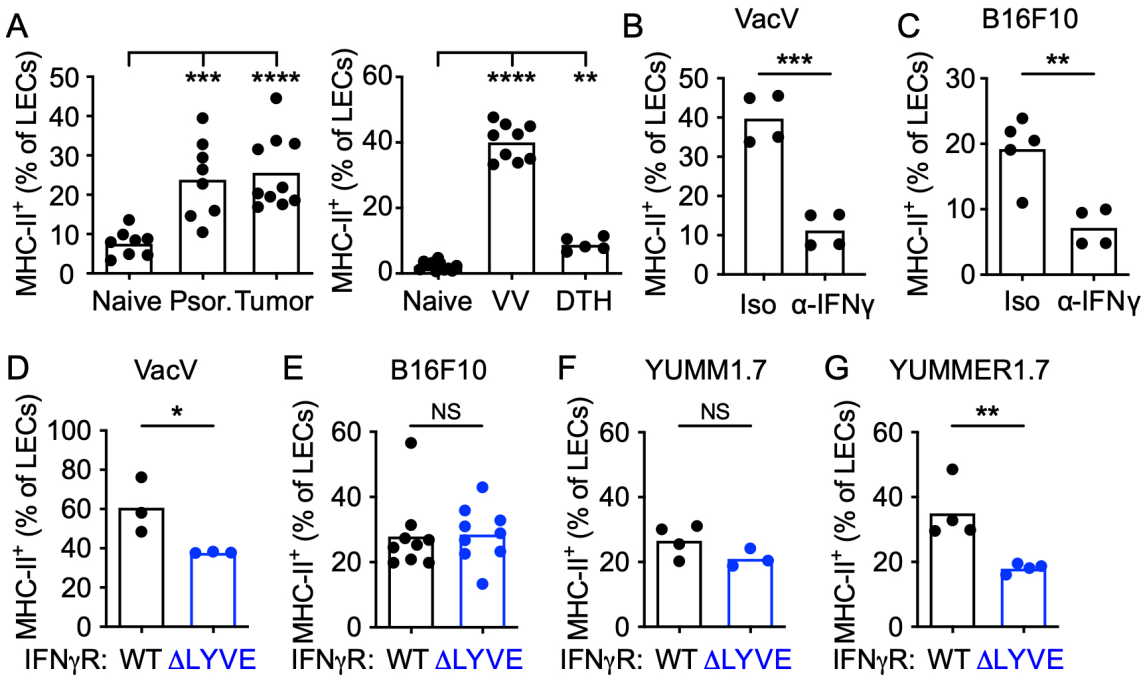

Figure 4.1: LEC MHC-II expression is dependent upon IFNγ signal directly on LECs (A) PD-L1 expression by LECs in naive or inflamed skin of mice challenged with imiquimod-induced psoriasis (Psor.), B16F10 melanoma (tumor) Vaccinia virus (VV), or delayed-type hypersensitivity (DTH). (B & C) MHC-II expression by LECs in skin infected with VacV (B) or in B16F10 tumors (C) of mice treated with α-IFNγ or isotype control. (D) MHC-II expression by LECs in ears on day 10 post infection in IFNγR$^{\Delta LYVE1}$ mice (blue) or littermate controls (black). (E-G) MHC-II expression by tumor associated LECs in B16F10 (E), YUMM1.7 (F), or YUMMER1.7 (G) tumors implanted into IFNγR$^{\Delta LYVE1}$ mice (blue) or littermate controls (black). One-way ANOVA corrected for multiple comparisons (A). Students T test (B-G). NS = not statistically significant, $*p<0.05$, $**p<0.01$, $***p<0.001$, $****p<0.0001$.

PD-L1 may also be inhibiting antitumor T cells. A complete understanding of the multiple mechanisms by which PD-L1 inhibits T cell function both within *and* outside of the TME is needed to improve therapy and to develop better biomarkers to identify those patients likely to have favorable response. Tumor cell PD-L1 prevents T cell mediated killing *in vivo*[73], however, a role for host hematopoietic PD-L1 has also recently emerged. PD-L1$^+$ myeloid cells in the TME *and* draining LNs may contribute by negatively regulating T cell activation[90,107].

Here I show that non-hematopoietic PD-L1 inhibits T cell mediated tumor control by limiting T cell accumulation in tumors. Though PD-L1 expression has previously been reported on tumor associated blood and lymphatic vessels[91,111], the specific mechanisms by which BEC and LEC PD-L1 expression contributes to T cell accumulation in tumors remains unclear. PD-L1 delivers an inhibitory signal to T cells that dampens TCR signal propagation during antigen encounter. PD-L1 expressed by infected BECs protects them from T cell-mediated killing during chronic viral infection[92] and PD-L1 blockade during *in vitro* coculture experiments increases naive CD8$^+$ T cell activation by BECs and

LECs[111,270]. Therefore, when ECs are presenting viral antigens or pulsed with peptide, they can inhibit antigen-specific T cell function. Whether tumor associated ECs present tumor antigens such that they can directly affect tumor specific T cell proliferation or apoptosis is unknown. Interestingly, LECs can scavenge and cross-present tumor antigens in the TME[145], however the functional relevance of this on antigen specific T cell function in the TME is not known. Alternatively, since BECs and LECs represent entry and exit points of the TME, respectively, it is also possible that their PD-L1 expression impacts T cell accumulation by regulating T cell trafficking into or out of the TME. Tumor associated vasculature selectively regulates leukocyte entry by several mechanisms including endothelin-1 and VEGF-A mediated down regulation of cell adhesion molecules and expression of Fas ligand[206]. Tumor associated EC PD-L1 expression may be another mechanism that selectively inhibits T cell entry into tumors. PD-L1 ligation to PD-1 on T cells, recruits SHP-2 to the cell membrane, where it dephosphorylates CD28[80]. SHP-2 however, also dephosphorylates other targets, such as focal adhesion kinase[271] and contributes to increased cellular motility[271–273]. Therefore PD-L1 expressed by tumor associated ECs may impact T cell motility on the lumenal surface and alter kinetics of adhesion, rolling, and subsequent transmigration across the endothelium independent of antigen presentation. It remains to be seen whether EC PD-L1 inhibits T cell accumulation only in tumors or may also do so other non-tumor tissues. As such, if tumor antigen is not required, then α-PD-L1 blockade may increase T cell accumulation into any tissue possessing PD-L1$^+$ BECs and contribute to irAEs in this way. A complete understanding of the mechanisms that contribute to patient response following immune checkpoint blockade will improve response and may provide insight into how to limit irAEs.

My work (Chapter 2 & Appendix A) shows that hematopoietic PD-L1 contributes to antitumor T cell activation, and therefore demonstrates that hematopoietic PD-L1 functions *outside* of the TME to limit antitumor immunity. This is important because sources of PD-L1 outside of the TME are not used to qualify patients for α-PD-L1 therapy. Despite data that demonstrates a role for hematopoietic PD-L1 in limiting T cell priming during chronic viral infection[76], the response to α-PD-1/α-PD-L1 blockade is thought to

be mediated directly in the TME. This model is supported by experiments demonstrating that the T cells present in B16F10 tumors on day 4 post implantation are sufficient to control tumors during α-PD-L1/α-CTLA4 combination therapy[69]. These studies, also demonstrated that combination therapy increases the number of circulating tumor specific T cells at later timepoints, therefore indicating that combination therapy may also increase T cell activation[69]. Whether systemic activation contributes to tumor control in patients is unknown. Further, recent data demonstrates that T cell activation is increased in tumor dLNs of mice treated with α-PD-L1[107] and the benefit of α-PD-L1 is lost in mice that have been depleted of PD-L1$^+$ CD11b$^+$ myeloid cells[90]. This, along with my data, is consistent with studies in melanoma patients showing increased circulating T cells three weeks after α-PD-1 therapy[89]. Altogether this supports a new model whereby PD-L1 both inhibits T cell function in the TME *and* restrains T cell priming in tumor dLNs, such that the efficacy of clinical blockade may stem from a release of priming inhibition independent of whether tumor cells express PD-L1 or not. Thus, biomarkers are needed for α-PD-L1 therapy beyond biopsies of the tumor, as these may identify patients with PD-L1-mediated inhibition of T cell priming that are likely to respond.

Appendix A:

T cell activation in BATF3$^{-/-}$:PD-L1$^{-/-}$ mixed bone marrow chimeras

During chronic viral infection, both hematopoietic and non-hematopoietic PD-L1 limit CD8$^+$ T cell activation and local effector function, respectively, contributing to protecting the host from viral immunopathology[76]. I demonstrated that in tumors both of these compartments contribute to decreased CD8$^+$ T cell accumulation and function within tumor microenvironments(Figure 2.1). However, while non-hematopoietic PD-L1 only had a local affect on accumulation, it appeared that hematopoietic PD-L1 also had a systemic affect on T cell activation (Figure 2.2). Interestingly, I found that CD103$^+$ and CD8α^+ cross-presenting DCs have increased PD-L1 expression in tumor DLNs compared to those in non-tumor DLNs (Figure 2.2), indicating that they may be the source of hematopoietic PD-L1 that contributes to increased systemic activation. Consistent with this, CD103$^+$ DCs are the DC responsible for CD8$^+$ T cell priming in B16F10 tumors[54]. Altogether these observations led to the hypothesis that CD103$^+$ DC PD-L1 limits antitumor T cell activation.

To test this hypothesis I implanted tumors into mice whose cross-presenting BATF3$^+$ DCs lack PD-L1 expression. To accomplish this, I generated mixed bone marrow chimeras by reconstituting lethally irradiated WT mice with a 50:50 mix of BATF3$^{-/-}$:PD-L1$^{-/-}$ bone marrow. Since BATF3$^{-/-}$ hematopoietic cells cannot form cross-presenting DCs, any cross-presenting DC in these mice is generated from the PD-L1$^{-/-}$ bone marrow and is PD-L1 deficient. Additionally, any other hematopoietic cell derived from the BATF3$^{-/-}$ bone marrow will still possess PD-L1. Thus these mice possess a PD-L1$^+$ hematopoietic compartment except for BATF3$^+$ cross-presenting DCs. I also generated WT into WT and full PD-L1$^{-/-}$ into WT (W-W, P-W, respectively) control mice. Upon verification of

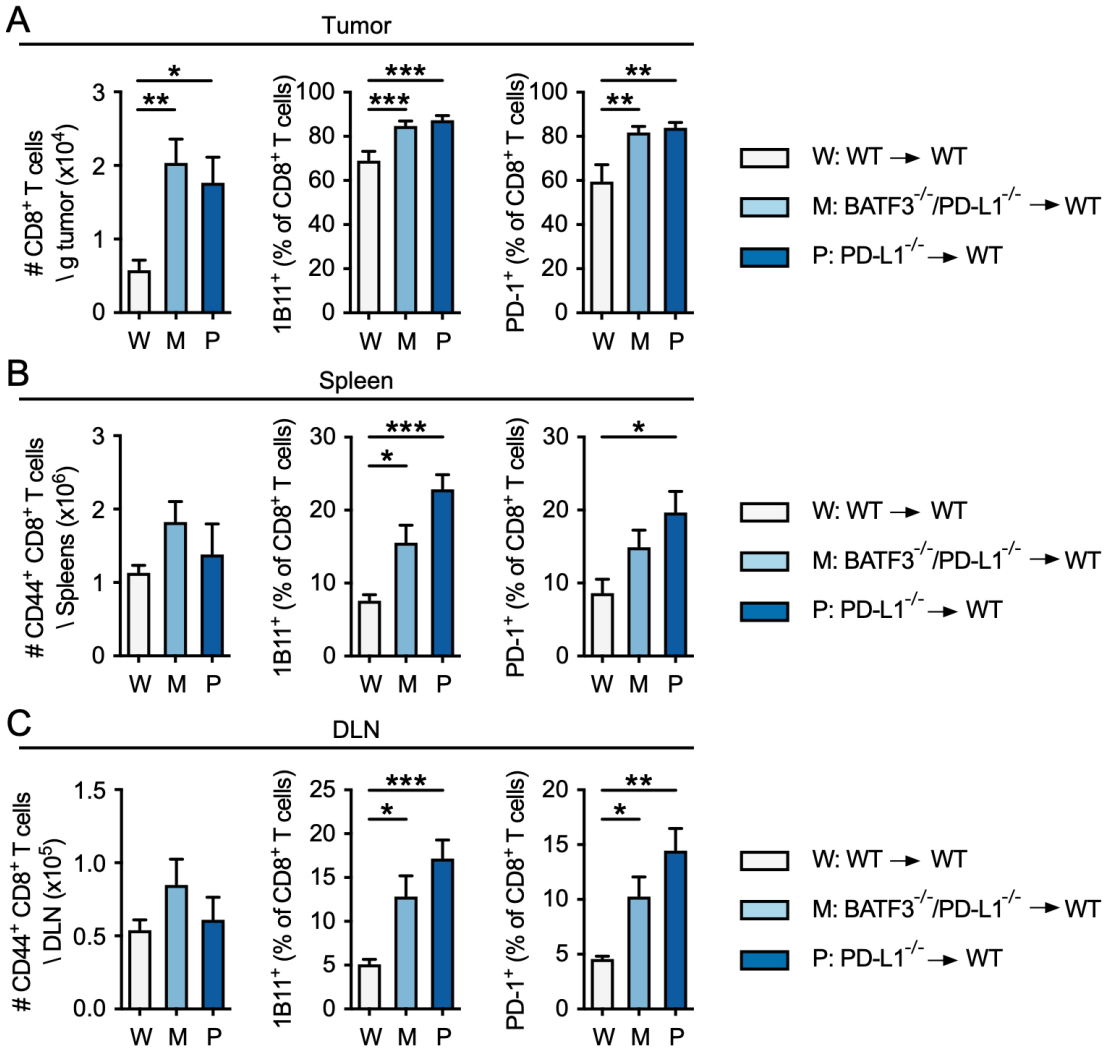

Figure A.1: Increased systemic T cell activation in BATF3-/-:PD-L1-/- mixed bone marrow chimeras Lethally irradiated WT mice were reconstituted with either WT, 50:50 mix of BATF3$^{-/-}$:PD-L1$^{-/-}$, or PD-L1$^{-/-}$ bone marrow generating WT controls (W, white), BATF3$^{-/-}$:PD-L1$^{-/-}$ mixed chimeras (M, light blue), or hematopoietic PD-L1$^{-/-}$ chimeras (P, dark blue). B16F10.OVA tumors were implanted intradermally into reconstituted chimeras. (A-C) Quantification of total number CD8$^+$ T cells (left panel) and expression of activation markers (middle and right panels) of T cells collected from tumors (A), spleens (B), and draining lymph nodes (C) of WT, mixed, and PD-L1$^{-/-}$ bone marrow chimeras on day 14 post implantation. One-way ANOVA corrected for multiple comparisons. $*p<0.05$, $**p<0.01$, $***p<0.001$

successful engraftment, I implanted tumors into these mice, monitored tumor growth, and harvested tumors and lymphoid organs on day 14 post implantation. Similar to full PD-L1$^{-/-}$ chimeras, mixed BATF3$^{-/-}$:PD-L1$^{-/-}$ chimeras also had increased tumor infiltrating CD8$^+$ T cells that expressed higher levels of activation markers (1B11 and PD-1) compared to W-W controls (Figure A.1 A). We saw no significant difference in the number of circulating CD44$^+$ activated CD8$^+$ T cells in spleens, however they expressed higher levels of activation markers in both mixed BATF3$^{-/-}$:PD-L1$^{-/-}$ and full PD-L1$^{-/-}$ chimeras, although the extent of expression in mixed chimeras was not as high as full knockouts (Figure A.1B). Similarly, there was no difference in the number of activated CD8$^+$ T cells

in draining LNs, but they expressed higher levels of activation markers (Figure A.1C). Again, the BATF3$^{-/-}$:PD-L1$^{-/-}$ mixed bone marrow chimeras did express increased activation markers, but not to the same extent as full PD-L1$^{-/-}$ chimeras (Figure A.1 C). Altogether this indicates that loss of PD-L1 by BATF3^{+} DCs, which includes both CD103^{+} and CD8α^{+} subsets, contributes to dampened antitumor CD8^{+} T cell activation.

Together, this data indicates that PD-L1 expressed by cross-presenting DCs limits antitumor T cell activation. Interestingly, circulating CD8^{+} T cells increase in melanoma patients within the first three weeks following α-PD-1 treatment[89], indicating that the effect of PD-1 therapy might occur during T cell activation or reinvigoration of exhausted T cells in LNs or spleens. Further studies are needed to determine the other cell types that contribute PD-L1. Additionally, a BATF3-cre:PD-L1$^{\text{floxed}}$ mouse is needed to definitively determine the role of cross presenting DC PD-L1 on antitumor T cell activation.

Appendix B:

Methods

Mice

Specific pathogen free C57BL/6J, and B6 CD45.1 Pep Boy mice were purchased from The Jackson Laboratory. PD-L1$^{-/-}$ were provided by Dr. Halina Offner Vandenbark, Oregon Health & Science University and Prox1:Cre-ERT2 were provided by Dr. Victor H. Engelhard, University of Virginia in agreement with Dr. Taija Makinen, Uppsala University. Tg(TcraTcrb)1100Mjb/J (OT-I mice, Stock No. 003831), Lyve1:Cre (Stock No. 012601), IFNγRfl/fl (Stock No. 025394) mice were purchased from Jackson, and all breeding was maintained at OHSU in specific pathogen free facilities. All mice were previously backcrossed over ten generations to the C57BL/6 background. Tyr:Cre-ER (Stock No. 012328), BrafV600E(Stock No. 017837), Ptenfl/fl (Stock No. 006440) mice were purchased from Jackson Labs and crossed in-house to generate Tyr::CreER;BrafCA/$^{+}$;Ptenfl/fl (BPC) mice for tumor induction. For all in vivo studies sex matched 8-10-week-old mice were used with at least 3-5 mice per group. Bone marrow chimeras were sexed matched 16-20-week-old mice. Lymph nodes from STAT1-/- mice were generously donated by the Dr. Timothy J. Nice Lab, Oregon Health & Science University. All animal procedures were approved by and performed in accordance with the Institutional Animal Care and Use Committee (IACUC) at Oregon Health & Science University.

Cell Lines

B16F10 (ATCC, Stock No. CRL-6475), B16F10.OVA murine melanoma, and MC38 murine adenocarcinoma cells (ATCC, Stock No. CRL-6475) were passaged in Dulbeccos Modified Eagle Medium (Invitrogen) supplemented with 10% fetal bovine serum (Atlanta Biologicals) and 1% penicillin streptomycin (Gibco). Yumm1.1, Yumm1.7[239], and YUM-

MER1.7[238] were passaged in 1:1 DMEM:F-12 supplemented with 1% L-glutamate, 1% non-essential amino acids, 10% FBS and 1% penicillin streptomycin. iLECs[144] passaged in 1:1 low glucose DMEM:F12 (Gibco), supplemented with 20% FBS, 1% penicillin streptomycin, Bovine endothelial cell growth supplement (10μg/mL, BD Biosciences), heparin (56μg/mL, Sigma), and IFNγ (100ng/mL). Primary human LECs (lonza hmVEC-dLy, CC-2810), cultured according to manufacturers recommendation.

Tumor Studies

5 x 105 B16F10.OVA, MC38, YUMM1.7, or YUMMER1.7 tumor cells were implanted intradermal into the flank of mice. Tumor growth was measured daily using digital calipers to measure the long and short axis. Average diameters were used to calculate spherical volume. Tumors were harvested and digested with collagenase I & II (Gibco), collagenase IV (Gibco), or Collagenase D (Sigma-aldrich) for 30-60 min at 37°C. Digests were then passed through a metal screen and 70 μm pore filter. Enrichment for lymphocytes was performed using a Lymphoprep gradient (StemCell Technologies) according to manufacturers protocol.

Listeria monocytogenes infection

ActA-deficient Listeria monocytogenes was grown in tryptic soy broth (Sigma-Aldrich) supplemented with 50μg/mL Streptomycin (Sigma-Aldrich) at 37°C until OD600 = 0.1 (108 CFU/mL). 107 CFU in 200 μL PBS were transferred intravenously into mice.

Vaccinia Virus Infection

Vaccinia virus expressing the recombinant antigen (VacV-GP33) was propagated in BSC-40 cells using standard protocols. Mice were infected cutaneously by 25 pokes with a 29-guage needle following administration of 5x106 plaque forming units (PFU) VacV in 10μl PBS to the ventral side of the ear pinna (scarification). Virus is propagated using standard protocols. Ear thickness was measure by digital calipers.

Imiquimod induced psoriasis

Psoriasis was induced using imiquimod, as previously described. Specifically, the back hair of C57BL6 mice was removed using electric razor. Mice received a daily topical dose of 62.5 mg 5% Imiquimod Cream (Perrigo) or Cetaphil cream, as vehicle control, for 4 days. Mice were sacrificed and skin collected on day 5.

Delayed Type Hypersensitivity

DTH was induced by application of DNFB solution (150μL 0.5%) in acetone/olive oil (4:1) to shaved backs of mice. 4 days later, right ears were challenged with DNFB solution (20μL 0.3%) and left ears treated with vehicle. Animals were sacrificed 2 days later.

Human Melanoma samples

5 μm sections of archived formalin fixed-paraffin embedded (FFPE) of stage I and II human primary melanoma resections were obtained Oregon Health and Science University (OHSU) Knight Biolibrary and the OHSU Department of Dermatology research repository (Table S1). Acquisition and use of human samples was performed in accordance with the Institutional Review Board (IRB) at Oregon Health & Science University.

Flow cytometry and antibodies

The following fluorescent dye-conjugated antibodies against surface and intracellular antigens were used: B2-20 (RA3-6B2, BioLegend), CD103 (2E7, BioLegend), CD106 (429, BioLegend), CD11b (M1/70, BioLegend), CD11c (N418, BioLegend), CD31 (MEC 13.3, BD Biosciences), CD3e (145-2C11, BioLegend), CD4 (GK1.5, BioLegend), CD43 activation-glycoform (1B11, BioLegend), CD44 (IM7, Tonbo), CD45 (30-F11, BioLegend), CD45.1 (A20, BioLegend), CD45.2 (104, Tonbo), CD8 (53-6.7, Tonbo), CD90.1 (OX-7, BioLegend), F4/80 (BM8, BioLegend), I-A/I-E (M5/114.15.2, BD Biosciences), IFNγ (XMG1.2, Tonbo), PD-1 (29F.1A12,), PD-L1 (MIH5, BD Biosceinces), Podoplanin (8.1.1, BioLegend), pSTAT1 (612564, BD Biosciences), TNFa (MP6-XT22, BioLegend). Single-cell suspensions were prepared from tumors by digestion with Collagenase D (1

mg/mL, Sigma) and DNAse (50 U/mL, Sigma, for leukocyte extraction) or collagenase IV (2200 U/mL, Worthington Biomedical) and DNAse (50 U/mL, Sigma, for endothelial cell extraction). Whole-tissue suspensions were then generated by gently forcing the tissue through a wire mesh screen and then filtered through 70μm pore nylon cell strainers. Leukocytes were enriched using Lymphoprep (StemCell Technologies) as per manufactures instructions. Single cell suspensions were stained and fixed with 2% paraformaldehyde. All data were acquired with a BD Biosciences Fortessa or LSRII flow cytometer and analyzed using FlowJo Software (TreeStar Inc.). Intracellular cytokine staining was performed as described above and fixed with BD Cytofix/Cytoperm (BD Biosciences). All antibodies were obtained from BD Biosciences, BioLegend (San Diego, CA), or Tonbo Biosciences (San Diego, CA) unless otherwise specified. H2-Kb restricted, B8R20-27 and Ova.SIINFEKL Tetramers were obtained from the National Institutes of Health tetramer core facility.

Immunohistochemistry and Immunofluorescence

Immunofluorescence: Lymph nodes were fixed in 1% paraformaldehyde (24 hours at 4°C) transferred to 15% sucrose (overnight at 4°C) followed by 30% sucrose (overnight at 4°C) then indirectly frozen in O.C.T. Compound (cat. no. 23-730-571, Fischer Scientific). 30μm sections (Fischer Scientific Cryotome) were blocked using 1:1 2.5% normal goat serum: 2.5% BSA solution, primaries were added for 2 hours at room temperature. Sections were stained with secondary in 1.25% BSA for 1 hour at room temperature, followed by incubation with DAPI nuclei stain (ThermoFisher Scientific) for 5 minutes at room temperature. Slides were sealed with SlowFade Gold antifade reagent (Invitrogen) and imaged a Zeiss ApoTome.2 fluorescent microscope(CarlZeiss) and processed using ZEN software (CarlZeiss). Antibodies: CD3ε (Cat. No. 550277, BD biosciences), B220 (RA3-6B2, BioLegend), and LYVE1 (103-PA50, Reliatech), Anti-hamster A546 (A21111), anti-rabbit A488 (A21206), and anti-rat A647 (A21472) from Life Technologies. Immunohistochemistry: Tissues were isolated from mice and fixed in 10% formalin for 24h at room temperature. Tissues were dehydrated and then embedded in paraffin wax

and cut in 7μm sections. Heated, citrate antigen retrieval was performed for 15 minutes (cat. No. HK086, BioGenex). Sections were blocked with 2.5% BSA for 1 hour at room temperature and then stained for 2 hours with primary antibodies in 1.25% BSA at room temperature. Sections were stained with species-matched HRP-conjugated ImmPRESS polymers (VectorLabs) for 1 hour at room temperature and visualized using Bajoran Purple (SKU BJP811, BioCare Medical). Sections were imaged on a Leica Aperio Scanscope AT slide scanner and processed using Aperio Imagescope (Leica Biosystems). Antibodies: CD3ε (550277, BD Biosciences), B220 (RA3-6B2, BioLegend), LYVE1 (103-PA50, Reliatech), F4-80 (CL;A3-1, BioRad), CD45 (30-F11, BD Biosciences), GP38 (AF3244, R & D Systems. Image analysis of infiltrating leukocytes was performed using Aperio ImageScope software (Leica) and their Membrane Image Analysis algorithm to classify positive cells (+3) or by manual count (mast cells, F4/80$^+$, vessels) in blinded samples and enumerated per length of tissue. Number of cells/length from two sections of each ear were averaged. Epidermal and dermal thickness was determined through direct measurement of epidermis at 5 places along length of ear. Two sections of each ear were averaged. Lymphatic and blood vessel density was determined by manual count in blinded samples per length of tissue or as percent positive pixel area in $>$6 representative regions of interest per sample.

Bone Marrow Chimeras

8-12-week-old recipient mice received two doses of whole-body radiation (500 rads and 450 rads, 4 hours apart) using an X-ray Irradiator. Bone marrow was isolated from hind limbs of donor mice and 5-10x106 cells injected intravenously into recipients. Mice were maintained on 2 mg/mL Ampicillin (Fisher Bioreagents) antibiotic water changed twice per week for 6 weeks. Mice were bled to check for efficient chimerism ($>$80%) and enrolled in studies 8 weeks post radiation.

T Cell Activation and Adoptive Transfer

Spleens were passed through a 70 μm filter and lysed with ammonium-chloride-potassium (ACK) lysis buffer. 5-6 x 106 splenocytes were plated in RPMI media (Gibco) supplemented with 10% fetal bovine serum (Atlanta Biologicals) and 1% penicillin streptomycin (Gibco). Wildtype splenocytes were activated by plate-bound α-CD3 (10 μg/mL, 145-2C11, Tonbo) and α-CD28 (2 μg/mL, 37.51, eBioscience) supplemented with 100 U/mL IL-2 (Peprotech) for 72 hours at 37°C. OT-I splenocytes were stimulated with SIINFEKL (1nM, Biosynthesis) supplemented with 100 U/mL IL-2 for 72 hours at 37°C. Alternatively, T cells were activated in vivo following transfer of naïve $CD8^+$ TCR-tg OT-I T cells into WT mice and infection one day later with 107 CFU attenuated WT Listeria monocytogenes (LM) or LM expressing the cognate antigens ovalbumin (LM-OVA). Spleens were harvested on day 7 post LM infection, passed through 70 μm-pore filter (VWR) and RBCs lysed with ACK lysis buffer. $CD8^+$ effector T cells were isolated using EasySep Mouse $CD8^+$ T cell isolation kit (StemCell Technologies) according to manufactures instructions. 106 activated $CD8^+$ T cells were transferred into tumor-bearing mice by intravenous injection.

LN digestion protocol

Cervical, inguinal, axillary, brachial, and mesenteric lymph nodes were harvested into digestion buffer (DMEM -pyruvate, Gibco 41965-062, 1% pen/strep, 1.2 mM CaCl2, 2% FBS, no β-mercaptoethanol) and capsule teased apart with 26G needle. Single cell suspensions were generated by sequential digestion with collagenase IV (220U/mL) and DNAse (>80U/mL) followed by collagenase D (0.7854U/mL) and DNAse (>80U.mL) as previously described[144,145].

TCGA

Upper-quartile normalized RSEM (RNAseq by Expectation Maximization) expected counts from the Cancer Genome Atlas (TCGA) were taken from the Broad Institute Firehose and clinical variables taken from the UCSC Genome Browser. Non-glabrous melanoma

samples (n=231) representing primary cutaneous (n=103), regional cutaneous metastases (n=74), and distant metastasis (n=54) but not regional lymph node metastases were extracted and log-transformed for analysis. Scores were calculated as the first principal component of each gene set: Lymphatic Score, VEGFC, LYVE1, PDPN; T cell inflammation score, CD8A, CCL2, CCL3, CCL4, CXCL9, CXCL10, ICOS, GZMK, IRF1, HLA-DMA, HLA-DMB, HLA-DOA, HLA-DOB[274]; Type II IFN score, IFNγ, STAT1, CCR5, CXCL9, PRF1, HLA-DRA, CXCL10, CXCL11, IDO1, GZMA[275]. Lymphatic score was stratified to high and low cohorts LSlo ($<$ mean-0.5$*$SD; n=71), LShi ($>$ mean^{+}0.5$*$SD, n=68).

Multiplexed, sequential immunohistochemistry (mIHC)

Sequential chromogenic immunohistochemistry was performed as previously described[242], using a modified protocol. In brief, 5 μm FFPE tissue sections of human primary melanoma were de-paraffinized and subsequently stained with hematoxylin (GHS116, Sigma-Aldrich) to visualize nuclei. Following whole-tissue scanning using Aperio ImageScope AT (Leica Biosystems), heat-mediated antigen retrieval in antigen retrieval Citra Plus solution (HK080-9K, BioGenex) was performed. Subsequent iterative cycles of standard IHC were performed using primary antibodies against CD8 (C8/144B, Thermo Fisher), CD31 (JC70A, Dako) or CD34 (QBEnd-10, Thermo Fisher), podoplanin (D2-40, Covance), and S100 (antibody cocktail, Biocare Medical), followed by detection with ImmPressTM IgG-polymerized peroxidase reagents (Vector Laboratories) and visualization with AEC (Vector Laboratories). After whole tissue scanning, AEC was removed using ethanol, antibody was stripped in heated citrate buffer, and the next staining cycle with the next primary antibody was performed. Tissues were treated with 10% H2O2 (Fisher Chemical) for 10 min at 60 °C immediately after deparaffinization to remove pigmentation.

Image processing

Serial digitized images were processed using a computational image analysis workflow described previously[242] to align and visualize several markers simultaneously in a single

pseudo-colored image. From whole-tissue serial images rectangular regions of interest with an area of 6.25 mm2 were selected based on quantitative analysis of $CD8^+$ cell-density. One to three high-density $CD8^+$ T cell-regions of interest (ROI) that included both stromal tissue and tumor parenchyma were chosen from each patient sample for analysis. Images of nuclei, CD8, CD31 or CD34, podoplanin and S100 staining were processed to obtain quantitative and spatial information of staining intensity on a single cell-level, and analyzed using FCS Express 5 Image Cytometry Version 5.01.0080 (De Novo Software). Tumor segmentation masks to distinguish intratumoral and peritumoral regions were generated from the images of cell nuclei and the tumor marker S100 of the same tissue region. The segmentation pipeline is a succession of thresholding and mathematical morphology operations: First, the nuclei image is used to define the parts of the image covered by tissue using triangle thresholding. S100-positive areas are detected within the ROI by computing an alternate sequential filter (a succession of opening and closing with structuring elements of increasing sizes), followed by a triangle thresholding and a cleaning with closing and opening operations which fill gaps and holes and remove artifacts, to generate a black and white-mask for the image region covered by tumor.

Vessel segmentation

Whole vessel segmentation was performed using Otsus method to segment blood and lymphatic vessels based on the intensity of $CD31^+$ or $CD34^+$ and $podoplanin^+$ staining: Blood vessels were defined as CD31 or CD34-single positive, lymphatic vessel masks were generated using the intersection of masks generated from podoplanin staining with CD31 masks, or, when staining with CD34, from podoplanin staining alone. The segmentation masks were refined with morphologic operation such as closing operation, i.e. dilation, followed by erosion using the same structuring element for both operations. Endothelial cell type was identified based on mIHC marker expression using image cytometry analysis, and vessel annotation was refined using the identified endothelial cell types and their location data; the image analysis output and threshold values from image cytometry were used to identify endothelial cells. The most frequent endothelial cell type within

the individual segmented vessels was determined, and vessel type was re-annotated based on the most frequent cell types in the segmented region. Finally, vessel segmentation and annotation was validated by visual assessment by an investigator to exclude objects falsely annotated as vessels due to unspecific staining, background, or errors in annotation overlooked by the automated procedure described above.

Extraction of Spatial Proximity and Distance Measurements

$CD8^+$ T cell positional data was used to measure distance from each individual T cell to the annotated vessels and tumor border. Using the Quickhull Algorithm for Convex Hulls, dsearchn function in MATLAB R2016, the shortest distance between T cell centroids and the boundary of the vessel segmentation mask was measured to determine T cell distance to vessels within peri- and intra-tumoral regions, respectively. Similarly, the shortest distance between T cell centroids or centroid of the vessels segmentation masks to the tumor border (boundary of the tumor tissue segmentation mask) were determined.

Statistical Analysis

Statistical analyses were performed using GraphPad (Prism). In all cases parametric or non-parametric Students t-test (2 groups), or One-way ANOVA for multiple pairwise testing ($>$2 groups) were performed as indicated. Changes in tumor growth were determined following approximation of linear regression and comparison of mean slope and variation. Analysis of survival was performed using Mantel-Cox test. $p<0.05$ was considered significant in all studies, indicated by $*$. All experiments were performed independently 2-3 times and data presented as cumulative or representative data as indicated. Details may be found in each figure legend.

Bibliography

[1] R. L. Siegel, K. D. Miller, and A. Jemal. Cancer statistics, 2019. *CA Cancer J Clin*, 69(1):7–34, 2019.

[2] R. S. Strern. Prevelane of a history of skin cancer in 2007. *Arch Dermatol*, 146(3):279–282, 2010.

[3] National Cancer Institute, Surveillance Epidemiology Program, and End Results. Cancer stat facts: Melanoma of the skin, 2016.

[4] Z. Ali, N. Yousaf, and J. Larkin. Melanoma epidemiology, biology and prognosis. *EJC Suppl*, 11(2):81–91, 2013. Ali, Z Yousaf, N Larkin, J eng Review England EJC Suppl. 2013 Sep;11(2):81-91. doi: 10.1016/j.ejcsup.2013.07.012.

[5] D. Lubin and E. H. Jensen. Effects of clouds and stratospheric ozone depletion on ultraviolet radiation trends. *Nature*, 377(6551):710–713, 1995.

[6] R. P. Rastogi, Richa, A. Kumar, M. B. Tyagi, and R. P. Sinha. Molecular mechanisms of ultraviolet radiation-induced dna damage and repair. *Journal of Nucleic Acids*, 2010:1–32, 2010.

[7] A. H. Shain and B. C. Bastian. From melanocytes to melanomas. *Nat Rev Cancer*, 16(6):345–58, 2016.

[8] M. Cichorek, M. Wachulska, A. Stasiewicz, and A. Tymińska. Skin melanocytes: biology and development. *Advances in Dermatology and Allergy*, 1:30–41, 2013.

[9] B. T. Fitzpatrick and S. A. Breathnach. *The Epidermal Melanin Unit System*, volume 147. Dermatol Wochenschr, 1963.

[10] H. Ando, Y. Niki, M. Ito, K. Akiyama, M. S. Matsui, D.l B. Yarosh, and M. Ichihashi. Melanosomes are transferred from melanocytes to keratinocytes through the processes of packaging, release, uptake, and dispersion. *Journal of Investigative Dermatology*, 132(4):1222–1229, 2012.

[11] J. P. Ortonne. Photoprotective properties of skin melanin. *British Journal of Dermatology*, 146(s61):7–10, 2002.

[12] John D'Orazio, Stuart Jarrett, Alexandra Amaro-Ortiz, and Timothy Scott. Uv radiation and the skin. *International Journal of Molecular Sciences*, 14(6):12222–12248, 2013.

[13] J. E. Hauser, A. L. Kadekaro, R. J. Kavanagh, K. Wakamatsu, S. Terzieva, S. Schwemberger, G. Babcock, M. B. Rao, S. Ito, and Z. A. Abdel-Malek. Melanin content and mc1r function independently affect uvr-induced dna damage in cultured human melanocytes. *Pigment Cell Res*, 19(4):303–314, 2006.

[14] K. H. Kaidbey, P. P. Agin, R. M. Sayre, and A. M. Kligman. Photoprotection by melanin—a comparison of black and caucasian skin. *Journal of the American Academy of Dermatology*, 1(3):249–260, 1979.

[15] I. Suzuki, R. D. Cone, S. Im, J. J. Nordlund, and Z. A. Abdel-Malek. Binding of melanotropic hormones to the melanocortin receptor mc1r on human melanocytes stimulates proliferation and melanogenesis. *Endocrinology*, 137(5):1627–1633, 1996.

[16] M. T. Landi, J. Bauer, R. M. Pfeiffer, D. E. Elder, B. Hulley, P. Minghetti, D. Calista, P. A. Kanetsky, D. Pinkle, and B. C. Bastian. Mc1r germline variants confer risk for braf-mutant melanoma. *Science*, 313(5786):521–522, 2006.

[17] G. C. Leonardi, L. Falzone, R. Salemi, A. Zanghi, D. A. Spandidos, J. A. McCubrey, S. Candido, and M. Libra. Cutaneous melanoma: From pathogenesis to therapy (review). *Int J Oncol*, 52(4):1071–1080, 2018.

[18] M. S. Carlino, G. V. Long, R. F. Kefford, and H. Rizos. Targeting oncogenic braf and aberrant mapk activation in the treatment of cutaneous melanoma. *Crit Rev Oncol Hematol*, 96(3):385–98, 2015. Carlino, Matteo S Long, Georgina V Kefford, Richard F Rizos, Helen eng Review Netherlands Crit Rev Oncol Hematol. 2015 Dec;96(3):385-98. doi: 10.1016/j.critrevonc.2015.08.021. Epub 2015 Aug 28.

[19] J. A. Curtin, J. Fridlyand, T. Kageshita, H. N. Patel, K. J. Busam, H. Kutzner, K.H. Cho, S. Aiba, E. B. Brocker, P. E. Leboit, D. Pinkel, and B. C. Bastian. Distinct sets of genetic alterations in melanoma. *New England Journal of Medicine*, 353(20):2135–2147, 2005.

[20] C. M. Lovly, K. B. Dahlman, L. E. Fohn, Z. Su, D. Dias-Santagata, D. J. Hicks, D. Hucks, E. Berry, C. Terry, M. Duke, Y. Su, T. Sobolik-Delmaire, A. Richmond, M. C. Kelley, C. L. Vnencak-Jones, A. J. Iafrate, J. Sosman, and W. Pao. Routine multiplex mutational profiling of melanomas enables enrollment in genotype-driven therapeutic trials. *PLoS One*, 7(4):e35309, 2012.

[21] H. Davies, G. R. Bignell, C. Cox, P. Stephens, S. Edkins, S. Clegg, J. Teague, H. Woffendin, M.J. Garnett, W. Bottomley, N. Davis, E. Dicks, R. Ewing, Y. Floyd, K. Gray, S. Hall, R. Hawes, J. Hughes, V. Kosmidou, A. Menzies, C. Mould, A. Parker, C. Stevens, S. Watt, S. Hooper, R. P. Wilson, H. Jayatilake, B. A. Gusterson, C. Cooper, J. Shipley, D. Hargrave, K. Pritchard-Jones, N. Maitland, G. Chenevix-Trench, G. J. Riggins, D.D. Bigner, G. Palmieri, A. Cossu, A. Flanagan, A. Nicholson, J.W. C. Ho, S.Y. Leung, S.T. Yuen, B. L. Weber, H. F. Seigler, T. L. Darrow, H. Paterson, R. Marais, C. J. Marshall, R. Wooster, M.R. Stratton, and P. A. Futreal. Mutations of the braf gene in human cancer. *Nature*, 417(6892):949–954, 2002.

[22] P. T. C. Wan, M. J. Garnett, S. M. Roe, S. Lee, D. Niculescu-Duvaz, V. M. Good, C. M. Jones, C.J. Marshall, C.J. Springer, D. Barford, and R. Marais. Mechanism of activation of the raf-erk signaling pathway by oncogenic mutations of b-raf. *Cell*, 116(6):855–867, 2004.

[23] B. C. Bastian. The molecular pathology of melanoma: an integrated taxonomy of melanocytic neoplasia. *Annu Rev Pathol*, 9:239–71, 2014. Bastian, Boris C eng P01-CA025874/CA/NCI NIH HHS/ R01-CA131524/CA/NCI NIH HHS/ R01-CA142873/CA/NCI NIH HHS/ Research Support, N.I.H., Extramural Review 2014/01/28 06:00 Annu Rev Pathol. 2014;9:239-71. doi: 10.1146/annurev-pathol-012513-104658.

[24] P. M. Pollock, U. L. Harper, K. S. Hansen, L. M. Yudt, M. Stark, C. M. Robbins, T. Y. Moses, G. Hostetter, U. Wagner, J. Kakareka, G. Salem, T. Pohida, P. Heenan, P. Duray, O. Kallioniemi, N. K. Hayward, J. M. Trent, and P. S. Meltzer. High frequency of braf mutations in nevi. *Nat Genet*, 33(1):19–20, 2003.

[25] C. Michaloglou, L. C. Vredeveld, M. S. Soengas, C. Denoyelle, T. Kuilman, C. M. van der Horst, D. M. Majoor, J. W. Shay, W. J. Mooi, and D. S. Peeper. Brafe600-associated senescence-like cell cycle arrest of human naevi. *Nature*, 436(7051):720–4, 2005.

[26] M. Serrano, A. W. Lin, M. E. McCurrach, D. Beach, and S. W. Lowe. Oncogenic ras provokes premature cell senescence associated with accumulation of p53 and p16ink4a. *Cell*, 88(5):593–602, 1997.

[27] A. H. Shain, I. Yeh, I. Kovalyshyn, A. Sriharan, E. Talevich, A. Gagnon, R. Dummer, J. North, L. Pincus, B. Ruben, W. Rickaby, C. D'Arrigo, A. Robson, and B. C. Bastian. The genetic evolution of melanoma from precursor lesions. *N Engl J Med*, 373(20):1926–36, 2015.

[28] B. Domingues, J. M. Lopes, P. Soares, and H. Populo. Melanoma treatment in review. *ImmunoTargets and Therapy*, 7:35–49, 2018.

[29] P. B. Chapman, A. Hauschild, C. Robert, J. B. Haanen, P. A. Ascierto, J. Larkin, R. Dummer, C. Garbe, A. Testori, M. Maio, D. Hogg, P. Lorigan, C. Lebbe, T. Jouary, D. Schadendorf, A. Ribas, S. J. O'Day, J. A. Sosman, J. M. Kirkwood, A. M. M. Eggermont, B. Dreno, K. Nolop, J. Li, B. Nelson, J. Hou, R. J. Lee, K. T. Flaherty, and G. A. McArthur. Improved survival with vemurafenib in melanoma with braf v600e mutation. *New England Journal of Medicine*, 364(26):2507–2516, 2011.

[30] R. J. Sullivan and K. T. Flaherty. Resistance to braf-targeted therapy in melanoma. *Eur J Cancer*, 49(6):1297–304, 2013.

[31] H. Rizos, A. M. Menzies, G. M. Pupo, M. S. Carlino, C. Fung, J. Hyman, L. E. Haydu, B. Mijatov, T. M. Becker, S. C. Boyd, J. Howle, R. Saw, J. F. Thompson, R. F. Kefford, R. A. Scolyer, and G. V. Long. Braf inhibitor resistance mechanisms in metastatic melanoma: Spectrum and clinical impact. *Clinical Cancer Research*, 20(7):1965–1977, 2014.

[32] A. Niezgoda, P. Niezgoda, and R. Czajkowski. Novel approaches to treatment of advanced melanoma: A review on targeted therapy and immunotherapy. *Biomed Res Int*, 2015:851387, 2015.

[33] J. Larkin, P. A. Ascierto, B. Dréno, V. Atkinson, G. Liszkay, M. Maio, M. Mandalà, L. Demidov, D. Stroyakovskiy, L. Thomas, L. De La Cruz-Merino, C. Dutriaux, C. Garbe, M.A. Sovak, I. Chang, N. Choong, S. P. Hack, G. A. McArthur, and A. Ribas. Combined vemurafenib and cobimetinib in braf-mutated melanoma. *New England Journal of Medicine*, 371(20):1867–1876, 2014.

[34] D. S. Chen and I. Mellman. Oncology meets immunology: the cancer-immunity cycle. *Immunity*, 39(1):1–10, 2013.

[35] T.N. Schumacher and R. D. Schreiber. Neoantigens in cancer immunotherapy. *Science*, 348(6230):69–74, 2015.

[36] F. S. Hodi, S. J. O'Day, D. F. McDermott, R. W. Weber, J. A. Sosman, J.B. Haanen, R. Gonzalez, C. Robert, D. Schadendorf, J. C. Hassel, W. Akerley, A. J. M. Van Den Eertwegh, J. Lutzky, P. Lorigan, J. M. Vaubel, G. P. Linette, D. Hogg, C. H. Ottensmeier, C. Lebbé, C. Peschel, I. Quirt, J. I. Clark, J. D. Wolchok, J. S. Weber, J. Tian, M.l J. Yellin, G. M. Nichol, A. Hoos, and W. J. Urba. Improved survival with ipilimumab in patients with metastatic melanoma. *New England Journal of Medicine*, 363(8):711–723, 2010.

[37] C. Robert, L. Thomas, I. Bondarenko, S. J. O'Day, J. S. Weber, C. Garbe, C. Lebbe, J.-F. Baurain, A. Testori, J.-J. Grob, N. Davidson, J. Richards, M. Maio, A. Hauschild, W. H. Miller, P. Gascon, M. Lotem, K. Harmankaya, R. Ibrahim, S. Francis, T.-T. Chen, R. Humphrey, A. Hoos, and J. D. Wolchok. Ipilimumab plus dacarbazine for previously untreated metastatic melanoma. *New England Journal of Medicine*, 364(26):2517–2526, 2011.

[38] D. Schadendorf, F. S. Hodi, C. Robert, J. S. Weber, K. Margolin, O. Hamid, D. Patt, T.T. Chen, D.M. Berman, and J. D. Wolchok. Pooled analysis of long-term survival data from phase ii and phase iii trials of ipilimumab in unresectable or metastatic melanoma. *Journal of Clinical Oncology*, 33(17):1889–1894, 2015.

[39] A. Ribas, O. Hamid, A. Daud, F. S. Hodi, J. D. Wolchok, R. Kefford, A. M. Joshua, A. Patnaik, W. J. Hwu, J. S. Weber, T. C. Gangadhar, P. Hersey, R. Dronca, R. W. Joseph, H. Zarour, B. Chmielowski, D. P. Lawrence, A. Algazi, N. A. Rizvi, B. Hoffner, C. Mateus, K. Gergich, J. A. Lindia, M. Giannotti, X. N. Li, S. Ebbinghaus, S. P. Kang, and C. Robert. Association of pembrolizumab with tumor response and survival among patients with advanced melanoma. *JAMA*, 315(15):1600–9, 2016.

[40] J. D. Wolchok, V. Chiarion-Sileni, R. Gonzalez, P. Rutkowski, J. J. Grob, C. L. Cowey, C. D. Lao, J. Wagstaff, D. Schadendorf, P. F. Ferrucci, M. Smylie, R. Dummer, A. B. Hill, D. Hogg, J. B. Haanen, M. S. Carlino, O. Bechter, M. Maio, I. Marquez-Rodas, M. Guidoboni, G. A. McArthur, Ce. Lebbé, P. A. Ascierto, G. V. Long, J. Cebon, J. Sosman, M. A. Postow, M. K. Callahan, D. Walker, L. Rollin, R. Bhore, F. S. Hodi, and J. Larkin. Overall survival with combined nivolumab and ipilimumab in advanced melanoma. *New England Journal of Medicine*, 377(14):1345–1356, 2017.

[41] C. Robert, J. Schachter, G. V. Long, A. Arance, J. J. Grob, L. Mortier, A. Daud, M. S. Carlino, C. McNeil, M. Lotem, J. Larkin, P. Lorigan, B. Neyns, C. U.

Blank, O. Hamid, C. Mateus, R. Shapira-Frommer, M. Kosh, H. Zhou, N. Ibrahim, S. Ebbinghaus, and A. Ribas. Pembrolizumab versus ipilimumab in advanced melanoma. *N Engl J Med*, 372(26):2521–32, 2015.

[42] Antoni Ribas, Igor Puzanov, Reinhard Dummer, Dirk Schadendorf, Omid Hamid, Caroline Robert, F. Stephen Hodi, Jacob Schachter, Anna C. Pavlick, Karl D. Lewis, Lee D. Cranmer, Christian U. Blank, Steven J. O'Day, Paolo A. Ascierto, April K. S. Salama, Kim A. Margolin, Carmen Loquai, Thomas K. Eigentler, Tara C. Gangadhar, Matteo S. Carlino, Sanjiv S. Agarwala, Stergios J. Moschos, Jeffrey A. Sosman, Simone M. Goldinger, Ronnie Shapira-Frommer, Rene Gonzalez, John M. Kirkwood, Jedd D. Wolchok, Alexander Eggermont, Xiaoyun Nicole Li, Wei Zhou, Adriane M. Zernhelt, Joy Lis, Scot Ebbinghaus, S. Peter Kang, and Adil Daud. Pembrolizumab versus investigator-choice chemotherapy for ipilimumab-refractory melanoma (keynote-002): a randomised, controlled, phase 2 trial. *The Lancet Oncology*, 16(8):908–918, 2015.

[43] F. Martins, L. Sofiya, G. P. Sykiotis, F. Lamine, M. Maillard, M. Fraga, K. Shabafrouz, C. Ribi, A. Cairoli, Y. Guex-Crosier, T. Kuntzer, O. Michielin, S. Peters, G. Coukos, F. Spertini, J. A. Thompson, and M. Obeid. Adverse effects of immune-checkpoint inhibitors: epidemiology, management and surveillance. *Nature Reviews Clinical Oncology*, 2019.

[44] Bruno Kyewski and Ludger Klein. A central role for central tolerance. *Annual Review of Immunology*, 24(1):571–606, 2006.

[45] Daniel L. Mueller. Mechanisms maintaining peripheral tolerance. *Nature Immunology*, 11(1):21–27, 2010.

[46] D. Hanahan and R. A. Weinberg. Hallmarks of cancer: the next generation. *Cell*, 144(5):646–74, 2011.

[47] Naiyer A. Rizvi, Matthew D. Hellmann, Alexandra Snyder, Pia Kvistborg, Vladimir Makarov, Jonathan J. Havel, William Lee, Jianda Yuan, Phillip Wong, Teresa S. Ho, Martin L. Miller, Natasha Rekhtman, Andre L. Moreira, Fawzia Ibrahim, Cameron Bruggeman, Billel Gasmi, Roberta Zappasodi, Yuka Maeda, Chris Sander, Edward B. Garon, Taha Merghoub, Jedd D. Wolchok, Ton N. Schumacher, and Timothy A. Chan. Mutational landscape determines sensitivity to pd-1 blockade in non–small cell lung cancer. *Science*, 348:124–128, 2015.

[48] S. Spranger, J. J. Luke, R. Bao, Y. Zha, K. M. Hernandez, Y. Li, A. P. Gajewski, J. Andrade, and T. F. Gajewski. Density of immunogenic antigens does not explain the presence or absence of the t-cell-inflamed tumor microenvironment in melanoma. *Proc Natl Acad Sci U S A*, 113(48):E7759–E7768, 2016.

[49] H. D. Hickman, K. Takeda, C. N. Skon, F. R. Murray, S. E. Hensley, J. Loomis, G. N. Barber, J. R. Bennink, and J. W. Yewdell. Direct priming of antiviral cd8+ t cells in the peripheral interfollicular region of lymph nodes. *Nat Immunol*, 9(2):155–65, 2008.

[50] E. Scandella, K. Fink, T. Junt, B. M. Senn, E. Lattmann, R. Forster, H. Hengartner, and B. Ludewig. Dendritic cell-independent b cell activation during acute virus

infection: A role for early ccr7-driven b-t helper cell collaboration. *The Journal of Immunology*, 178(3):1468–1476, 2007.

[51] M. Sixt, N. Kanazawa, M. Selg, T. Samson, G. Roos, D. P. Reinhardt, R. Pabst, M. B. Lutz, and L. Sorokin. The conduit system transports soluble antigens from the afferent lymph to resident dendritic cells in the t cell area of the lymph node. *Immunity*, 22(1):19–29, 2005.

[52] P. Rantakari, K. Auvinen, N. Jappinen, M. Kapraali, J. Valtonen, M. Karikoski, H. Gerke, E. Khuda I. Iftakhar, J. Keuschnigg, E. Umemoto, K. Tohya, M. Miyasaka, K. Elima, S. Jalkanen, and M. Salmi. The endothelial protein plvap in lymphatics controls the entry of lymphocytes and antigens into lymph nodes. *Nat Immunol*, 16(4):386–96, 2015.

[53] C. P. Loo, N. A. Nelson, R. S. Lane, J. L. Booth, S. C. Loprinzi Hardin, A. Thomas, M. K. Slifka, J. C. Nolz, and A. W. Lund. Lymphatic vessels balance viral dissemination and immune activation following cutaneous viral infection. *Cell Rep*, 20(13):3176–3187, 2017.

[54] E. W. Roberts, M. L. Broz, M. Binnewies, M. B. Headley, A. E. Nelson, D. M. Wolf, T. Kaisho, D. Bogunovic, N. Bhardwaj, and M. F. Krummel. Critical role for cd103(+)/cd141(+) dendritic cells bearing ccr7 for tumor antigen trafficking and priming of t cell immunity in melanoma. *Cancer Cell*, 30(2):324–336, 2016.

[55] A. W. Lund, M. Wagner, M. Fankhauser, E. S. Steinskog, M. A. Broggi, S. Spranger, T. F. Gajewski, K. Alitalo, H. P. Eikesdal, H. Wiig, and M. A. Swartz. Lymphatic vessels regulate immune microenvironments in human and murine melanoma. *J Clin Invest*, 126(9):3389–402, 2016.

[56] E. Ingulli, D. R. Ulman, M. M. Lucido, and M. K. Jenkins. In situ analysis reveals physical interactions between cd11b+ dendritic cells and antigen-specific cd4 t cells after subcutaneous injection of antigen. *Journal of Immunology*, 169(5):2247–2252, 2002.

[57] S. Bedoui, P. G. Whitney, J. Waithman, L. Eidsmo, L. Wakim, I. Caminschi, R. S. Allan, M. Wojtasiak, K. Shortman, F. R. Carbone, A. G. Brooks, and W. R. Heath. Cross-presentation of viral and self antigens by skin-derived cd103+ dendritic cells. *Nat Immunol*, 10(5):488–95, 2009.

[58] R. S. Allan, J. Waithman, S. Bedoui, C. M. Jones, J. A. Villadangos, Y. Zhan, A. M. Lew, K. Shortman, W. R. Heath, and F. R. Carbone. Migratory dendritic cells transfer antigen to a lymph node-resident dendritic cell population for efficient ctl priming. *Immunity*, 25(1):153–62, 2006.

[59] D. L. Mueller, M. K. Jenkins, and R. H. Schwartz. Clonal expansion versus functional clonal inactivation: A costimulatory signalling pathway determines the outcome of t cell antigen receptor occupancy. *Annual Review of Immunology*, 7(1):445–480, 1989.

[60] C. H. June, J. A. Ledbetter, M. M. Gillespie, T. Lindsten, and C. B. Thompson. T-cell proliferation involving the cd28 pathway is associated with cyclosporine-resistant interleukin 2 gene expression. *Molecular and Cellular Biology*, 7(12):4472–4481, 1987.

[61] A. D. S. Linhares, J. Leitner, K. Grabmeier-Pfistershammer, and P. Steinberger. Not all immune checkpoints are created equal. *Frontiers in Immunology*, 9, 2018.

[62] E. A. Tivol, F. Borriello, A. N. Schweitzer, W. P. Lynch, J. A. Bluestone, and A. H. Sharpe. Loss of ctla-4 leads to massive lymphoproliferation and fatal multiorgan tissue destruction, revealing a critical negative regulatory role of ctla-4. *Immunity*, 3(5):541–547, 1995.

[63] M. F. Krummel. Cd28 and ctla-4 have opposing effects on the response of t cells to stimulation. *Journal of Experimental Medicine*, 182(2):459–465, 1995.

[64] D. M. Pardoll. The blockade of immune checkpoints in cancer immunotherapy. *Nat Rev Cancer*, 12(4):252–64, 2012.

[65] D. R. Leach, M. F. Krummel, and J. P. Allison. Enhancement of antitumor immunity by ctla-4 blockade. *Science*, 271(5256):1734–1736, 1996.

[66] T. N. Khan, J. L. Mooster, A. M. Kilgore, J. F. Osborn, and J. C. Nolz. Local antigen in nonlymphoid tissue promotes resident memory cd8+ t cell formation during viral infection. *J Exp Med*, 213(6):951–66, 2016.

[67] Ryan S. Lane and Amanda W. Lund. Non-hematopoietic control of peripheral tissue t cell responses: Implications for solid tumors. *Frontiers in Immunology*, 9:2662, 2018.

[68] M. M. Steele, M. J. Churchill, A. P. Breazeale, R. S. Lane, N. A. Nelson, and A. W. Lund. Quantifying leukocyte egress via lymphatic vessels from murine skin and tumors. *Journal of Visualized Experiments*, 143:e58704, 2019.

[69] S. Spranger, K.H. Koblish, B. Horton, P.A. Scherle, R. Newton, and T.F. Gajewski. Mechanism of tumor rejection with doublets of ctla-4, pd-1/pd-l1, or ido blockade involves restored il-2 production and proliferation of cd8+ t cells directly within the tumor microenvironment. *Journal for ImmunoTherapy of Cancer*, 2(3), 2014.

[70] R. S. Lane, J. Femel, A. P. Breazeale, C. P. Loo, G. Thibault, A. Kaempf, M. Mori, T. Tsujikawa, Y. H. Chang, and A. W. Lund. Ifng-activated dermal lymphatic vessels inhibit cytotoxic t cell in melanoma and inflamed skin. *Journal of Experimental Medicine*, 2018.

[71] A. Ribas. Adaptive immune resistance: How cancer protects from immune attack. *Cancer Discov*, 5(9):915–9, 2015.

[72] T. F. Gajewski, H. Schreiber, and Y. X. Fu. Innate and adaptive immune cells in the tumor microenvironment. *Nat Immunol*, 14(10):1014–22, 2013.

[73] V. R. Juneja, K. A. McGuire, R. T. Manguso, M. W. LaFleur, N. Collins, W. N. Haining, G. J. Freeman, and A. H. Sharpe. Pd-l1 on tumor cells is sufficient for immune evasion in immunogenic tumors and inhibits cd8 t cell cytotoxicity. *J Exp Med*, 214(4):895–904, 2017.

[74] A. I. Daud, J. D. Wolchok, C. Robert, W. J. Hwu, J. S. Weber, A. Ribas, F. S. Hodi, A. M. Joshua, R. Kefford, P. Hersey, R. Joseph, T. C. Gangadhar, R. Dronca,

A. Patnaik, H. Zarour, C. Roach, G. Toland, J. K. Lunceford, X. N. Li, K. Emancipator, M. Dolled-Filhart, S. P. Kang, S. Ebbinghaus, and O. Hamid. Programmed death-ligand 1 expression and response to the anti-programmed death 1 antibody pembrolizumab in melanoma. *J Clin Oncol*, 34(34):4102–4109, 2016.

[75] E. John Wherry, Sang-Jun Ha, Susan M. Kaech, W. Nicholas Haining, Surojit Sarkar, Vandana Kalia, Shruti Subramaniam, Joseph N. Blattman, Daniel L. Barber, and Rafi Ahmed. Molecular signature of cd8+ t cell exhaustion during chronic viral infection. *Immunity*, 27(5):670–684, 2007.

[76] S. N. Mueller, V. K. Vanguri, S. J. Ha, E. E. West, M. E. Keir, J. N. Glickman, A. H. Sharpe, and R. Ahmed. Pd-l1 has distinct functions in hematopoietic and nonhematopoietic cells in regulating t cell responses during chronic infection in mice. *J Clin Invest*, 120(7):2508–15, 2010.

[77] Y. Agata, A. Kawasaki, H. Nishimura, Y. Ishida, T. Tsubat, H. Yagita, and T. Honjo. Expression of the pd-1 antigen on the surface of stimulated mouse t and b lymphocytes. *International Immunology*, 8(5):765–772, 1996.

[78] L. V. Riella, A. M. Paterson, A. H. Sharpe, and A. Chandraker. Role of the pd-1 pathway in the immune response. *American Journal of Transplantation*, 12(10):2575–2587, 2012.

[79] G. J. Freeman, A. J. Long, Y. Iwai, K. Bourque, T. Chernova, H. Nishimura, L. J. Fitz, N. Malenkovich, T. Okazaki, M. C. Byrne, H. F. Horton, L. Fouser, L. Carter, V. Ling, M. R. Bowman, B. M. Carreno, M. Collins, C. R. Wood, and T. Honjo. Engagement of the pd-1 immunoinhibitory receptor by a novel b7 family member leads to negative regulation of lymphocyte activation. *The Journal of Experimental Medicine*, 192(7):1027–1034, 2000.

[80] E. Hui, J. Cheung, J. Zhu, X. Su, M. J. Taylor, H. A. Wallweber, D. K. Sasmal, J. Huang, J. M. Kim, I. Mellman, and R. D. Vale. T cell costimulatory receptor cd28 is a primary target for pd-1–mediated inhibition. *Science*, 355(6332):1428–1433, 2017.

[81] N. Patsoukis, J. Brown, V. Petkova, F. Liu, L. Li, and V. A. Boussiotis. Selective effects of pd-1 on akt and ras pathways regulate molecular components of the cell cycle and inhibit t cell proliferation. *Sci. Signaling*, 5(230):ra46–ra46, 2012.

[82] M. Quigley, F. Pereyra, B. Nilsson, F. Porichis, C. Fonseca, Q. Eichbaum, B. Julg, J. L. Jesneck, K. Brosnahan, S. Imam, K. Russell, I. Toth, A. Piechocka-Trocha, D. V. Dolfi, J. Angelosanto, A. Crawford, H. Shin, D. S. Kwon, J. Zupkosky, L. M. Francisco, G. J. Freeman, E. J. Wherry, D. E. Kaufmann, B. D. Walker, B. Ebert, and W. N. Haining. Transcriptional analysis of hiv-specific cd8+ t cells shows that pd-1 inhibits t cell function by upregulating batf. *Nature Medicine*, 16(10):1147–1151, 2010.

[83] B. T. Fife, K. E. Pauken, T. N. Eagar, T. Obu, J. Wu, Q. Tang, M. Azuma, M. F. Krummel, and J. A. Bluestone. Interactions between pd-1 and pd-l1 promote tolerance by blocking the tcr-induced stop signal. *Nat Immunol*, 10(11):1185–92, 2009.

[84] D. L. Barber, E. J. Wherry, D. Masopust, B. Zhu, J. P. Allison, A. H. Sharpe, G. J. Freeman, and R. Ahmed. Restoring function in exhausted cd8 t cells during chronic viral infection. *Nature*, 439(7077):682–7, 2006.

[85] K. E. Pauken and E. J. Wherry. Overcoming t cell exhaustion in infection and cancer. *Trends Immunol*, 36(4):265–76, 2015.

[86] E. John Wherry. T cell exhaustion. *Nature Immunology*, 131(6):492–499, 2011.

[87] L. Baitsch, P. Baumgaertner, E. Devevre, S. K. Raghav, A. Legat, L. Barba, S. Wieckowski, H. Bouzourene, B. Deplancke, P. Romero, N. Rufer, and D. E. Speiser. Exhaustion of tumor-specific cd8(+) t cells in metastases from melanoma patients. *J Clin Invest*, 121(6):2350–60, 2011.

[88] L. M. McLane, M. S. Abdel-Hakeem, and E. J. Wherry. Cd8 t cell exhaustion during chronic viral infection and cancer. *Annual Review of Immunology*, 37:457–495, 2019.

[89] A. C. Huang, M. A. Postow, R. J. Orlowski, R. Mick, B. Bengsch, S. Manne, W. Xu, S. Harmon, J. R. Giles, B. Wenz, M. Adamow, D. Kuk, K. S. Panageas, C. Carrera, P. Wong, F. Quagliarello, B. Wubbenhorst, K. D'Andrea, K. E. Pauken, R. S. Herati, R. P. Staupe, J. M. Schenkel, S. McGettigan, S. Kothari, S. M. George, R. H. Vonderheide, R. K. Amaravadi, G. C. Karakousis, L. M. Schuchter, X. Xu, K. L. Nathanson, J. D. Wolchok, T. C. Gangadhar, and E. J. Wherry. T-cell invigoration to tumour burden ratio associated with anti-pd-1 response. *Nature*, 545(7652):60–65, 2017.

[90] Haidong Tang, Yong Liang, Robert A. Anders, Janis M. Taube, Xiangyan Qiu, Aditi Mulgaonkar, Xin Liu, Susan M. Harrington, Jingya Guo, Yangchun Xin, Yahong Xiong, Kien Nham, William Silvers, Guiyang Hao, Xiankai Sun, Mingyi Chen, Raquibul Hannan, Jian Qiao, Haidong Dong, Hua Peng, and Yang-Xin Fu. Pd-l1 on host cells is essential for pd-l1 blockade–mediated tumor regression. *Journal of Clinical Investigation*, 2018.

[91] M. Schmittnaegel, N. Rigamonti, E. Kadioglu, A. Cassara, C.W. Rmili, A. Kialainen, Y. Kienast, H. J. Mueller, C. H. Ooi, D. Laoui, and M. De Palma. Dual angiopoietin-2 and vegfa inhibition elicits antitumor immunity that is enhanced by pd-1 checkpoint blockade. *Science Translational Medicine*, 9(385):eaak9670, 2017.

[92] H. Frebel, V. Nindl, R. A. Schuepbach, T. Braunschweiler, K. Richter, J. Vogel, C. A. Wagner, D. Loffing-Cueni, M. Kurrer, B. Ludewig, and A. Oxenius. Programmed death 1 protects from fatal circulatory failure during systemic virus infection of mice. *J Exp Med*, 209(13):2485–99, 2012.

[93] H. Nishimura, M. Nose, H. Hiai, N. Minato, and T. Honjo. Development of lupus-like autoimmune diseases by disruption of the pd-1 gene encoding an itim motif-carrying immunoreceptor. *Immunity*, 11(2):141–151, 1999.

[94] Y. E. Latchman, S. C. Liang, Y. Wu, T. Chernova, R. A. Sobel, M. Klemm, V. K. Kuchroo, G. J. Freeman, and A. H. Sharpe. Pd-l1-deficient mice show that pd-l1 on

t cells, antigen-presenting cells, and host tissues negatively regulates t cells. *PNAS*, 101(29):10691–10696, 2004.

[95] L. L. Carter, M. W. Leach, M. L. Azoitei, J. Cui, J. W. Pelker, J. Jussif, S. Benoit, G. Ireland, D. Luxenberg, G. R. Askew, K. L. Milarski, C. Groves, T. Brown, B. A. Carito, K. Percival, B. M. Carreno, M. Collins, and S. Marusic. Pd-1/pd-l1, but not pd-1/pd-l2, interactions regulate the severity of experimental autoimmune encephalomyelitis. *Journal of Neuroimmunology*, 182(1-2):124–134, 2007.

[96] P. T. Sage, F. A. Schildberg, R. A. Sobel, V. K. Kuchroo, G. J. Freeman, and A. H. Sharpe. Dendritic cell pd-l1 limits autoimmunity and follicular t cell differentiation and function. *The Journal of Immunology*, 200(8):2592–2602, 2018.

[97] L. Scandiuzzi, K. Ghosh, K. A. Hofmeyer, Y. M. Abadi, E. Lazar-Molnar, E. Y. Lin, Q. Liu, H. Jeon, S. C. Almo, L. Chen, S. G. Nathenson, and X. Zang. Tissue-expressed b7-h1 critically controls intestinal inflammation. *Cell Rep*, 6(4):625–32, 2014.

[98] J. El Annan, S. Goyal, Q. Zhang, G. J. Freeman, A. H. Sharpe, and R. Dana. Regulation of t-cell chemotaxis by programmed death-ligand 1 (pd-l1) in dry eye-associated corneal inflammation. *Invest Ophthalmol Vis Sci*, 51(7):3418–23, 2010.

[99] C.L. Pittet, J. Newcombe, A. Prat, and N. Arbour. Human brain endothelial cells endeavor to immunoregulate cd8 t cells via pd-1 ligand expression in multiple sclerosis. *Journal of Neuroinflammation*, 8(155), 2011.

[100] X. Ren, K. Akiyoshi, A. A. Vandenbark, P. D. Hurn, and H. Offner. Programmed death-1 pathway limits central nervous system inflammation and neurologic deficits in murine experimental stroke. *Stroke*, 42(9):2578–83, 2011.

[101] S. Bodhankar, Y. Chen, A. V. Arthur, S. J. Murphy, and H. Offner. Pd-l1 enhances cns inflammation and infarct volume following experimental stroke in mice in opposition to pd-1. *Journal of neuroinflammation*, 10(111), 2013.

[102] S. Bodhankar, Y. Chen, A. Lapato, A. L. Dotson, J. Wang, A. A. Vandenbark, J. A. Saugstad, and H. Offner. Pd-l1 monoclonal antibody treats ischemic stroke by controlling central nervous system inflammation. *Stroke*, 46(10):2926–34, 2015.

[103] K. E. Pauken, M. K. Jenkins, M. Azuma, and B. T. Fife. Pd-1, but not pd-l1, expressed by islet-reactive cd4+ t cells suppresses infiltration of the pancrease during type 1 diabetes. *Diabetes*, 62(8):2859–2869, 2013.

[104] R. Califano, R. Lal, C. Lewanski, M. C. Nicolson, C. H. Ottensmeier, S. Popat, M. Hodgson, and P. E. Postmus. Patient selection for anti-pd-1/pd-l1 therapy in advanced non-small-cell lung cancer: implications for clinical practice. *Future Oncology*, 14(23):2415–2431, 2018.

[105] Mari Mino-Kenudson. Programmed cell death ligand-1 (pd-l1) expression by immunohistochemistry: could it be predictive and/or prognostic in non-small cell lung cancer? *Cancer Biology and Medicine*, 13(2):157–170, 2016.

[106] Antoni Ribas and Siwen Hu-Lieskovan. What does pd-l1 positive or negative mean? *The Journal of Experimental Medicine*, page jem.20161462, 2016.

[107] Heng Lin, Shuang Wei, Elaine M. Hurt, Michael D. Green, Lili Zhao, Linda Vatan, Wojciech Szeliga, Ronald Herbst, Paul W. Harms, Leslie A. Fecher, Pankaj Vats, Arul M. Chinnaiyan, Christopher D. Lao, Theodore S. Lawrence, Max Wicha, Junzo Hamanishi, Masaki Mandai, Ilona Kryczek, and Weiping Zou. Host expression of pd-l1 determines efficacy of pd-l1 pathway blockade–mediated tumor regression. *Journal of Clinical Investigation*, 2018.

[108] R. S. Herbst, J. C. Soria, M. Kowanetz, G. D. Fine, O. Hamid, M. S. Gordon, J. A. Sosman, D. F. McDermott, J. D. Powderly, S. N. Gettinger, H. E. Kohrt, L. Horn, D. P. Lawrence, S. Rost, M. Leabman, Y. Xiao, A. Mokatrin, H. Koeppen, P. S. Hegde, I. Mellman, D. S. Chen, and F. S. Hodi. Predictive correlates of response to the anti-pd-l1 antibody mpdl3280a in cancer patients. *Nature*, 515(7528):563–7, 2014.

[109] E.F. Tewalt, J.N. Cohen, S.J. Rouhani, C.J. Guidi, H. Qaio, S.P. Fahl, M.R. Conaway, T.P. Bender, K.S. Tung, A.T. Vella, A.J. Adler, L. Chen, and V.H. Engelhard. Lymphatic endothelial cells induce tolerance via pd-l1 and lack of costimulation leading to high-level pd-1 expression on cd8 t cells. *Blood*, 120(24):4772–4782, 2012.

[110] J. N. Cohen, E. F. Tewalt, S. J. Rouhani, E. L. Buonomo, A. N. Bruce, X. Xu, S. Bekiranov, Y. X. Fu, and V. H. Engelhard. Tolerogenic properties of lymphatic endothelial cells are controlled by the lymph node microenvironment. *PLoS One*, 9(2):e87740, 2014.

[111] C.D. Dieterich, K. Ikenberg, T. Cetintas, K. Kapaklikaya, C. Hutmacher, and M. Detmar. Tumor-associated lymphatic vessels upregulate pdl1 to inhibit t-cell activation. *Frontiers in Immunology*, 8:66, 2017.

[112] Y. Nakamura, H. Yasuoka, M. Tsujimoto, S. Imabun, M. Nakahara, K. Nakao, M. Nakamura, I. Mori, and K. Kakudo. Lymph vessel density correlates with nodal status, vegf-c expression, and prognosis in breast cancer. *Breast Cancer Research and Treatment*, 91(2):125–132, 2005.

[113] Y. Zeng, K. Opeskin, L. G. Horvath, R. L. Sutherland, and E. D. Williams. Lymphatic vessel density and lymph node metastasis in prostate cancer. *The Prostate*, 65(3):222–230, 2005.

[114] M. A. Swartz and A. W. Lund. Lymphatic and interstitial flow in the tumour microenvironment: linking mechanobiology with immunity. *Nat Rev Cancer*, 12(3):210–9, 2012.

[115] A. W. Lund, T. R. Medler, S. A. Leachman, and L. M. Coussens. Lymphatic vessels, inflammation, and immunity in skin cancer. *Cancer Discov*, 6(1):22–35, 2016.

[116] G. J. Randolph and N. E. Miller. Lymphatic transport of high-density lipoproteins and chylomicrons. *Journal of Clinical Investigation*, 124(3):929–935, 2014.

[117] S. A. Stacker, S. P. Williams, T. Karnezis, R. Shayan, S. B. Fox, and M. G. Achen. Lymphangiogenesis and lymphatic vessel remodelling in cancer. *Nat Rev Cancer*, 14(3):159–72, 2014.

[118] J. Andrew Carlson. Lymphedema and subclinical lymphostasis (microlymphedema) facilitate cutaneous infection, inflammatory dermatoses, and neoplasia: A locus minoris resistentiae. *Clinics in Dermatology*, 32(5):599–615, 2014.

[119] F. Zhang, G. Zarkada, J. Han, J. Li, A. Dubrac, R. Ola, G. Genet, K. Boyé, P. Michon, S. E. Künzel, J. P. Camporez, A. K. Singh, G. H. Fong, M. Simons, P. Tso, C. Fernández-Hernando, G. I. Shulman, W. C. Sessa, and A. Eichmann. Lacteal junction zippering protects against diet-induced obesity. *Science*, 361(6402):599, 2018.

[120] R. M. Steinman, D.l Hawiger, and M. C. Nussenzweig. Tolerogenic dendritic cells. *Annual Review of Immunology*, 21(1):685–711, 2003.

[121] L. Ohl, M. Mohaupt, N. Czeloth, G. Hintzen, Z. Kiafard, J. Zwirner, T. Blankenstein, G. Henning, and R. Förster. Ccr7 governs skin dendritic cell migration under inflammatory and steady-state conditions. *Immunity*, 21(2):279–288, 2004.

[122] E. Russo, A. Teijeira, K. Vaahtomeri, A. H. Willrodt, J. S. Bloch, M. Nitschke, L. Santambrogio, D. Kerjaschki, M. Sixt, and C. Halin. Intralymphatic ccl21 promotes tissue egress of dendritic cells through afferent lymphatic vessels. *Cell Rep*, 14(7):1723–1734, 2016.

[123] L. A. Johnson, S. Banerji, W. Lawrance, U. Gileadi, G. Prota, K. A. Holder, Y. M. Roshorm, T. Hanke, V. Cerundolo, N. W. Gale, and D. G. Jackson. Dendritic cells enter lymph vessels by hyaluronan-mediated docking to the endothelial receptor lyve-1. *Nat Immunol*, 18(7):762–770, 2017.

[124] A. Teijeira, M. C. Hunter, E. Russo, S. T. Proulx, T. Frei, G. F. Debes, M. Coles, I. Melero, M. Detmar, A. Rouzaut, and C. Halin. T cell migration from inflamed skin to draining lymph nodes requires intralymphatic crawling supported by icam-1/lfa-1 interactions. *Cell Rep*, 18(4):857–865, 2017.

[125] K. D. Klonowski, K. J. Williams, A. L. Marzo, D. A. Blair, E. G. Lingenheld, and L. Lefrancois. Dynamics of blood-borne cd8 memory t cell migration in vivo. *Immunity*, 20(5):551–62, 2004.

[126] X. Jiang, R. A. Clark, L. Liu, A. J. Wagers, R. C. Fuhlbrigge, and T. S. Kupper. Skin infection generates non-migratory memory cd8+ t(rm) cells providing global skin immunity. *Nature*, 483(7388):227–31, 2012.

[127] T. Seabrook, B. Au, J. Dickstein, X. Zhang, B. Ristevski, and J. B. Hay. The traffic of resting lymphocytes through delayed hypersensitivity and chronic inflammatory lesions: a dynamic equilibrium. *Semin Immunol*, 11(2):115–23, 1999.

[128] T. Seabrook, B. Au, J. Dickstein, X. Zhang, B. Ristevski, and J. B. Hay. The traffic of resting lymphocytes through delayed hypersensitivity and chronic inflammatory lesions: a dynamic equilibrium. *Semin Immunol*, 11(2):115–23, 1999.

[129] M. Weber, R. Hauschild, J. Schwarz, C. Moussion, I. de Vries, D. F. Legler, S. A. Luther, T. Bollenbach, and M. Sixt. Interstitial dendritic cell guidance by haptotactic chemokine gradients. *Science*, 339:328–332, 2013.

[130] S. A. Geherin, R. P. Wilson, S. Jennrich, and G. F. Debes. Cxcr4 is dispensable for t cell egress from chronically inflamed skin via the afferent lymph. *PLoS One*, 9(4):e95626, 2014.

[131] B. Vigl, D. Aebischer, M. Nitschké, M. Iolyeva, T. Röthlin, O. Antsiferova, and Halin. Tissue inflammation modulates gene expression of lymphatic endothelial cells and dendritic cell migration in a stimulus-dependent manner. *Blood*, 118(1):205–215, 2011.

[132] L. A. Johnson and D. G. Jackson. Inflammation-induced secretion of ccl21 in lymphatic endothelium is a key regulator of integrin-mediated dendritic cell transmigration. *Int Immunol*, 22(10):839–49, 2010.

[133] L. A. Johnson, S. Clasper, A. P. Holt, P. F. Lalor, D. Baban, and D. G. Jackson. An inflammation-induced mechanism for leukocyte transmigration across lymphatic vessel endothelium. *J Exp Med*, 203(12):2763–77, 2006.

[134] Y. Sawa, E. Tsuruga, K. Iwasawa, H. Ishikawa, and S. Yoshida. Leukocyte adhesion molecule and chemokine production through lipoteichoic acid recognition by toll-like receptor 2 in cultured human lymphatic endothelium. *Cell Tissue Res*, 333(2):237–52, 2008.

[135] D. O. Miteva, J. M. Rutkowski, J. B. Dixon, W. Kilarski, J. D. Shields, and M. A. Swartz. Transmural flow modulates cell and fluid transport functions of lymphatic endothelium. *Circ Res*, 106(5):920–31, 2010.

[136] M. Salmi, M. Karikoski, K. Elima, P. Rantakari, and S. Jalkanen. Cd44 binds to macrophage mannose receptor on lymphatic endothelium and supports lymphocyte migration via afferent lymphatics. *Circ Res*, 112(12):1577–82, 2013.

[137] M. Karikoski, H. Irjala, M. Maksimow, M. Miiluniemi, K. Granfors, S. Hernesniemi, K. Elima, G. Moldenhauer, K. Schledzewski, J. Kzhyshkowska, S. Goerdt, M. Salmi, and S. Jalkanen. Clever-1/stabilin-1 regulates lymphocyte migration within lymphatics and leukocyte entrance to sites of inflammation. *Eur J Immunol*, 39(12):3477–87, 2009.

[138] H. Pflicke and M. Sixt. Preformed portals facilitate dendritic cell entry into afferent lymphatic vessels. *J Exp Med*, 206(13):2925–35, 2009.

[139] L. C. Yao, P. Baluk, R. S. Srinivasan, G. Oliver, and D. M. McDonald. Plasticity of button-like junctions in the endothelium of airway lymphatics in development and inflammation. *Am J Pathol*, 180(6):2561–75, 2012.

[140] J. N. Cohen, C. J. Guidi, E. F. Tewalt, H. Qiao, S. J. Rouhani, A. Ruddell, A. G. Farr, K. S. Tung, and V. H. Engelhard. Lymph node-resident lymphatic endothelial cells mediate peripheral tolerance via aire-independent direct antigen presentation. *J Exp Med*, 207(4):681–8, 2010.

[141] L. A. Nichols, Y. Chen, T. A. Colella, C. L. Bennett, B. E. Clausen, and V. H. Engelhard. Deletional self-tolerance to a melanocyte/melanoma antigen derived from tyrosinase is mediated by a radio-resistant cell in peripheral and mesenteric lymph nodes. *The Journal of Immunology*, 179(2):993–1003, 2007.

[142] T. A. Colella, T. N. J. Bullock, L. B. Russell, D. W. Mullins, W. W. Overwijk, C. J. Luckey, R. A. Pierce, N. P. Restifo, and V. H. Engelhard. Self-tolerance to the murine homologue of a tyrosinase-derived melanoma antigen. *The Journal of Experimental Medicine*, 191(7):1221–1232, 2000.

[143] S. J. Rouhani, J. D. Eccles, P. Riccardi, J. D. Peske, E. F. Tewalt, J. N. Cohen, R. Liblau, T. Makinen, and V. H. Engelhard. Roles of lymphatic endothelial cells expressing peripheral tissue antigens in cd4 t-cell tolerance induction. *Nat Commun*, 6:6771, 2015.

[144] S. Hirosue, E. Vokali, V. R. Raghavan, M. Rincon-Restrepo, A. W. Lund, P. Corthesy-Henrioud, F. Capotosti, C. Halin Winter, S. Hugues, and M. A. Swartz. Steady-state antigen scavenging, cross-presentation, and cd8+ t cell priming: a new role for lymphatic endothelial cells. *J Immunol*, 192(11):5002–11, 2014.

[145] A. W. Lund, F. V. Duraes, S. Hirosue, V. R. Raghavan, C. Nembrini, S. N. Thomas, A. Issa, S. Hugues, and M. A. Swartz. Vegf-c promotes immune tolerance in b16 melanomas and cross-presentation of tumor antigen by lymph node lymphatics. *Cell Rep*, 1(3):191–9, 2012.

[146] V. Lukacs-Kornek, D. Malhotra, A. L. Fletcher, S. E. Acton, K. G. Elpek, P. Tayalia, A. R. Collier, and S. J. Turley. Regulated release of nitric oxide by nonhematopoietic stroma controls expansion of the activated t cell pool in lymph nodes. *Nat Immunol*, 12(11):1096–104, 2011.

[147] J. Dubrot, F. V. Duraes, L. Potin, F. Capotosti, D. Brighouse, T. Suter, S. LeibundGut-Landmann, N. Garbi, W. Reith, M. A. Swartz, and S. Hugues. Lymph node stromal cells acquire peptide-mhcii complexes from dendritic cells and induce antigen-specific cd4(+) t cell tolerance. *J Exp Med*, 211(6):1153–66, 2014.

[148] S. Podgrabinska, O. Kamalu, L. Mayer, M. Shimaoka, H. Snoeck, G. J. Randolph, and M. Skobe. Inflamed lymphatic endothelium suppresses dendritic cell maturation and function via mac-1/icam-1-dependent mechanism. *J Immunol*, 183(3):1767–79, 2009.

[149] M. C. Hunter, A. Teijeira, R. Montecchi, E. Russo, P. Runge, F. Kiefer, and C. Halin. Dendritic cells and t cells interact within murine afferent lymphatic capillaries. *Front Immunol*, 10:520, 2019.

[150] J. C. Nolz. Molecular mechanisms of cd8(+) t cell trafficking and localization. *Cell Mol Life Sci*, 72(13):2461–73, 2015.

[151] J. S. Pober and W. C. Sessa. Evolving functions of endothelial cells in inflammation. *Nat Rev Immunol*, 7(10):803–15, 2007.

[152] C. Bouzin, A. Brouet, J. De Vriese, J. DeWever, and O. Feron. Effects of vascular endothelial growth factor on the lymphocyte-endothelium interactions: Identification of caveolin-1 and nitric oxide as control points of endothelial cell anergy. *The Journal of Immunology*, 178(3):1505–1511, 2007.

[153] D. Tousoulis, A.M. Kampoli, C.T.N. Papageorgiou, and C. Stefanadis. The role of nitric oxide in endothelial function. *Current Vascular Pharmacology*, 10(1):4–18, 2012.

[154] B. Walzog and P. Gaehtgens. Adhesion molecules: The path to a new understanding of acute inflammation. *News in Physiological Sciences*, 15:107–113, 2000.

[155] D. Vestweber. How leukocytes cross the vascular endothelium. *Nat Rev Immunol*, 15(11):692–704, 2015.

[156] X. Ye, J. Ding, X. Zhou, G. Chen, and S. F. Liu. Divergent roles of endothelial nf-kappab in multiple organ injury and bacterial clearance in mouse models of sepsis. *J Exp Med*, 205(6):1303–15, 2008.

[157] J. M. Munro, J. S. Pober, and R. S. Cotran. Tumor necrosis factor and interferon-ey induce distinct patterns of endothelial activation and associated leukocyte accumulation in skin of papio anubis. *American Journal of Pathology*, 135(1):121–133, 1989.

[158] R. P. McEver. Selectins: initiators of leucocyte adhesion and signalling at the vascular wall. *Cardiovasc Res*, 107(3):331–9, 2015.

[159] H. M. McGettrick, E. Smith, A. Filer, S. Kissane, M. Salmon, C. D. Buckley, G. E. Rainger, and G. B. Nash. Fibroblasts from different sites may promote or inhibit recruitment of flowing lymphocytes by endothelial cells. *Eur J Immunol*, 39(1):113–25, 2009.

[160] M. Chimen, H. M. McGettrick, B. Apta, S. J. Kuravi, C. M. Yates, A. Kennedy, A. Odedra, M. Alassiri, M. Harrison, A. Martin, F. Barone, S. Nayar, J. R. Hitchcock, A. F. Cunningham, K. Raza, A. Filer, D. A. Copland, A. D. Dick, J. Robinson, N. Kalia, L. S. K. Walker, C. D. Buckley, G. B. Nash, P. Narendran, and G. E. Rainger. Homeostatic regulation of t cell trafficking by a b cell-derived peptide is impaired in autoimmune and chronic inflammatory disease. *Nat Med*, 21(5):467–475, 2015.

[161] R. Martinelli, M. Kamei, P. T. Sage, R. Massol, L. Varghese, T. Sciuto, M. Toporsian, A. M. Dvorak, T. Kirchhausen, T. A. Springer, and C. V. Carman. Release of cellular tension signals self-restorative ventral lamellipodia to heal barrier microwounds. *J Cell Biol*, 201(3):449–65, 2013.

[162] C. V. Carman and R. Martinelli. T lymphocyte-endothelial interactions: Emerging understanding of trafficking and antigen-specific immunity. *Frontiers in Immunology*, 6(603), 2015.

[163] S. K. Shaw, S. Ma, M. B. Kim, R. M. Rao, C. U. Hartman, R. M. Froio, L. Yang, T. Jones, Y. Liu, A. Nusrat, C. A. Parkos, and F. W. Luscinskas. Coordinated redistribution of leukocyte lfa-1 and endothelial cell icam-1 accompany neutrophil transmigration. *J Exp Med*, 200(12):1571–80, 2004.

[164] C. V. Carman and T. A. Springer. A transmigratory cup in leukocyte diapedesis both through individual vascular endothelial cells and between them. *J Cell Biol*, 167(2):377–88, 2004.

[165] C. V. Carman, P. T. Sage, T. E. Sciuto, M. A. de la Fuente, R. S. Geha, H. D. Ochs, H. F. Dvorak, A. M. Dvorak, and T. A. Springer. Transcellular diapedesis is initiated by invasive podosomes. *Immunity*, 26(6):784–97, 2007.

[166] D. Schulte, V. Kuppers, N. Dartsch, A. Broermann, H. Li, A. Zarbock, O. Kamenyeva, F. Kiefer, A. Khandoga, S. Massberg, and D. Vestweber. Stabilizing the ve-cadherin-catenin complex blocks leukocyte extravasation and vascular permeability. *EMBO J*, 30(20):4157–70, 2011.

[167] J. Song, X. Zhang, K. Buscher, Y. Wang, H. Wang, J. Di Russo, L. Li, S. Lutke-Enking, A. Zarbock, A. Stadtmann, P. Striewski, B. Wirth, I. Kuzmanov, H. Wiendl, D. Schulte, D. Vestweber, and L. Sorokin. Endothelial basement membrane laminin 511 contributes to endothelial junctional tightness and thereby inhibits leukocyte transmigration. *Cell Rep*, 18(5):1256–1269, 2017.

[168] F. Wessel, M. Winderlich, M. Holm, M. Frye, R. Rivera-Galdos, M. Vockel, R. Linnepe, U. Ipe, A. Stadtmann, A. Zarbock, A. F. Nottebaum, and D. Vestweber. Leukocyte extravasation and vascular permeability are each controlled in vivo by different tyrosine residues of ve-cadherin. *Nat Immunol*, 15(3):223–30, 2014.

[169] J. S. Reyat, M. Chimen, P. J. Noy, J. Szyroka, G. E. Rainger, and M. G. Tomlinson. Adam10-interacting tetraspanins tspan5 and tspan17 regulate ve-cadherin expression and promote t lymphocyte transmigration. *J Immunol*, 199(2):666–676, 2017.

[170] J. F. Osborn, J. L. Mooster, S. J. Hobbs, M. W. Munks, C. Barry, J. T. Harty, A. B. Hill, and J. C. Nolz. Enzymatic synthesis of core 2 o-glycans governs the tissue-trafficking potential of memory cd8+ t cells. *Science Immunology*, 2:eaan6049, 2017.

[171] Y. Simoni, E. Becht, M. Fehlings, C. Y. Loh, S. L. Koo, K. W. W. Teng, J. P. S. Yeong, R. Nahar, T. Zhang, H. Kared, K. Duan, N. Ang, M. Poidinger, Y. Y. Lee, A. Larbi, A. J. Khng, E. Tan, C. Fu, R. Mathew, M. Teo, W. T. Lim, C. K. Toh, B. H. Ong, T. Koh, A. M. Hillmer, A. Takano, T. K. H. Lim, E. H. Tan, W. Zhai, D. S. W. Tan, I. B. Tan, and E. W. Newell. Bystander cd8(+) t cells are abundant and phenotypically distinct in human tumour infiltrates. *Nature*, 557(7706):575–579, 2018.

[172] Alexei Y. Savinov, F. Susan Wong, Austin C. Stonebraker, and Alexander V. Chervonsky. Presentation of antigen by endothelial cells and chemoattraction are required for homing of insulin-specific cd8+t cells. *The Journal of Experimental Medicine*, 197(5):643–656, 2003.

[173] I. Galea, M. Bernardes-Silva, P. A. Forse, N. van Rooijen, R. S. Liblau, and V. H. Perry. An antigen-specific pathway for cd8 t cells across the blood-brain barrier. *J Exp Med*, 204(9):2023–30, 2007.

[174] R. Bagai, A. Valujskikh, D. H. Canaday, E. Bailey, P. N. Lalli, C. V. Harding, and P. S. Heeger. Mouse endothelial cells cross-present lymphocyte-derived antigen on class i mhc via a tap1- and proteasome-dependent pathway. *The Journal of Immunology*, 174(12):7711–7715, 2005.

[175] James E. Greening, Timothy I.M. Tree, Karolena T. Kotowicz, Astrid G. van Halteren, Bart O. Roep, Nigel J. Klein, and Mark Peakman. Processing and presentation of the islet autoantigen gad by vascular endothelial cells promotes transmigration of autoreactive t-cells. *Diabetes*, 52:717–725, 2003.

[176] P. T. Sage, L. M. Varghese, R. Martinelli, T. E. Sciuto, M. Kamei, A. M. Dvorak, T. A. Springer, A. H. Sharpe, and C. V. Carman. Antigen recognition is facilitated by invadosome-like protrusions formed by memory/effector t cells. *J Immunol*, 188(8):3686–99, 2012.

[177] F. M. Marelli-Berg, M. J. James, J. Dangerfield, J. Dyson, M. Millrain, D. Scott, E. Simpson, S. Nourshargh, and R. I. Lechler. Cognate recognition of the endothelium induces hy-specific cd8+ t-lymphocyte transendothelial migration (diapedesis) in vivo. *Blood*, 103(8), 2004.

[178] T. D. Manes and J. S. Pober. Antigen presentation by human microvascular endothelial cells triggers icam-1-dependent transendothelial protrusion by, and fractalkine-dependent transendothelial migration of, effector memory cd4+ t cells. *The Journal of Immunology*, 180(12):8386–8392, 2008.

[179] A. Limmer, J. Ohl, C. Kurts, H. Ljunggren, Y. Reiss, M. Groettrup, F. Momburg, B. Arnold, and P. Knolle. Efficient presentation of exogenous antigen by liber endothelial cells to cd8+ t cells results in antigen-speciic t-cell tolerance. *Nature Medicine*, 6(12):1348–1354, 2000.

[180] A. Schurich, M. Berg, D. Stabenow, J. Bottcher, M. Kern, H. J. Schild, C. Kurts, V. Schuette, S. Burgdorf, L. Diehl, A. Limmer, and P. A. Knolle. Dynamic regulation of cd8 t cell tolerance induction by liver sinusoidal endothelial cells. *J Immunol*, 184(8):4107–14, 2010.

[181] I. Bartholomaus, N. Kawakami, F. Odoardi, C. Schlager, D. Miljkovic, J. W. Ellwart, W. E. Klinkert, C. Flugel-Koch, T. B. Issekutz, H. Wekerle, and A. Flugel. Effector t cell interactions with meningeal vascular structures in nascent autoimmune cns lesions. *Nature*, 462(7269):94–8, 2009.

[182] E. Korpos, C. Wu, J. Song, R. Hallmann, and L. Sorokin. Role of the extracellular matrix in lymphocyte migration. *Cell Tissue Res*, 339(1):47–57, 2010.

[183] M. B. Voisin, D. Probstl, and S. Nourshargh. Venular basement membranes ubiquitously express matrix protein low-expression regions: characterization in multiple tissues and remodeling during inflammation. *Am J Pathol*, 176(1):482–95, 2010.

[184] N. Petajaniemi, M. Korhonen, J Kortesmaa, K. Tryggvason, K. Sekiguchi, H. Fujiwara, L. Sorokin, L. E. Thornell, Z. Wondimu, D. Assefa, M. Patarroyo, and I. Virtanen. Localization of laminin a4-chain in developint and adult human tissues. *The Journal of Histochemistry & Cytochemistry*, 50(8):1113–1130, 2002.

[185] C. Wu, F. Ivars, P. Anderson, R. Hallmann, D. Vestweber, P. Nilsson, H. Robenek, K. Tryggvason, J. Song, E. Korpos, K. Loser, S. Beissert, E. Georges-Labouesse, and L. M. Sorokin. Endothelial basement membrane laminin alpha5 selectively inhibits t lymphocyte extravasation into the brain. *Nat Med*, 15(5):519–27, 2009.

[186] Michael Sixt, Britta Engelhardt, Friederike Pausch, Rupert Hallmann, Olaf Wendler, and Lydia M. Sorokin. Endothelial cell laminin isoforms, laminins 8 and 10, play decisive roles in t cell recruitment across the blood–brain barrier in experimental autoimmune encephalomyelitis. *The Journal of Cell Biology*, 153(5):933–946, 2001.

[187] M. B. Voisin, A. Woodfin, and S. Nourshargh. Monocytes and neutrophils exhibit both distinct and common mechanisms in penetrating the vascular basement membrane in vivo. *Arterioscler Thromb Vasc Biol*, 29(8):1193–9, 2009.

[188] M. S. Buzza, L. Zamurs, J. Sun, C. H. Bird, A. I. Smith, J. A. Trapani, C. J. Froelich, E. C. Nice, and P. I. Bird. Extracellular matrix remodeling by human granzyme b via cleavage of vitronectin, fibronectin, and laminin. *J Biol Chem*, 280(25):23549–58, 2005.

[189] M. D. Prakash, M. A. Munoz, R. Jain, P. L. Tong, A. Koskinen, M. Regner, O. Kleifeld, B. Ho, M. Olson, S. J. Turner, P. Mrass, W. Weninger, and P. I. Bird. Granzyme b promotes cytotoxic lymphocyte transmigration via basement membrane remodeling. *Immunity*, 41(6):960–72, 2014.

[190] Jérôme Galon, Anne Costes, Fatima Sanchez-Cabo, Amos Kirilovsky, Bernhard Mlecnik, Christine Lagorce-Pagès, Marie Tosolini, Matthieu Camus, Anne Berger, Philippe Wind, Franck Zinzindohoué, Patrick Bruneval, Paul-Henri Cugnenc, Zlatko Trajanoski, Wolf-Herman Fridman, and Franck Pagès. Type, density, and location of immune cells within human colorectal tumors predict clinical outcome. *Science*, 313:1960–1964, 2006.

[191] T. Duhen, R. Duhen, R. Montler, J. Moses, T. Moudgil, N. F. de Miranda, C. P. Goodall, T. C. Blair, B. A. Fox, J. E. McDermott, S. C. Chang, G. Grunkemeier, R. Leidner, R. B. Bell, and A. D. Weinberg. Co-expression of cd39 and cd103 identifies tumor-reactive cd8 t cells in human solid tumors. *Nat Commun*, 9(1):2724, 2018.

[192] J. A. Joyce and D. T. Fearon. T cell exclusion, immune privilege, and the tumor microenvironment. *Science*, 348(6230):74–80, 2015.

[193] Y. Nakagawa, Y. Negishi, M. Shimizu, M. Takahashi, M. Ichikawa, and H. Takahashi. Effects of extracellular ph and hypoxia on the function and development of antigen-specific cytotoxic t lymphocytes. *Immunol Lett*, 167(2):72–86, 2015.

[194] K. Fischer, P. Hoffmann, S. Voelkl, N. Meidenbauer, J. Ammer, M. Edinger, E. Gottfried, S. Schwarz, G. Rothe, S. Hoves, K. Renner, B. Timischl, A. Mackensen, L. Kunz-Schughart, R. Adreesen, S. W. Krause, and M. Kruetz. Inhibitory effect of tumor cell-derived lactic acid on human t cells. *Blood*, 109(9):3812–3819, 2007.

[195] J. Ahamed, N. Burg, K. Yoshinaga, C. A. Janczak, D. B. Rifkin, and B. S. Coller. In vitro and in vivo evidence for shear-induced activation of latent transforming growth factor-beta1. *Blood*, 112(9):3650–60, 2008.

[196] M. Ahmadzadeh and S. A. Rosenberg. Tgf- 1 attenuates the acquisition and expression of effector function by tumor antigen-specific human memory cd8 t cells. *The Journal of Immunology*, 174(9):5215–5223, 2005.

[197] L. Broderick and R. B. Bankert. Membrane-associated tgf- 1 inhibits human memory t cell signaling in malignant and nonmalignant inflammatory microenvironments. *The Journal of Immunology*, 177(5):3082–3088, 2006.

[198] G. T. Motz and G. Coukos. Deciphering and reversing tumor immune suppression. *Immunity*, 39(1):61–73, 2013.

[199] H. Jiang, S. Hegde, and D. G. DeNardo. Tumor-associated fibrosis as a regulator of tumor immunity and response to immunotherapy. *Cancer Immunol Immunother*, 66(8):1037–1048, 2017.

[200] R. Kalluri and M. Zeisberg. Fibroblasts in cancer. *Nat Rev Cancer*, 6(5):392–401, 2006.

[201] P. P. Provenzano, K. W. Eliceiri, J. M. Campbell, D. R. Inman, J. G. White, and P. J. Keely. Collagen reorganization at the tumor-stromal interface facilitates local invasion. *BMC Med*, 4(1):38, 2006.

[202] I. Acerbi, L. Cassereau, I. Dean, Q. Shi, A. Au, C. Park, Y. Y. Chen, J. Liphardt, E. S. Hwang, and V. M. Weaver. Human breast cancer invasion and aggression correlates with ecm stiffening and immune cell infiltration. *Integrative Biology*, 7(10):1120–1134, 2015.

[203] H. Salmon, K. Franciszkiewicz, D. Damotte, M. C. Dieu-Nosjean, P. Validire, A. Trautmann, F. Mami-Chouaib, and E. Donnadieu. Matrix architecture defines the preferential localization and migration of t cells into the stroma of human lung tumors. *J Clin Invest*, 122(3):899–910, 2012.

[204] A. Boissonnas, L. Fetler, I. S. Zeelenberg, S. Hugues, and S. Amigorena. In vivo imaging of cytotoxic t cell infiltration and elimination of a solid tumor. *J Exp Med*, 204(2):345–56, 2007.

[205] M. B. Schaaf, A. D. Garg, and P. Agostinis. Defining the role of the tumor vasculature in antitumor immunity and immunotherapy. *Cell Death Dis*, 9(2):115, 2018.

[206] E. Lanitis, M. Irving, and G. Coukos. Targeting the tumor vasculature to enhance t cell activity. *Curr Opin Immunol*, 33:55–63, 2015.

[207] D. Lambrechts, E. Wauters, B. Boeckx, S. Aibar, D. Nittner, O. Burton, A. Bassez, H. Decaluwe, A. Pircher, K. Van den Eynde, B. Weynand, E. Verbeken, P. De Leyn, A. Liston, J. Vansteenkiste, P. Carmeliet, S. Aerts, and B. Thienpont. Phenotype molding of stromal cells in the lung tumor microenvironment. *Nat Med*, 2018.

[208] R. J. Buckanovich, A. Facciabene, S. Kim, F. Benencia, D. Sasaroli, K. Balint, D. Katsaros, A. O'Brien-Jenkins, P. A. Gimotty, and G. Coukos. Endothelin b receptor mediates the endothelial barrier to t cell homing to tumors and disables immune therapy. *Nat Med*, 14(1):28–36, 2008.

[209] A. W. Griffioen, C. A. Damen, G. H. Blijham, and G. Groenewegen. Tumor angiogenesis is accompanied by a decreased inflammatory response of tumor-associated endothelium. *Blood*, 88(2):667–673, 1996.

[210] G. T. Motz, S. P. Santoro, L. P. Wang, T. Garrabrant, R. R. Lastra, I. S. Hagemann, P. Lal, M. D. Feldman, F. Benencia, and G. Coukos. Tumor endothelium fasl establishes a selective immune barrier promoting tolerance in tumors. *Nat Med*, 20(6):607–15, 2014.

[211] John S. Yu, Paul K. Lee, Moneeb Ehtesham, Ken Samoto, Keith L. Black, and Christopher J. Wheeler. Intratumoral t cell subset ratios and fas ligand expression on brain tumor endothelium. *Journal of neuro-oncology*, 64(1-2):55–61, 2003.

[212] Rakesh K. Jain. Normalizing tumor vasculature with anti-angiogenic therapy: A new paradigm for combination therapy. *Nature Medicine*, 7:987, 2001.

[213] E. Allen, A. Jabouille, L. B. Rivera, O. Lodewijckx, R. Missiaen, V. Steri, K. Feyen, J. Tawney, D. Hanahan, I. P. Michael, and G. Bergers. Combined antiangiogenic and anti-pd-l1 therapy stimulates tumor immunity through hev formation. *Science Translational Medicine*, 9:eaak9679, 2017.

[214] W. H. Fridman, F. Pages, C. Sautes-Fridman, and J. Galon. The immune contexture in human tumours: impact on clinical outcome. *Nat Rev Cancer*, 12(4):298–306, 2012.

[215] L. Martinet, I. Garrido, T. Filleron, S. Le Guellec, E. Bellard, J. J. Fournie, P. Rochaix, and J. P. Girard. Human solid tumors contain high endothelial venules: association with t- and b-lymphocyte infiltration and favorable prognosis in breast cancer. *Cancer Res*, 71(17):5678–87, 2011.

[216] X. Zheng, Z. Fang, X. Liu, S. Deng, P. Zhou, X. Wang, C. Zhang, R. Yin, H. Hu, X. Chen, Y. Han, Y. Zhao, S. H. Lin, S. Qin, X. Wang, B. Y. Kim, P. Zhou, W. Jiang, Q. Wu, and Y. Huang. Increased vessel perfusion predicts the efficacy of immune checkpoint blockade. *J Clin Invest*, 128(5):2104–2115, 2018.

[217] H. Harlin, Y. Meng, A. C. Peterson, Y. Zha, M. Tretiakova, C. Slingluff, M. McKee, and T. F. Gajewski. Chemokine expression in melanoma metastases associated with cd8+ t-cell recruitment. *Cancer Res*, 69(7):3077–85, 2009.

[218] R. Muthuswamy, J. M. Corman, K. Dahl, G. S. Chatta, and P. Kalinski. Functional reprogramming of human prostate cancer to promote local attraction of effector cd8(+) t cells. *Prostate*, 76(12):1095–105, 2016.

[219] V. Chew, J. Chen, D. Lee, E. Loh, J. Lee, K. H. Lim, A. Weber, K. Slankamenac, R. T. Poon, H. Yang, L. L. Ooi, H. C. Toh, M. Heikenwalder, I. O. Ng, A. Nardin, and J. P. Abastado. Chemokine-driven lymphocyte infiltration: an early intratumoural event determining long-term survival in resectable hepatocellular carcinoma. *Gut*, 61(3):427–38, 2012.

[220] B. Molon, S. Ugel, F. Del Pozzo, C. Soldani, S. Zilio, D. Avella, A. De Palma, P. Mauri, A. Monegal, M. Rescigno, B. Savino, P. Colombo, N. Jonjic, S. Pecanic,

L. Lazzarato, R. Fruttero, A. Gasco, V. Bronte, and A. Viola. Chemokine nitration prevents intratumoral infiltration of antigen-specific t cells. *J Exp Med*, 208(10):1949–62, 2011.

[221] C. Feig, J. O. Jones, M. Kraman, R. J. Wells, A. Deonarine, D. S. Chan, C. M. Connell, E. W. Roberts, Q. Zhao, O. L. Caballero, S. A. Teichmann, T. Janowitz, D. I. Jodrell, D. A. Tuveson, and D. T. Fearon. Targeting cxcl12 from fap-expressing carcinoma-associated fibroblasts synergizes with anti-pd-l1 immunotherapy in pancreatic cancer. *Proc Natl Acad Sci U S A*, 110(50):20212–7, 2013.

[222] A. K. Alitalo, S. T. Proulx, S. Karaman, D. Aebischer, S. Martino, M. Jost, N. Schneider, M. Bry, and M. Detmar. Vegf-c and vegf-d blockade inhibits inflammatory skin carcinogenesis. *Cancer Res*, 73(14):4212–21, 2013.

[223] Bernhard Mlecnik, Gabriela Bindea, Amos Kirilovsky, Helen K. Angell, Anna C. Obenauf, Marie Tosolini, Sarah E. Church, Pauline Maby, Angela Vasaturo, Mihaela Angelova, Tessa Fredriksen, Stéphanie Mauger, Maximilian Waldner, Anne Berger, Michael R. Speicher, Franck Pagès, Viia Valge-Archer, and Jérôme Galon. The tumor microenvironment and immunoscore are critical determinants of dissemination to distant metastasis. *Science Translational Medicine*, 8(327):327ra26, 2016.

[224] Natacha Bordry, Maria A. S. Broggi, Kaat de Jonge, Karin Schaeuble, Philippe O. Gannon, Periklis G. Foukas, Esther Danenberg, Emanuela Romano, Petra Baumgaertner, Manuel Fankhauser, Noémie Wald, Laurène Cagnon, Samia Abed-Maillard, Hélène Maby-El Hajjami, Timothy Murray, Kalliopi Ioannidou, Igor Letovanec, Pu Yan, Olivier Michielin, Maurice Matter, Melody A. Swartz, and Daniel E. Speiser. Lymphatic vessel density is associated with cd8+ t cell infiltration and immunosuppressive factors in human melanoma. *OncoImmunology*, 2018.

[225] M. Fankhauser, M.A.S. Broggi, L. Potin, N. Bordry, L. Jeanbart, A.W. Lund, E. Da Costa, S. Hauert, M. Rincon-Restrepo, C. Tremblay, E. Cabello, K. Homicsko, O. Michielin, D. Hanahan, D.E. Speiser, and M.A. Swartz. Tumor lymphangiogenesis promotes t cell infiltration and potentiates immunotherapy in melanoma. *Science Translational Medicine*, 9:1–12, 2017.

[226] A. Reuben, C. N. Spencer, P. A. Prieto, V. Gopalakrishnan, S. M. Reddy, J. P. Miller, X. Mao, M. P. De Macedo, J. Chen, X. Song, H. Jiang, P. L. Chen, H. C. Beird, H. R. Garber, W. Roh, K. Wani, E. Chen, C. Haymaker, M. A. Forget, L. D. Little, C. Gumbs, R. L. Thornton, C. W. Hudgens, W. S. Chen, J. Austin-Breneman, R. S. Sloane, L. Nezi, A. P. Cogdill, C. Bernatchez, J. Roszik, P. Hwu, S. E. Woodman, L. Chin, H. Tawbi, M. A. Davies, J. E. Gershenwald, R. N. Amaria, I. C. Glitza, A. Diab, S. P. Patel, J. Hu, J. E. Lee, E. A. Grimm, M. T. Tetzlaff, A. J. Lazar, II Wistuba, K. Clise-Dwyer, B. W. Carter, J. Zhang, P. A. Futreal, P. Sharma, J. P. Allison, Z. A. Cooper, and J. A. Wargo. Genomic and immune heterogeneity are associated with differential responses to therapy in melanoma. *NPJ Genom Med*, 2, 2017.

[227] A. W. Lund. Rethinking lymphatic vessels and antitumor immunity. *Trends in Cancer*, 2(10):548–551, 2016.

[228] D. M. Fonseca, T. W. Hand, S. J. Han, M. Y. Gerner, A. Glatman Zaretsky, A. L. Byrd, O. J. Harrison, A. M. Ortiz, M. Quinones, G. Trinchieri, J. M. Brenchley, I. E. Brodsky, R. N. Germain, G. J. Randolph, and Y. Belkaid. Microbiota-dependent sequelae of acute infection compromise tissue-specific immunity. *Cell*, 163(2):354–66, 2015.

[229] A. Ruddell, S. B. Kirschbaum, S. N. Ganti, C. L. Liu, R. R. Sun, and S. C. Partridge. Tumor-induced alterations in lymph node lymph drainage identified by contrast-enhanced mri. *J Magn Reson Imaging*, 42(1):145–52, 2015.

[230] N. A. Rohner, J. McClain, S. L. Tuell, A. Warner, B. Smith, Y. Yun, A. Mohan, M. Sushnitha, and S. N. Thomas. Lymph node biophysical remodeling is associated with melanoma lymphatic drainage. *FASEB J*, 29(11):4512–22, 2015.

[231] B. A. Tamburini, M. A. Burchill, and R. M. Kedl. Antigen capture and archiving by lymphatic endothelial cells following vaccination or viral infection. *Nat Commun*, 5:3989, 2014.

[232] S. Spranger, R. M. Spaapen, Y. Zha, J. Williams, Y. Meng, T. T. Ha, and T. F. Gajewski. Up-regulation of pd-l1, ido, and t(regs) in the melanoma tumor microenvironment is driven by cd8(+) t cells. *Sci Transl Med*, 5(200):200ra116, 2013.

[233] S. Topalian, F. S. Hodi, J. Brahmer, S. N. Gettinger, D. C. Smith, D. F. McDermott, J. D. Powderly, R. D. Carvajal, J. A. Sosman, M. B. Atkins, P. D. Leming, D. R. Spigel, S. J. Antonia, L. Horn, C. Drake, D. M. Pardoll, L. Chen, W. H. Sharfman, R. A. Anders, J. M. Taube, T. L. McMiller, H. Xu, A. J. Korman, M. Jure-Kunkel, S. Agrawa, D. M. McDonald, G. D. Kollia, A. Gupta, J. M. Wigginton, and M. Sznol. Safety, activity, and immune correlates of anti–pd-1 antibody in cancer. *New England Journal of Medicine*, 366(26), 2012.

[234] J. D. Wolchok, H. Kluger, M. K. Callahan, M. A. Postow, N. A. Rizvi, A. M. Lesokhin, N. H. Segal, C. E. Ariyan, R. A. Gordon, K. Reed, M. M. Burke, A. Caldwell, S. A. Kronenberg, B. U. Agunwamba, X. Zhang, I. Lowy, H. D. Inzunza, W. Feely, C. E. Horak, Q. Hong, A. J. Korman, J. M. Wigginton, A. Gupta, and M. Sznol. Nivolumab plus ipilimumab in advanced melanoma. *N Engl J Med*, 369(2):122–33, 2013.

[235] A. Ribas, O. Hamid, A. Daud, F. S. Hodi, J. D. Wolchok, R. Kefford, A. M. Joshua, A. Patnaik, W. J. Hwu, J. S. Weber, T. C. Gangadhar, P. Hersey, R. Dronca, R. W. Joseph, H. Zarour, B. Chmielowski, D. P. Lawrence, A. Algazi, N. A. Rizvi, B. Hoffner, C. Mateus, K. Gergich, J. A. Lindia, M. Giannotti, X. N. Li, S. Ebbinghaus, S. P. Kang, and C. Robert. Association of pembrolizumab with tumor response and survival among patients with advanced melanoma. *JAMA*, 315(15):1600–9, 2016.

[236] S. Kleffel, C. Posch, S. R. Barthel, H. Mueller, C. Schlapbach, E. Guenova, C. P. Elco, N. Lee, V. R. Juneja, Q. Zhan, C. G. Lian, R. Thomi, W. Hoetzenecker, A. Cozzio, R. Dummer, Jr. Mihm, M. C., K. T. Flaherty, M. H. Frank, G. F. Murphy, A. H. Sharpe, T. S. Kupper, and T. Schatton. Melanoma cell-intrinsic pd-1 receptor functions promote tumor growth. *Cell*, 162(6):1242–56, 2015.

[237] J. C. Nolz and J. T. Harty. Il-15 regulates memory cd8+ t cell o-glycan synthesis and affects trafficking. *J Clin Invest*, 124(3):1013–26, 2014.

[238] J. Wang, C. J. Perry, K. Meeth, D. Thakral, W. Damsky, G. Micevic, S. Kaech, K. Blenman, and M. Bosenberg. Uv-induced somatic mutations elicit a functional t cell response in the yummer1.7 mouse melanoma model. *Pigment Cell Melanoma Res*, 30(4):428–435, 2017.

[239] K. Meeth, J. X. Wang, G. Micevic, W. Damsky, and M. W. Bosenberg. The yumm lines: a series of congenic mouse melanoma cell lines with defined genetic alterations. *Pigment Cell Melanoma Res*, 29(5):590–7, 2016.

[240] H. D. Hickman, G. V. Reynoso, B. F. Ngudiankama, E. J. Rubin, J. G. Magadan, S. S. Cush, J. Gibbs, B. Molon, V. Bronte, J. R. Bennink, and J. W. Yewdell. Anatomically restricted synergistic antiviral activities of innate and adaptive immune cells in the skin. *Cell Host Microbe*, 13(2):155–68, 2013.

[241] A. Garcia-Diaz, D. S. Shin, B. H. Moreno, J. Saco, H. Escuin-Ordinas, G. A. Rodriguez, J. M. Zaretsky, L. Sun, W. Hugo, X. Wang, G. Parisi, C. P. Saus, D. Y. Torrejon, T. G. Graeber, B. Comin-Anduix, S. Hu-Lieskovan, R. Damoiseaux, R. S. Lo, and A. Ribas. Interferon receptor signaling pathways regulating pd-l1 and pd-l2 expression. *Cell Rep*, 19(6):1189–1201, 2017.

[242] T. Tsujikawa, S. Kumar, R. N. Borkar, V. Azimi, G. Thibault, Y. H. Chang, A. Balter, R. Kawashima, G. Choe, D. Sauer, E. El Rassi, D. R. Clayburgh, M. F. Kulesz-Martin, E. R. Lutz, L. Zheng, E. M. Jaffee, P. Leyshock, A. A. Margolin, M. Mori, J. W. Gray, P. W. Flint, and L. M. Coussens. Quantitative multiplex immunohistochemistry reveals myeloid-inflamed tumor-immune complexity associated with poor prognosis. *Cell Rep*, 19(1):203–217, 2017.

[243] M. J. Cannon, P. J. M. Openshaw, and B. A. Askonas. Cytotoxic t cells clear virus but augment lung pathology in mice infected with respiratory syncytial virus. *Journal of Experimental Medicine*, 168(3):1163–1168, 1988.

[244] R. P. Kataru, H. Kim, C. Jang, D. K. Choi, B. I. Koh, M. Kim, S. Gollamudi, Y. K. Kim, S. H. Lee, and G. Y. Koh. T lymphocytes negatively regulate lymph node lymphatic vessel formation. *Immunity*, 34(1):96–107, 2011.

[245] E. D. Lucas, J. M. Finlon, M. A. Burchill, M. K. McCarthy, T. E. Morrison, T. M. Colpitts, and B. A. J. Tamburini. Type 1 ifn and pd-l1 coordinate lymphatic endothelial cell expansion and contraction during an inflammatory immune response. *J Immunol*, 2018.

[246] Louise A. Johnson, Remko Prevo, Steven Clasper, and David G. Jackson. Inflammation-induced uptake and degradation of the lymphatic endothelial hyaluronan receptor lyve-1. *Journal of Biological Chemistry*, 282(46):33671–33680, 2007.

[247] C. J. Nirschl, M. Suarez-Farinas, B. Izar, S. Prakadan, R. Dannenfelser, I. Tirosh, Y. Liu, Q. Zhu, K. S. P. Devi, S. L. Carroll, D. Chau, M. Rezaee, T. G. Kim, R. Huang, J. Fuentes-Duculan, G. X. Song-Zhao, N. Gulati, M. A. Lowes, S. L. King, F. J. Quintana, Y. S. Lee, J. G. Krueger, K. Y. Sarin, C. H. Yoon, L. Garraway,

A. Regev, A. K. Shalek, O. Troyanskaya, and N. Anandasabapathy. Ifngamma-dependent tissue-immune homeostasis is co-opted in the tumor microenvironment. *Cell*, 170(1):127–141 e15, 2017.

[248] H. Ikeda, L. J. Old, and R. D. Schreiber. Roles of ifng in protection against tumor development and cancer immunoediting. *Cytokine & Growth Factor Reviews*, 13:95–109, 2002.

[249] ET Creagan, CL Loprinzi, DL Ahmann, and DJ Schaid. A phase i–ii trial of the combination of recombinant leukocyte a interferon and recombinant human interferon-gamma in patients with metastatic malignant melanoma. *Cancer*, 62:2472–2474, 1988.

[250] S. Osanto, R. Jansen, A.M.I.H. Naipal, J.M. Gratama, A.V. Leeuwen, and F.J. Cleton. in vivo effects of combination treatment with recombinant interferongamma and alpha in metastatic melanoma. *Int. J. Cancer*, 43(6):1001–1006, 1989.

[251] W. Pan, S. Zhu, K. Qu, K. Meeth, J. Cheng, K. He, H. Ma, Y. Liao, X. Wen, C. Roden, Z. Tobiasova, Z. Wei, J. Zhao, J. Liu, J. Zheng, B. Guo, S. A. Khan, M. Bosenberg, R. A. Flavell, and J. Lu. The dna methylcytosine dioxygenase tet2 sustains immunosuppressive function of tumor-infiltrating myeloid cells to promote melanoma progression. *Immunity*, 47(2):284–297 e5, 2017.

[252] C. J. Perry, A. R. Munoz-Rojas, K. M. Meeth, L. N. Kellman, R. A. Amezquita, D. Thakral, V. Y. Du, J. X. Wang, W. Damsky, A. L. Kuhlmann, J. W. Sher, M. Bosenberg, K. Miller-Jensen, and S. M. Kaech. Myeloid-targeted immunotherapies act in synergy to induce inflammation and antitumor immunity. *J Exp Med*, 215(3):877–893, 2018.

[253] S. Hoves, C. H. Ooi, C. Wolter, H. Sade, S. Bissinger, M. Schmittnaegel, O. Ast, A. M. Giusti, K. Wartha, V. Runza, W. Xu, Y. Kienast, M. A. Cannarile, H. Levitsky, S. Romagnoli, M. De Palma, D. Ruttinger, and C. H. Ries. Rapid activation of tumor-associated macrophages boosts preexisting tumor immunity. *J Exp Med*, 215(3):859–876, 2018.

[254] S. Pasquali, A. P. van der Ploeg, S. Mocellin, J. R. Stretch, J. F. Thompson, and R. A. Scolyer. Lymphatic biomarkers in primary melanomas as predictors of regional lymph node metastasis and patient outcomes. *Pigment Cell Melanoma Res*, 26(3):326–37, 2013.

[255] M. Skobe, T. Hawighorst, D.G. Jackson, R. Prevo, L. Janes, P. Velasco, L. Riccardi, K. Alitalo, K. Claffey, and M. Detmar. Induction of tumor lymphangiogenesis by vegf-c promotes breast cancer metastasis. *Nature Medicine*, 7(2):192–198, 2001.

[256] J. Naidoo, D. B. Page, B. T. Li, L. C. Connell, K. Schindler, M. E. Lacouture, M. A. Postow, and J. D. Wolchok. Toxicities of the anti-pd-1 and anti-pd-l1 immune checkpoint antibodies. *Annals of Oncology*, page mdv383, 2015.

[257] F. Jean, P. Tomasini, and F. Barlesi. Atezolizumab: feasible second-line therapy for patients with non-small cell lung cancer? a review of efficacy, safety and place in therapy. *Ther Adv Med Oncol*, 9(12):769–779, 2017.

[258] O. Hasan Ali, S. Diem, E. Markert, W. Jochum, K. Kerl, L. E. French, D. E. Speiser, M. Früh, and L. Flatz. Characterization of nivolumab-associated skin reactions in patients with metastatic non-small cell lung cancer. *OncoImmunology*, page e1231292, 2016.

[259] J. Larkin, V. Chiarion-Sileni, R. Gonzalez, J. J. Grob, C. L. Cowey, C. D. Lao, D. Schadendorf, R. Dummer, M. Smylie, P. Rutkowski, P. F. Ferrucci, A. Hill, J. Wagstaff, M. S. Carlino, J. B. Haanen, M. Maio, I. Marquez-Rodas, G. A. McArthur, P. A. Ascierto, G. V. Long, M. K. Callahan, M. A. Postow, K. Grossmann, M. Sznol, B. Dreno, L. Bastholt, A. Yang, L. M. Rollin, C. Horak, F. S. Hodi, and J. D. Wolchok. Combined nivolumab and ipilimumab or monotherapy in untreated melanoma. *N Engl J Med*, 373(1):23–34, 2015.

[260] M. A. Postow, J. Chesney, A. C. Pavlick, C. Robert, K. Grossmann, D. McDermott, G. P. Linette, N. Meyer, J. K. Giguere, S. S. Agarwala, M. Shaheen, M. S. Ernstoff, D. Minor, A. K. Salama, M. Taylor, P. A. Ott, L. M. Rollin, C. Horak, P. Gagnier, J. D. Wolchok, and F. S. Hodi. Nivolumab and ipilimumab versus ipilimumab in untreated melanoma. *N Engl J Med*, 372(21):2006–17, 2015.

[261] S. L. Topalian, M. Sznol, D. F. McDermott, H. M. Kluger, R. D. Carvajal, W. H. Sharfman, J. R. Brahmer, D. P. Lawrence, M. B. Atkins, J. D. Powderly, P. D. Leming, E. J. Lipson, I. Puzanov, D. C. Smith, J. M. Taube, J. M. Wigginton, G. D. Kollia, A. Gupta, D. M. Pardoll, J. A. Sosman, and F. S. Hodi. Survival, durable tumor remission, and long-term safety in patients with advanced melanoma receiving nivolumab. *J Clin Oncol*, 32(10):1020–30, 2014.

[262] K. Nishino, S. Ohe, M. Kitamura, K. Kunimasa, M. Kimura, T. Inoue, M. Tamiya, T. Kumagai, S. I. Nakatsuka, T. Isei, and F. Imamura. Nivolumab induced vitiligo-like lesions in a patient with metastatic squamous cell carcinoma of the lung. *J Thorac Dis*, 10(6):E481–E484, 2018.

[263] Leonidas C. Platanias. Mechanisms of type-i- and type-ii-interferon-mediated signalling. *Nature Reviews Immunology*, 5(5):375–386, 2005.

[264] P. Kubes and S. M. Kerfoot. Leukocyte recruitment in the microcirculation: the rolling paradigm revisited. *News Physiol. Sci.*, 16:76–80, 2001.

[265] A. Zahr, P. Alcaide, J. Yang, A. Jones, M. Gregory, N. G. dela Paz, S. Patel-Hett, T. Nevers, A. Koirala, F. W. Luscinskas, M. Saint-Geniez, B. Ksander, P. A. D'Amore, and P. Argueso. Endomucin prevents leukocyte-endothelial cell adhesion and has a critical role under resting and inflammatory conditions. *Nat Commun*, 7:10363, 2016.

[266] M. Gato-Canas, M. Zuazo, H. Arasanz, M. Ibanez-Vea, L. Lorenzo, G. Fernandez-Hinojal, R. Vera, C. Smerdou, E. Martisova, I. Arozarena, C. Wellbrock, D. Llopiz, M. Ruiz, P. Sarobe, K. Breckpot, G. Kochan, and D. Escors. Pdl1 signals through conserved sequence motifs to overcome interferon-mediated cytotoxicity. *Cell Rep*, 20(8):1818–1829, 2017.

[267] S.-H. Chen, D. A. Murphy, W. Lassoued, G. Thurston, M. D. Feldman, and W. M. F. Lee. Activated stat3 is a mediator and biomarker of vegf endothelial activation. *Journal Cancer Biology & Therapy*, 7(12):1994–2003, 2008.

[268] H. Alsaffar, N. Martino, J. P. Garrett, and A. P. Adam. Interleukin-6 promotes a sustained loss of endothelial barrier function via janus kinase-mediated stat3 phosphorylation and de novo protein synthesis. *American Journal of Physiology-Cell Physiology*, 314(5):C589–C602, 2018.

[269] F. Orsenigo, C. Giampietro, A. Ferrari, M. Corada, A. Galaup, S. Sigismund, G. Ristagno, L. Maddaluno, G. Y. Koh, D. Franco, V. Kurtcuoglu, D. Poulikakos, P. Baluk, D. McDonald, M. Grazia Lampugnani, and E. Dejana. Phosphorylation of ve-cadherin is modulated by haemodynamic forces and contributes to the regulation of vascular permeability in vivo. *Nat Commun*, 3:1208, 2012. Orsenigo, Fabrizio Giampietro, Costanza Ferrari, Aldo Corada, Monica Galaup, Ariane Sigismund, Sara Ristagno, Giuseppe Maddaluno, Luigi Koh, Gou Young Franco, Davide Kurtcuoglu, Vartan Poulikakos, Dimos Baluk, Peter McDonald, Donald Grazia Lampugnani, Maria Dejana, Elisabetta eng P01 HL024136/HL/NHLBI NIH HHS/ R01 HL059157/HL/NHLBI NIH HHS/ HL24136/HL/NHLBI NIH HHS/ HL59157/HL/NHLBI NIH HHS/ Research Support, N.I.H., Extramural Research Support, Non-U.S. Gov't England Nat Commun. 2012;3:1208. doi: 10.1038/ncomms2199.

[270] N. Rodig, T. Ryan, J. A. Allen, H. Pang, N. Grabie, T. Chernova, E. A. Greenfield, S. C. Liang, A. H. Sharpe, A. H. Lichtman, and G. J. Freeman. Endothelial expression of pd-l1 and pd-l2 down-regulates cd8+ t cell activation and cytolysis. *Eur J Immunol*, 33(11):3117–26, 2003.

[271] Z. R. Hartman, M. D. Schaller, and Y. M. Agazie. The tyrosine phosphatase shp2 regulates focal adhesion kinase to promote egf-induced lamellipodia persistence and cell migration. *Molecular Cancer Research*, 11(6):651–664, 2013.

[272] R. D. Chernock, R. P. Cherla, and R. K. Ganju. Shp2 and cbl participate in alpha-chemokine receptor cxcr4-mediated signaling pathways. *Blood*, 97(3):608–615, 2001.

[273] K. Hagihara, E. E. Zhang, Y.-H. Ke, G. Liu, J.-J. Liu, Y. Rao, and G.-S. Feng. Shp2 acts downstream of sdf-1/cxcr4 in guiding granule cell migration during cerebellar development. *Dev Biol.*, 334(1):276–284, 2009.

[274] S. Spranger, R. Bao, and T. F. Gajewski. Melanoma-intrinsic beta-catenin signalling prevents anti-tumour immunity. *Nature*, 523(7559):231–5, 2015.

[275] M. Ayers, J. Lunceford, M. Nebozhyn, E. Murphy, A. Loboda, D. R. Kaufman, A. Albright, J. D. Cheng, S. P. Kang, V. Shankaran, S. A. Piha-Paul, J. Yearley, T. Y. Seiwert, A. Ribas, and T. K. McClanahan. Ifn-gamma-related mrna profile predicts clinical response to pd-1 blockade. *J Clin Invest*, 127(8):2930–2940, 2017.